MOLECULAR PATHOGENICITY OF DISEASE-ASSOCIATED MUTATIONS IN CONE CNG CHANNEL SUBUNITS

By

CHUNMING LIU

A dissertation/thesis submitted in partial fulfillment of
the requirements for the degree of

DOCTOR OF PHILOSOPHY

WASHINGTON STATE UNIVERSITY
COLLEGE OF VETERINARY MEDICINE

May 2008

To the Faculty of Washington State University:

The members of the Committee appointed to examine the dissertation/thesis of CHUNMING LIU find it satisfactory and recommend that it be accepted.

_____
Chair

_____

_____

_____

_____

ACKNOWLEDGMENT

First and foremost, I would like to thank my mentor, Michael D Varnum, for his continuous guidance in both of my academic research and career advancement. I also want to thank my family for their constant emotional support. Without their encouragement, I would not be able to withstand the lonely days thousands of miles away from my home country and familiar environment. I would also like to thank all the members of the Varnum Lab for all the technical and emotional support. Finally, I would like to thank all the faculty members and stuff in our department for creating such a supportive environment to work in. I owe my success in this endeavor to all of you.

MOLECULAR PATHOGENICITY OF DISEASE-ASSOCIATED MUTATIONS IN CONE CNG CHANNEL SUBUNITS

Abstract

By Chunming Liu, Ph.D.
Washington State University
February 2008

Chair: Michael D. Varnum

Located at the outer segment membrane of photoreceptor cells, cyclic nucleotide-gated CNG channels are a critical step in the phototransduction cascade by which light stimulation is converted into electrical responses that can be processed by the central nervous system. The abundance and proper functioning of CNG channels are critical for photoreceptor survival. Multiple mutations in genes encoding CNG channel subunits have been identified in patients with inherited retinal degenerative diseases, a genetically heterogeneous group of disorders characterized by loss of rod, cone, or both photoreceptor cells. The resulting blindness is one of the major causes of disability. However, the pathogenic mechanisms arising from these mutations have remained largely undetermined.

To address this question, we have focused on cone specific CNG channels and functionally characterized three mutations associated with severe progressive cone dystrophy. Complex effects, including altered channel-gating properties, impaired channel subunit processing and

maturation, and disrupted plasma membrane localization, were observed with these mutations. These results provide evidence for the pathogenecity of the mutations in humans, and suggest that changes in channel activity and/or localization may ultimately lead to the reported clinical features.

To further identify the possible cellular and molecular pathways by which CNG channel mutations initiate photoreceptor degeneration, two achromatopsia-associated, gain-of-function mutations in CNGB3 were studied using heterologous expression in photoreceptor derived 661W cell. Mutant channels exhibited increased apparent affinity for CPT-cGMP compared to wild-type channels. Increased cytotoxicity induced by a low concentration of CPT-cGMP was observed in mutant channel-expressing 661W cells. The elevation in cytotoxicity was found to be dependent on the presence of extracellular calcium. The increased susceptibility to cell death could be rescued by applying CNG channel blockers L-*cis*-diltiazem or tetracaine. These results suggest that cytotoxicity in this model depends on calcium entry through hyperactive CNG channels, supporting a Ca^{2+}-overload hypothesis. Our results are the first to show a direct connection between disease-associated mutations in cone CNG channel subunits, altered CNG channel-activation properties, and photoreceptor cytotoxicity.

TABLE OF CONTENTS

LIST OF FIGURES

Page

INTRODUCTION

Ⅰ. Phototransduction, recovery and light adaptation

How does an animal "see" things, i.e., how does light in the surrounding environment create an image in the brain? Since all neuronal responses are ultimately electrical responses, the first step of vision must be the conversion of light stimuli to electrical signals. This process is known as phototransduction and is carried out by retinal photoreceptor cells. In the resting state of photoreceptors in the absence of light, cyclic nucleotide-gated (CNG) channels located at the outer segment membrane, are opened by direct binding of intracellular guanosine 3', 5'-cyclic monophosphate (cGMP) (44, 80, 109). A "dark current" carried mostly by influx of Na^+ and Ca^{2+} through open CNG channels (63), leads to slight photoreceptor depolarization and excitatory neurotransmitter (glutamate) release at the photoreceptor synapse. The excitation process of phototransduction begins with absorption of photons by visual pigment, rhodopsin or opsin, which activates cGMP phosphodiesterase (PDE) through a specific GTP-binding protein, transducin. The activated cGMP PDE then catalyzes the hydrolysis of cGMP to the inactive form GMP. In response to the drop of intracellular cGMP, CNG channels close and the influx of Na^+ and Ca^{2+} decreases. The resulting membrane hyperpolarization leads to attenuation in tonic glutamate release (194). Through a network of interneurons, including bipolar, horizontal and amacrine cells, these electrical signals are processed and relayed to retinal ganglion cells. Signals evoked by light in photoreceptors are transmitted as trains of action potentials through

the optic nerve formed by axons of ganglion cells, projected to higher order neurons in the central nervous system and ultimately processed as vision.

Within the outer segment, the drop in intracellular Ca^{2+} produced by closure of the CNG channels after light stimulation triggers a negative feedback loop. This negative feedback loop mediates recovery of the photoreceptor to its pre-activated state in the case of a transient stimulus, or light adaptation in the case of a sustained stimulus (141). The recovery of phototransduction also involves active turnoff and recycling of the transduction components. Rhodopsin kinase phosphorylates and inactivates rhodopsin, and the inactivated rhodopsin is subsequently capped by arrestin to be removed from further action. Transducin is deactivated through the hydrolysis of bound GTP to GDP, thereby allowing cGMP PDE to return to its inactive state and reducing the hydrolysis of cGMP. Guanylyl cyclase (GC) is activated through a Ca^{2+} sensor, guanylyl cyclase activating protein (GCAP), which responds to the decrease of cytoplasmic Ca^{2+} concentration ($[Ca^{2+}]_i$) after CNG channel closure. The enzymatic activity of GC thus produces more cGMP. Combined actions of reduced hydrolysis and activated synthesis leads to an increase in cytosolic cGMP levels, allowing more CNG channels to be opened and the photoreceptor to return to its resting state (27, 124, 159).

In order for photoreceptor cells to maintain a response over a broad range of light intensities and durations, photoreceptor cells alter their sensitivity to light, a process known as light adaptation (see review in (15) and (37)). The adaptation process occurs at multiple levels, such as shortened lifetime of active PDE (84) and altered ligand sensitivity of the CNG channel through Ca^{2+}-calmodulin (CaM) (71, 72, 90, 131).

Photoreceptor cells, including rods and cones, are highly differentiated in structure and protein components that carry out their primary task of phototransduction. Although the goals are basically the same, rods and cones work under different light spectra (see review in (15, 57)). The rods are sensitive to low intensity light and are responsible for night vision. High intensity light (day-light vision) and color vision depends on three types of cone photoreceptors in humans that are optimally sensitive to light of different wavelengths. Rods and cones express related but distinct genes for many important signaling proteins in the phototransduction cascade. One example of these specializations is that native CNG channel in rods and cones exhibits different apparent ligand affinities and different sensitivities to calcium-feedback regulation. Compared to rods, less is known about cone phototransduction and the specialized CNG channels of cone photoreceptors (40). To address this important gap in knowledge, research in our lab has been focused on characterizing the structure and function of cone CNG channels.

Environmental damage or gene defects, which result in disruption of normal phototransduction, can increase the risk of photoreceptor cell death and lead to retinal degenerative diseases (136). In the following section, we will briefly discuss some of the possible causes of these diseases.

Ⅱ. Photoreceptor degenerative diseases

Retinal dystrophies, a group of diseases that are characterized by degeneration of photoreceptor cells in the retina (rods, cones, or both) and subsequent loss of vision, affect millions of people worldwide. There are many identified environmental or genetic factors

thought to be related to photoreceptor degeneration. The most common damaging factors from the environment that cause photoreceptor cell death include excessive light exposure, hypoxic-ischemia insult and heavy metals such as lead exposure (14, 35, 50, 51). Another major cause for loss of rods and cones is genetic mutations, leading to inherited photoreceptor degenerative diseases (IPDs) such as retinitis pigmentosa (RP), achromatopsia, progressive cone dystrophy (PCD) and inherited forms of macular degeneration (MD). To date, 190 genes and loci have been mapped and 138 genes identified as linked to IPDs (see RetNet at http://www.sph.uth.tmc.edu/Retnet/; also reviewed by Pacione (123)). The resulting loss of vision is one of the most common causes of disability. According to the NEI National Plan for Eye and Vision Research (2004), the inherited forms of retinal diseases afflict approximately 100,000 people in the United States.

Common clinical phenotypes

IPDs are a genetically and phenotypically diverse group of inherited diseases. Heterogeneity in clinical symptoms and genetic defects is remarkable in this group of diseases, since autosomal dominant, autosomal recessive and X linked recessive inheritance have all been reported. In the majority of IPDs, both cone and rod photoreceptors die, but the time course and the degree to which these cell types are affected differs between various disorders. For example, RP is a heterogeneous group of diseases characterized initially by a progressive loss of rods. As a result, night vision and peripheral vision are affected at first. The subsequent degeneration of cones eventually leads to complete blindness (see review in (67) and (78)).

Similarly, disruptions in cone function and cone degeneration leads to day-light sensory deficiencies (legal blindness) and abnormalities in color-vision, as the primary symptoms in patients with achromatopsia (164), PCD (164, 165) and inherited forms of MD (173). Since cone photoreceptors are mostly enriched in the central part of retina (fovea), impairment of central vision usually occurs first. Other clinical symptoms include reduced visual acuity, photophobia and nystagmus (see reviews in (143, 164)). Based on diseases' clinical progression, cone degenerative diseases can be broadly divided into two groups, stationary and progressive cone dystrophy (164).

Achromatopsia, which is also called rod monochromatism, is a stationary form of cone dystrophy that denotes a group of congenital disorders where lack of cone function is evident from birth (160, 161). All three types of cones are affected in the complete form of achromatopsia, resulting in complete colorblindness and severe reduction of visual acuity. Less severe form of cone degeneration, where different degrees of residual cone function remain detectable, is called incomplete achromatopsia (see review (26, 114, 164)). In this type of disease, specific subtypes or all three types of cones are affected, yet symptoms are less severe compared to complete achromatopsia (164). Patients with PCD, on the other hand, usually present normal vision at birth. Deterioration of visual acuity and color vision starts at the adolescent or early adult stage (reviewed by Simunovic (164)). Yet this clinical definition of "stationary" or "progressive" is not absolute, since a progressive loss of residual cone function has been reported in patients diagnosed with "achromatopsia" (82). In this study, some affected individuals retain residual cone function into middle age, and then progressively lose this

functional remnant over a prolonged period (6-12 years). Thus, methods other than clinical characterization, such as genetic analysis and mechanistic study, may offer advantages for disease classification.

Affected genes in IPDs

Based on the known or presumed function of the encoded proteins, brief analysis of all the affected genes and loci revealed that the following biochemical pathways might be affected by mutations: phototransduction cascade, vitamin A metabolism, structural or cytoskeletal features, cell-cell interaction and signalling, synaptic interaction, RNA intron-splicing factors, trafficking of intracellular proteins, maintenance of cilia/ciliated cells, pH regulation (choriocapillaris) and phagocytosis (67). It is not clearly understood how the altered structure or function of critical proteins in the photoreceptors drives them toward cell death, producing barriers in developing prevention and treatment methods. As briefly described above, the opening and closure of CNG channels is crucial to phototransduction, recovery and light adaptation. Mutations in different components of the phototransduction pathway may result in abnormal CNG channel activity, triggering photoreceptor cell death. These include mutations in CNG channel subunits that directly alter channel gating (discussed later in this introduction), and mutations in critical enzymes that change channel ligand concentration in the photoreceptor outer segment, including cGMP phosphodiesterase (PDE), retinal guanylyl cyclase (retGC) and its activating protein (GCAP) (see review in (122, 138)).

Mutations resulting in abnormal cytoplasmic cyclic nucleotide levels have been linked to photoreceptor degeneration. Even prior to the identification and cloning of genes encoding CNG channels, an abnormal elevation in intracellular cGMP levels was observed in the *rd1* mouse, a classic model for RP (43), and in patients with RP (42). Genetic and functional studies demonstrated that elevated cGMP levels were a result of mutant PDE6 β-subunits that impair enzymatic activity (8, 17, 18, 111, 112). Recent studies by Stearns and coworkers suggest that rapid cone degeneration is also observed in the zebrafish retina after mutation of a cone specific *pde6* gene, providing further evidence that links the loss of functional cGMP PDE to photoreceptor degeneration *in vivo* (168). Additional studies showed that RP-associated mutations in retinal GC and GCAP both produced constitutively active GC (28, 55, 129, 135, 156), leading to a sustained increase in cGMP levels. Retinal explants and photoreceptor derived 661W cells treated with PDE inhibitor show a tonic increase in intracellular Ca^{2+} levels and subsequent cell death (106, 157, 180, 181), providing further evidence that appropriate intracellular cGMP levels are critical for photoreceptor survival.

Another group of IPD-related mutations are found in genes encoding CNG channel subunits. To better understand the effects of these mutations, we will take a closer look at the structural features and functional importance of photoreceptor CNG channels.

Ⅲ. CNG channels

Critical role of CNG channels in visual transduction, recovery and adaptation

Since the first discovery of CNG channels in the plasma membrane of vertebrate rod (44) and cone (68) photoreceptor outer segments, extensive studies have been carried out in this field. Consequently, a close relationship between these channels and primary sensory systems, including vision and olfaction, has been established (reviewed by Pifferi (137)). By helping to convert sensory input (absorption of light) into electrical responses (hyperpolarization of photoreceptors), CNG channels play a fundamental role in the visual transduction pathway.

CNG channels are also critical for recovery and light adaptation by controlling intracellular Ca^{2+} homeostasis. Ca^{2+} enters into photoreceptor outer segments mainly through CNG channels, and is extruded via the Na^{+}/Ca^{2+}-K^{+} exchanger (141). Important steps in both recovery and adaptation processes are Ca^{2+}-dependent (review in (45, 141)). For example, GC activation depends on GCAP, a Ca^{2+} sensor that responds to the decrease of cytoplasmic Ca^{2+} concentration ($[Ca^{2+}]_i$). With the closure of the CNG channels after light stimulation, intracellular Ca^{2+} concentration decreases and therefore initiates the recovery process by activating GC and enhancing synthesis of new cGMP molecules (27, 124, 159). Adaptation is also highly Ca^{2+}-dependent (37, 65, 90). The lowered intracellular Ca^{2+} concentration after light stimulation and CNG channel closure may initiate adjustment of the sensitivity of the transduction machinery.

Structural features of CNG channels

CNG channels are functionally classified as one member of ligand-gated, non-selective cation channels (44, 80, 109). Although they are only weakly sensitive to membrane depolarization, structural homology indicates that CNG channels are related to the superfamily of voltage-gated potassium (K^+) channels (see review in (198)). Each CNG channel subunit contains six transmembrane domains (S1-S6), cytoplasmic N- and C-termini, a conserved pore region, a cyclic nucleotide-biding domain (CNBD) and a C-linker region between S6 and CNBD (Chapter 1, Fig. 1). The S4 transmembrane domain contains multiple positively-charged residues, similar to that of voltage-gated K^+ channels in which S4 is believed to act as a voltage sensor (76, 97). Ligand docking at each CNBD initiates a conformational change in the channel that leads to opening of the channel pore. Cyclic GMP is the physiological activator of the photoreceptor CNG channels *in vivo*. Bound cGMP promotes an allosteric conformational change leading to opening of the channel pore. Adenosine 3', 5'-cyclic monophosphate (cAMP) is a partial agonist of the rod and cone CNG channel (80). The initial binding of cAMP is comparable to that of cGMP, but cAMP is much less efficient in promoting channel opening after binding to CNBD (61). The major structural determinant of cGMP efficacy and specificity has been localized to a single aspartic acid residue within the CNBD (182).

CNG channels are tetrameric proteins (61, 104, 183) composed of some combination of α (CNGA1, CNGA2, CNGA3 and CNGA4) and β (CNGB1 and CNGB3) subunits (7, 58, 91, 153). While CNGA1, CNGA2 and CNGA3 subunits can form active homomeric channels by themselves when expressed alone in heterologous expression systems, native CNG channels are

known to be heteromeric. Rod photoreceptor CNG channels contain three CNGA1 subunits and one CNGB1 subunit (186, 201, 203). A different stoichiometry is adopted by cone CNG channel: CNGA3 and CNGB3 subunits are arranged in a 2:2 configuration (134). CNG channels of olfactory receptor neurons are composed of two CNGA2 subunits, one CNGA4 subunit, and one alternatively spliced CNGB1 subunit (CNGB1b) (202). Although CNGA4, CNGB1 and CNGB3 do not form functional channels by themselves, they can modulate channel properties and fine-tune each cell type specific CNG channel to best perform its physiological role (7, 9, 10, 20, 58, 100, 153).

CNG Channelopathies

Mutations in ion channel genes that are linked to clinical diseases are known as channelopathies. More than 60 mutations in genes encoding CNG channel subunits have been identified in patients suffering from IPDs (see review (4)). Depending on cell-type expression of mutant protein, rods and cones are affected differently, leading to distinct clinical symptoms discussed above. Some forms of RP are caused by mutations in the *CNGA1* or *CNGB1* genes of the rod photoreceptor cells (33, 107, 177). Yet this can only account for a small portion (less than 9%) of patients having this disease (67). Mutations in the cone CNG channel genes *CNGA3* (62, 77, 88, 120, 184, 187, 188) and *CNGB3* (77, 86, 89, 113, 120, 121, 163, 170, 184, 189) have also been identified in patients with achromatopsia, PCD and inherited MD. Different from RP, mutations in cone channel subunits accounting for 60-80% of the cone dystrophy patients examined, with *CNGA3* accounting for 20-30% of achromatopsia cases and *CNGB3* accounting

for up to 50% ((77, 89), also see RetNet). Mutations in another gene, *GNAT2*, which encodes the α subunit of the G-protein transducin (87), accounts for a minor fraction (<2%). Obviously, there are still unidentified gene alterations related to inherited cone dysfunction.

How do these mutations in CNG channel genes affect protein activity? Several functional studies using heterologous expression methods have been carried out to answer this question and two major effects have been characterized in these mutant channels, as described below.

Functional consequences of CNG channel mutations

Some mutant alleles can produce functional channels in the plasma membrane with altered gating properties. Many mutations in cone specific CNGB3 subunits produce a gain-of-function phenotype (13, 121, 132). Such gain-of-function changes are evident as an increase in apparent ligand affinity and relative agonist efficacy. Some mutations in CNGA3 subunits exhibited a similar gain-of-function effect (103, 118, 133). Altered ion selectivity and single channel properties of heteromeric channels containing S435F, an achromatopsia-associated point mutation in CNGB3, have also been observed (132). In addition, an incomplete achromatopsia-associated mutation in CNGA3 (T369S) exhibits altered Ca^{2+} permeation and block (176).

Besides the direct gating changes observed in mutant CNG channels, many nonsense or deletion/frame shift mutations in *CNGB3* are null mutations that produce severely truncated CNGB3 subunits (127, 146). These mutant subunits do not form functional heteromeric channels with CNGA3 at the plasma membrane. One of the most prevalent mutations in achromatopsia patients, T383fsX in CNGB3 (77, 89), falls into this category (13, 132).

Channels formed after heterologous expression of CNGA3 plus CNGB3 subunits containing this mutation closely resembled homomeric CNGA3 channels (132). CNGA3 homomeric channels exhibit higher apparent affinity for cGMP compared to heteromeric channels, and they are insensitive to down-regulation by Ca^{2+}/calmodulin (131) and phospholipids including PIP_3 (11) and PIP_2 (data not published from our lab). Thus, this type of mutation can essentially be considered as producing a "gain-of-function" phenotype.

Others mutations disrupt channel protein trafficking and plasma membrane localization, thus resulting in loss of channels at the plasma membrane. Two RP-associated mutations in rod *CNGA1* (S316F and R654Dstop) produced channel subunits that fail to reach the plasma membrane (33, 177). For cone CNG channels, our studies have shown that an achromatopsia-associated mutation in CNGA3, Q655stop, disrupts plasma membrane localization (133). Another study, using bovine CNGA3 subunits with specific mutations in the S4 domain, indicated that these mutant channel subunits do not arrive at the plasma membrane, possibly due to disruption in channel maturation through glycosylation (36). Studies of four distinct achromatopsia-associated mutations in the CNGA3 S1 transmembrane region also demonstrated that mutant channel subunits were mainly retained within endoplasmic reticulum (ER) (127). Additional studies revealed that most *CNGA3* mutations (32 out of 39) do not form functional channels at the plasma membrane when expressed heterologously (118). Interestingly, one CNGA3 mutation (E593K) expressed in HEK293 cells produced functional homomeric channels with lowered apparent affinity for cGMP (118). In addition, a five-fold decrease in cGMP apparent affinity was also reported in incomplete achromatopsia-associated CNGA3 mutation

(T369S) (176). These gating alterations represent another type of loss-of-function change.

The functional importance of CNG channels in promoting photoreceptor survival has also been investigated by knocking out genes encoding the CNG subunits (5, 22, 73). These knockout animal models can mimic a loss-of-function change similar to some disease associated channel mutations. A knockdown mouse model with partial loss of CNGA1 via overexpressing CNGA1 antisense mRNA induced a reduction in photoreceptor cell number (98). Complete knock-out of *CNGB1* in mice abolished the rod-mediated response to light, possibly resulting from disruption of CNGA1 targeting to the rod outer segment (73). Retinal degeneration in this model was similar to human RP, with the loss of rods at birth followed by progressive degeneration of cones. Deletion of the *CNGA3* gene produced mice lacking functional CNG channels in the cone photoreceptor outer segment. This mouse model showed an absence of cone-mediated light response together with progressive cone degeneration, whereas the rod pathway was completely intact (5, 154). The retinal phenotype of *CNGA3*-knockout mice resembled clinical symptoms associated with achromatopsia and PCD in humans. Similar progressive loss of photoreceptors was also observed in the retina of a mouse *CNGA3*/*Rho* double-knockout model (22).

These converging lines of evidence from functional mutation studies and gene knockout models clearly indicate that proper CNG channel activity is crucial for maintaining photoreceptor survival.

Complexity of phenotype-genotype relationship in IPDs

Functional studies revealed that severity of some clinical syndromes was partially correlated to the gating changes induced by disease-associated channel mutations (13). Allelic analysis of some CNGA3 mutations in patients indicated similar correlation (120). However, this correlation is not definitive. In IPDs, phenotypic variation is rather evident among patients with the same disease-associated CNG mutations. For example, two most common CNGA3 mutations, R277C and R283W, were found in patients representing different clinical phenotypes, including complete and incomplete forms of achromatopsia as well as PCD (187). Similarly, homozygotes for the most common *CNGB3* mutation, T383fsX (89, 120, 189), presented severe cone dysfunction syndromes, yet another patient with the same T383fsX genotype exhibited an extremely mild phenotype (120). Two sisters carrying identical compound heterozygous *CNGA3* mutations (T224R/T369S) also exhibited different phenotypes. Although both suffer from incomplete achromatopsia, the severity of their symptoms in terms of reduced visual acuity and impaired color vision was different (176). This suggests that other factors contribute to their phenotype. Functional studies revealed that T224R is effectively a null mutation that does not give rise to functional channels, whereas T369S can form functional homomeric channels with altered gating properties, including significantly reduced cGMP apparent affinity (176). It seems that a fraction of channel function is sufficient to maintain partial cone photoreceptor function. Furthermore, some patients exhibit incomplete achromatopsia even though they are homozygous for presumptive *CNGA3* null mutations such as R283W (118, 187). It is difficult to explain these examples of residual cone function unless other genetic factors are considered.

Variability in phenotypes is a common phenomenon in inherited diseases. This may be due to allelic differences, environmental influences, modifier genes, or a combination of these factors (see review in (123)). The lack of obvious correlation between specific CNG mutations and the severity of cone dysfunction suggests that other genetic or environmental factors play a major role in these diseases. Modifier genes may participate in creating a permissive genetic background for single gene mutations to manifest a disease phenotype (123). Exact modifier loci need to be mapped to support this hypothesis.

Despite the identification of many mutations in CNG channels in patients with IPDs and the in-depth functional characterization of some disease-associated mutations, little is known about how such mutations lead to photoreceptor cell death *in vivo*. What are the cellular and molecular mechanisms underlying photoreceptor degeneration? One of our research goals is to understand the pathogenecity of these channel mutations and to elucidate underlying cellular and molecular mechanisms.

Ⅳ. Cellular and molecular mechanisms for photoreceptor degeneration

Common pathways for photoreceptor cell death

Cell death occurs in normal or damaged cells through two main pathways, apoptosis and necrosis. The programmed cell death, apoptosis, has been described as the common pathway in many forms of neuronal degeneration (see review in (12, 108)). Activation of critical components of the apoptotic signaling pathway, such as caspase-3 and caspase-9, is observed in some models of photoreceptor degeneration, indicating that apoptotic cell death may also be

involved in retina dystrophies. Elevated levels of active caspase-3 are evident in the *rd* mouse, a mouse model for autosomal recessive RP (arRP) (157). Similar caspase-3 activation is observed in photoreceptor derived 661W cell death induced by oxidative-stress or by application of a bioreductive agent (2-nitroimidazole radiosensitizer, CI-1010) (116). Caspase-1 and caspase-9 activation have also been reported for light-induced apoptosis in 661W cells (24, 79, 92). In addition, anti-apoptotic Bcl-2 overexpression offered protection against light damage in photoreceptor cell models through NF-kB preservation (24). Overall, apoptotic cell death has long been considered as the predominant form by which photoreceptor cell death occurs in many forms of eye disease such as hereditary retinal dystrophies, age related macular degeneration, retinal detachment, and retinal light damage (19, 34, 125, 148, 149, 178).

While apoptotic mechanisms play a critical role in photoreceptor degeneration, new evidence has emerged in recent years suggesting that other parallel pathways may be involved. One such alternative cell death mechanism is autophagy, the major cellular pathway for the degradation of aged proteins and organelles by the lysosome (83, 99). This idea is supported by the evidence that mRNA levels of both apoptotic and autophagic maker genes are elevated in oxidative stress induced photoreceptor damage in *vitro* (94, 95). The lack of complete rescue of cell loss by applying caspase 3 inhibitor to C3H mice carrying the *rd* mutation (196) or in Ca^{2+}-ionophore stimulated 661W cells (157) also suggests that apoptosis cannot account for all cell death observed with retina dystrophies. On the contrary, blocking the apoptotic pathway by caspase inhibitor may push the cell to undergo necrotic cell death (94). One Ca^{2+}-dependent cysteine protease, calpain, stands out in autophagic pathways as a critical component. Calpain

activation, followed by rupture of the lysosomal membrane and the activation of lysosomal cathepsins, is one of the characteristics in the autolytic digestion of the cell (191). Activation of calpain has been shown to be involved in retinal degeneration in several different animal models (2, 30, 32, 106, 126, 157).

Although apoptosis and autophagy are two morphologically distinct forms of cell death, boundaries between them are not clearly demarcated (see review in (105)). Both mechanisms may co-exist in photoreceptor degeneration (31, 95, 106, 145). Recent evidence suggests that autophagy might precede apoptosis and participate in photoreceptor cell death by initiating apoptosis (94). Research addressing these issues has failed to identify specific mechanisms by which altered CNG channel properties lead to photoreceptor degeneration. One important second messenger, Ca^{2+}, seems to stand on the crossroad of the two forms of cell death. Disruption of intracellular Ca^{2+} homeostasis may provide the link between altered channel function/abundance and retina dystrophies.

Ca^{2+}-overload may trigger the initiation of photoreceptor cell death

Ca^{2+} enters photoreceptor cells through Ca^{2+} permeable cation channels at the plasma membrane. Although there are voltage-gated L-type Ca^{2+} channels expressed at the inner segment of photoreceptor cells, CNG channels are the main pathway for Ca^{2+} influx into the outer segment where photo-pigments and other critical phototransduction proteins exist (see review in (93)). Such influx of Ca^{2+} is balanced by Ca^{2+} extrusion through the Na^{+}/Ca^{2+}-K^{+} exchanger (141) or is buffered by the intracellular Ca^{2+} pool (ER). The free intracellular Ca^{2+}

concentration in rod outer segments can change almost 80-fold in seconds (410 ± 37 nM in the dark-adapted outer segment; 5.5 ± 2.4 nM after saturating illumination) (151). This dynamic range of intracellular Ca^{2+} indicates a powerful buffering system, which is critical for normal cell function and survival. Only sustained elevation of intracellular Ca^{2+} levels is expected to lead to impairment of photoreceptor cells. Consistent with this idea, increased intracellular Ca^{2+} levels have been reported in several different photoreceptor degeneration models, as will be discussed below.

661W cells showed a rapid increase in intracellular Ca^{2+} after treatment with 8-br-cGMP, a cGMP analogue which continuously activates CNG channels, or the PDE inhibitor IBMX, which leads to increased intracellular cGMP levels; with both treatments subsequent cell degeneration was observed (157). An early increase in intracellular Ca^{2+} concentration prior to apoptotic photoreceptor cell death was also reported in light-induced retinal degeneration, possibly through neuronal nitric oxide (NO) activation of GC, resulting in increased [cGMP] and CNG channel opening (29). Similar to these manipulations, mutations in CNG channel subunits that produce gain-of-function changes in channel gating, or mutations in the cGMP PDE, GC or GCAP proteins that lead to increased intracellular cGMP levels, may all contribute to an abnormally high level of channel activity, as discussed in the previous section. The increased CNG channel open probability or prolonged open channel durations may result in a large Ca^{2+} influx that surpasses the buffering limit of the photoreceptor. In the second part of this dissertation, we will provide evidence showing that disease-associated, gain-of-function mutations in cone CNG channels can increase photoreceptor susceptibility to cell death, and that this effect is Ca^{2+}

dependent. Such a link between gain-of-function changes in channel activity and photoreceptor degeneration also has been observed in a *Drosophila* retinal degeneration model. In *Drosophila*, a light-activated, Ca^{2+}-selective transient receptor potential (TRP) channel plays a role similar to the CNG channel of vertebrate phototransduction (66). A mutation in *Trp*, resulting in a constitutively active TRP channel, leads to massive photoreceptor degeneration in the *Drosophila* retina (195). The severity of the photoreceptor cell loss is ameliorated by overexpressing a Na^{+}/Ca^{2+} exchanger, suggesting a direct link between increased intracellular Ca^{2+} entry through hyperactive channels and photoreceptor degeneration (185).

How does intracellular Ca^{2+}-overload trigger photoreceptor cell death? It has been established that a sustained elevation of intracellular Ca^{2+} can initiate apoptotic cell death (see review in (3, 21, 119)). Evidence shows that in photoreceptors, elevated intracellular Ca^{2+} is associated with photoreceptor apoptosis in *rd* mice (41), RP (19, 52) and cone dystrophy (129, 166), as well as other forms of retina dystrophy such as cancer-associated retinopathy (175), lead-exposed rats (50-52), rats injected with anti-recoverin antibodies (1), rats with hypoxic-ischemic injury (25), and rats (35) or mice (197) with light-induced damage. Studies performed in isolated rat retinas have demonstrated that Ca^{2+} overload can induce mitochondrial depolarization and the release of apoptosis-inducing factors (such as cytochrome *c*), which subsequently lead to the activation of caspase-9 and caspase-3 (70). Such changes have also been linked to oxidative stress induced apoptosis in 661W cells (106).

On the other hand, autophagy pathways are also Ca^{2+} dependent and may be involved in photoreceptor degeneration. The dissociation of calpain from its inhibitor calpastatin, which is

required for calpain activation, seems to be dependent on an increase in intracellular Ca^{2+} (reviewed by Goll (59)). And calpain activation, following the influx of Ca^{2+} through CNG channels, is observed in oxidative stress induced degeneration of 661W cells (106). Calpain activation could also lead to photoreceptor apoptotic cell death without cytochrome c release (139), which is thought to be a caspase-independent process. These converging lines of evidence suggest that Ca^{2+} overload might be an important trigger for initiation of photoreceptor cell death.

ER stress and unfolded protein response may be another trigger for the photoreceptor cell death

Although high channel activity/Ca^{2+} overload seems to be a likely mechanism by which photoreceptors degenerate, emerging evidence indicates that altered channel gating properties cannot account for all the possible mechanisms by which mutant channel subunits may cause cell degeneration. Several different aspects of channel processing and function can also be affected by disease-associated mutations. In some situations, such as CNG channel subunit knockout models and disease-associated null mutations, lack of functional CNG channels at the outer segment membrane is evident. Obviously, other factors must be involved in initiating photoreceptor cell death under these conditions. Recent studies by Tso and coworkers have demonstrated a significant increase in ER stress marker proteins in degenerating photoreceptors in both the *rd1* mouse model and light-induced retinal degeneration (192, 193). Such up-regulation of these proteins coincides with or foreshadows photoreceptor apoptosis. Results such

as these indicate that ER stress and the unfolded protein response (UPR) might be candidate mechanisms for initiation of photoreceptor cell death.

Stress in the endoplasmic reticulum (ER stress) is caused by accumulation of unfolded or misfolded proteins in the ER lumen. The unfolded protein response (UPR) that accompanies ER stress has been closely associated with neuronal cell death in stroke, Alzheimer's disease and Parkinson's disease (see review in (199, 200)). ER stress that results from accumulation of misfolded rhodopsin has been linked to apoptotic photoreceptor degeneration in a *Drosophila* model for autosomal dominant RP (adRP) (150). In other cases of autosomal dominant RP, mutant rhodopsin molecules are considered to be toxic to rods via interference with cell metabolism, formation of intracellular protein aggregates, a defect in intracellular transport, or a fault in the structure of the photoreceptor outer segment (23, 75, 81, 96, 117, 171, 172). Such toxicity may also arise from ER stress and the UPR. In support of this hypothesis, recent studies have shown that ER stress marker gene expression levels were significantly higher in mutant rhodopsin expressing HEK293 cells as well as in retinas from adRP transgenic rats expressing mutant rhodopsin (101). It also has been suggested that ER stress and the UPR might underlie tunicamycin induced apoptotic cell death in cultured retinal ganglion cells (162).

Little is known about the involvement of ER stress secondary to disease-associated mutations in CNG channels. The fact that many of these mutations lead to misfolded or immature channel subunits that aggregate within the ER (33, 127, 146, 177) suggests that ER stress might be involved in initiation of photoreceptor cell death in these cases. In the mouse *CNGA3* knockout model, impaired opsin targeting led to substantial accumulation of opsin in the

inner segments, somata, and terminals of cone photoreceptors (115). It thought that the CNG channel protein complex is pre-assembled in the ER prior to being transported to the outer segment. Lack of normal CNG channels, as in some null CNG mutations, may lead to failure of proper targeting of other critical outer segment proteins such as opsin.

Ⅴ. Protective effect of CNG channel blockers

One of the biggest difficulties that patients carrying inherited photoreceptor degenerative diseases may face is the lack of effective preventative methods and clinical treatments. A number of organic compounds, including L-*cis*-diltiazem (20, 46, 69, 103, 110) and tetracaine (48, 49, 155), are reported to block the ionic current through CNG channels. D-*cis*-diltiazem, which is more selective for blocking L-type Ca^{2+} channels, has also been shown to have a weak blocking effect for CNG channels (74, 85). Whether application of diltiazem can exert a protective effect against photoreceptor degeneration remains somewhat controversial. Alleviated apoptosis in rod photoreceptors by D-*cis*-diltiazem was observed in $Pde6b^{rd1}$ mice (30, 54), although others have reported no rescue after the same treatment with identical or similar animal models, including $Pde6b^{rd1}$ mice (128), dogs with a different PDE mutation (130), or rats with a rhodopsin P23H mutation (16). In contrast, Fox and coworkers (53) reported that block of Ca^{2+} influx through CNG channels with L-*cis*-diltiazem partially rescued rod degeneration in $Pde6b^{rd1}$ mice. The Ca^{2+}-overload hypothesis described here offers an explanation for the potential cell-protective effect of CNG channel blockers such as L-*cis*-diltiazem and tetracaine.

In Chapter One of this thesis, we describe the functional consequences of three progressive cone dystrophy-associated mutations in the CNGA3 subunit of cone CNG channels. In Chapter Two, we provide evidence that Ca^{2+}-overload mechanisms might underlie the pathogenicity of disease-associated mutations in the CNGB3 subunit. This work has significantly broadened our understanding of CNG channelopathies, providing a theoretical basis for developing effective therapeutic strategies.

CHAPTER ONE

Functional consequences of progressive cone dystrophy-associated mutations in the human cone photoreceptor cyclic nucleotide-gated channel CNGA3 subunit

Chunming Liu[1], and Michael D. Varnum[1, 2*]

[1] Dept. of Veterinary and Comparative Anatomy, Pharmacology, and Physiology and Program in Neuroscience, and [2]Center for Integrative Biotechnology
Washington State University, P. O. Box 646520, Pullman, WA 99164-6520

*To whom correspondence should be addressed: E-mail: varnum@wsu.edu; Telephone: 509-335-0701, Fax: 509-335-4650

Running Title: Effects of Progressive Cone Dystrophy Mutations in Human CNGA3

Chunming Liu and Michael D. Varnum. Progressive cone dystrophies are a genetically heterogeneous group of disorders characterized by early deterioration of visual acuity and color vision, together with psychophysical and electrophysiological evidence of abnormal cone function and cone degeneration. Recently, three mutations in the gene encoding the CNGA3 subunit of cone photoreceptor cyclic nucleotide-gated (CNG) channels have been linked to progressive cone dystrophy in humans. In order to investigate the functional consequences of these mutations, we expressed mutant human CNGA3 subunits in *Xenopus* oocytes, alone or together with human CNGB3, and studied these channels using patch-clamp recording. Compared to wild-type channels, homomeric and heteromeric channels containing CNGA3-N471S or -R563H subunits exhibited an increase in apparent affinity for cGMP and an increase in the relative agonist efficacy of cAMP compared to cGMP. In contrast, R277C subunits did not form functional homomeric or heteromeric channels. Cell surface expression levels, determined by confocal microscopy of green fluorescent protein (GFP)-tagged subunits and patch-clamp recording, were significantly reduced for both R563H and R277C but unchanged for N471S. Overall, these results suggest that the plasma membrane localization and gating properties of cone CNG channels are altered by progressive cone dystrophy-associated mutations, providing evidence supporting the pathogenicity of these mutations.

cyclic nucleotide-gated channel; cone; photoreceptor; subunit; severe progressive cone dystrophy

Normal high-acuity and color vision relies on the presence and functional integrity of three types of cone photoreceptors that are optimally sensitive to light of different wavelengths (reviewed in (20)). Located in the photoreceptor outer segment, cyclic nucleotide-gated (CNG) channels play a fundamental role in phototransduction by helping to convert sensory input into electrical responses. In the absence of light, the CNG channels are opened by binding of intracellular cGMP (29, 73) and conduct a "dark current" carried mostly by influx of Na^+ and Ca^{2+} (24). When photons are absorbed by the photo-pigments, sequential signaling events are initiated including activation of a photoreceptor G protein transducin, and activation of cGMP phosphodiesterase (PDE). The activated cGMP PDE then hydrolyzes and lowers the intracellular cGMP level. Hyperpolarization of the photoreceptors thus results from the closure of CNG channels in response to the lowered cGMP level and the tonic release of neurotransmitter (glutamate) from the photoreceptor terminal decreases (70). The CNG channels are also crucial for recovery and light adaptation processes by controlling intracellular Ca^{2+} homeostasis since they are the major pathway for Ca^{2+} entry into the photoreceptor outer segment (14, 16). Intracellular Ca^{2+} entry is balanced by Ca^{2+} extrusion through Na^+/Ca^{2+}-K^+ exchangers (reviewed by Pugh (51)). Within the outer segment, the fall in intracellular Ca^{2+} concentration due to the closure of CNG channels triggers a negative feedback loop that mediates recovery of the cell to its pre-activated state in the case of a transient stimulus, or light adaptation in the case of a sustained stimulus (33, 51).

CNG channels are tetrameric proteins (22, 39, 65) composed of some combination of CNGA1, CNGA2, CNGA3, CNGA4, CNGB1 and CNGB3 subunits (3, 21, 34, 57). The

CNGA1, CNGA2 or CNGA3 subunits can form functional homomeric channels when expressed alone (2, 11, 28, 67). While CNGB1, CNGB3 or CNGA4 subunits do not form functional channels by themselves, they can modulate the channel properties when co-assembled with the other subunit types (3-6, 21, 37, 57). Native rod CNG channels are heteromeric proteins formed by assembly of three CNGA1 and one CNGB1 subunit (66, 74, 76). Recent studies suggest that cone CNG channels adopt a different structure, being composed of CNGA3 and CNGB3 subunits in a 2:2 configuration (49). Each channel subunit contains six transmembrane regions, cytoplasmic N- and C-termini, a conserved pore domain and a cyclic nucleotide-binding domain (Fig. 1A) (reviewed by Kaupp and Seifert (29)). Loss or functional alterations in the cone photoreceptor CNG channels—due to missense mutations, deletions, or splice-site disruption in the genes encoding these subunits—result in abnormal cone function leading to daylight and color-vision deficiencies (reviewed in (52)). The general forms of color blindness, cone dystrophies, can be broadly divided into two groups: stationary and progressive cone dystrophy. The stationary form of cone dystrophy is also called ‘achromatopsia’ or ‘monochromatism’ (58). Progressive cone dystrophies are a group of clinically heterogeneous disorders. Patients with these diseases exhibit progressive loss of visual acuity and color vision, together with photophobia and nystagmus, in their late childhood or early adult life (59). Psychophysical and electrophysiological examinations show abnormal cone function while rod function is intact (58). The mechanisms underlying the pathophysiology of cone dystrophies are still poorly understood.

Functional characterization of disease-associated mutations in genes encoding CNG channel subunits can provide insight into the molecular mechanisms and pathogenicity of photoreceptor

degeneration. Studies of retinitis pigmentosa (RP)-associated mutations in the rod CNGA1 subunit suggest that some mutations may lead to absence of functional CNG channels at the plasma membrane (12, 40, 61). Similarly, an achromatopsia associated frame-shift mutation in the gene encoding the cone photoreceptor CNGB3 subunit (31, 60) results in a truncated form of the subunit unable to form functional heteromeric channels with CNGA3 subunits (48). This suggests that properly assembled heteromeric channels are critical for normal cone function and survival. Studies also show that an achromatopsia-associated missense mutation in the CNGB3 subunit (S435F) alters the gating properties of heteromeric channels when co-expressed with CNGA3 subunits (44, 48).

Recently, 51 mutations have been identified in the gene encoding the human CNGA3 subunit of cone photoreceptor CNG channels and linked to achromatopsia and progressive cone dystrophy (32, 68). Three of these mutations are present in patients with severe progressive cone dystrophy: R277C (in the S4 domain), N471S (in C-linker region) and R563H (in cyclic nucleotide-binding domain (CNBD)) (Fig. 1A). An important step towards understanding the development of this disease is to determine how individual mutations alter the functional properties of CNG channels and how abnormal channel function may lead to cone photoreceptor degeneration.

Here we report the functional consequences of three progressive cone dystrophy-associated mutations in CNGA3 subunits. Our results suggest that these mutations disrupt plasma membrane localization, impair channel protein post-translational modification and/or alter the gating properties of cone CNG channels, thus leading to abnormal cone photoreceptor function

and ultimately, degeneration.

MATERIALS AND METHODS

Mutagenesis and functional expression. For heterologous expression in *Xenopus laevis* oocytes, the coding sequence for human CNGA3 (71) was subcloned into pGEMHE (38), and an amino-terminal tag with green fluorescent protein (GFP) was generated as described previously (47). The human CNGB3 clone was isolated from human retinal cDNA and also subcloned into pGEMHE (47, 48). Mutations in the CNGA3 coding sequence were engineered using overlapping PCR mutagenesis (25, 55). All mutations and the fidelity of PCR-amplified cassettes were confirmed by automated DNA sequencing. For expression studies, identical amounts of cDNA were linearized using *Sph*I or *Nhe*I, and capped mRNA was transcribed *in vitro* using the T-7 RNA polymerase mMessage mMachine kit (Ambion, Austin, TX). mRNA concentrations and relative amounts were determined by denaturing gel electrophoresis and 1D image analysis software (Kodak, NY), and spectrophotometry.

Oocytes were isolated as previously described (64, 72) and microinjected with a fixed amount of mRNA for all constructs (~5 ng). For efficient generation of heteromeric channels, the ratio of wild type or mutant CNGA3 mRNA to CNGB3 mRNA was 1:5 (49). Oocytes were incubated in ND96 (96 mM NaCl, 2mM KCl, 1.8 mM $CaCl_2$, 1 mM $MgCl_2$, and 5 mM HEPES, pH 7.6, supplemented with 10 μg/ml gentamycin). For some experiments, oocytes were incubated in ND96 that also contained 5 μM tunicamycin (EMD Bioscience Inc. La Jolla, CA).

Electrophysiology. Two to 7 days after microinjection of mRNA, patch-clamp experiments were performed in the inside-out configuration with an Axopatch 200B amplifier (Axon Instruments, Foster City, CA). Recordings were made at 20–23 °C. Data were acquired using Pulse software

(HEKA Elektronik, Lambrecht, Germany). Current traces were elicited by voltage steps from a holding potential of 0 mV to +80 mV, then to -80 mV and back to 0 mV. Initial pipette resistances were 0.4–0.8 MΩ. Intracellular and extracellular solutions contained 130 mM NaCl, 0.2 mM EDTA, and 3 mM HEPES (pH 7.2). Intracellular solutions were changed using an RSC-160 rapid solution changer (Molecular Kinetics, Pullman, WA). Currents in the absence of cyclic nucleotide were subtracted. For channel activation by cGMP or cAMP, dose-response data were fitted to the Hill equation, $I/I_{max} = ([cNMP]^h/(K_{1/2}{}^h + [cNMP]^h))$, where I is the current amplitude, I_{max} is the maximum current elicited by saturating concentration of ligand, [cNMP] is the ligand concentration, $K_{1/2}$ is the apparent ligand affinity, and h is the Hill slope. For current block by tetracaine, data were fitted to a modified Hill equation in the form $I_{tetracaine}/I = (K_{1/2}{}^h/(K_{1/2}{}^h + [tetracaine]^h))$. To confirm the formation of heteromeric CNGB3 plus CNGA3 channels, we measured sensitivity to block by 25 μM L-*cis*-diltiazem (RBI, Natick, MA) applied to the intracellular face of the patch in the presence of 1 mM cGMP. Data were analyzed using Igor (Wavemetrics, Lake Oswego, OR), SigmaPlot, and SigmaStat (SPSS Inc.). All values are reported as the mean ± S.E. of n experiments (patches) unless otherwise indicated. Statistical significance was determined using a Student's t test or Mann-Whitney rank sum test, and a p value of < 0.05 was considered significant.

To describe the gating of homomeric CNGA3 channels, we used a simplified linear allosteric model where independent ligand-binding steps are followed by a single allosteric transition from the liganded but closed state to the open state (18, 23, 36, 64):

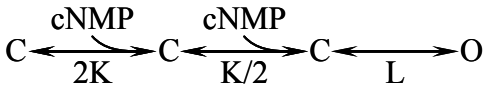

In this kinetic scheme, K is the equilibrium constant for the initial binding of cyclic nucleotide and L is the equilibrium constant of the allosteric conformational transition. We used the local anesthetic tetracaine (Sigma, St. Louis, MO), a known state-dependent blocker of CNG channels that binds to closed channels with nearly a thousand fold greater affinity compared to open channels (18), to investigate the altered gating properties of mutant homomeric channels. By applying a saturating concentration of cGMP (fully ligand-bound state), we isolated the allosteric conformational change associated with channel opening. Tetracaine sensitivity is a reporter for this equilibrium; thus, channels that spend more time in the open state are less sensitive to tetracaine block. We calculated the equilibrium constant for the allosteric transition (L) for cGMP-bound channels using the equation of Fodor and coworkers (18):

$$L_{cG} = \frac{K_{Do} \times (K_{1/2\ Tet} - K_{Dc})}{K_{Dc} \times (K_{Do} - K_{1/2\ Tet})}$$

Here, K_{Dc} (220 nM) and K_{Do} (170 μM) are dissociation constants for tetracaine binding to closed or open channels, respectively (18). L for cAMP-bound channels was determined using the relative agonist efficacy of cAMP compared to cGMP. K was determined from fits of the simple allosteric model described above to the dose-response data, using L values calculated from tetracaine apparent affinity and relative agonist efficacy. The free energy differences for L and for K were calculated as $\Delta G_X = -RT \times \ln (X)$. Also, $\Delta\Delta G = \Delta G_{mutant} - \Delta G_{wt}$. Tetracaine apparent affinity was not used to analyze the gating properties of heteromeric channels, since CNGB3 subunits lack the negatively-charged residue in the pore thought to be critical for state-

dependent binding of tetracaine (17) and tetracaine binding to channels containing CNGB3 subunits has not been characterized. Thus, the model of Fodor and coworkers (18) is not expected to apply to this channel type.

Confocal Microscopy. As described previously (48), confocal images of oocytes expressing GFP-tagged CNGA3 were obtained using a Bio-Rad MRC-1024 confocal laser-scanning system and a krypton-argon laser with a Nikon Eclipse TE 300 inverted microscope and 10x objective. Four days after injection of mRNA, oocytes expressing homomeric or heteromeric channels were placed in borosilicate coverglass chambers such that the equator was approximately perpendicular to the plane of imaging. GFP fluorescence was determined using an excitation wavelength of 488 nm and a 522 DF 32 emission filter. Laser intensity, pinhole aperture, and photo-multiplier gain were the same for all experiments. Images were analyzed using NIH ImageJ software. Surface fluorescence for each oocyte was determined from an area within the animal hemisphere, representing approximately 5% of the circumference in a single plane, and expressed as intensity of signal per unit area. Background fluorescence was determined for an equivalent area using a blank region of the same image and subtracted. Values were reported as the mean ± S.E. of *n* oocytes tested.

Protein Biochemistry. To assess the overall abundance and processing of CNGA3 subunits expressed in *Xenopus* oocytes, we used Western blot analysis of proteins from oocytes expressing GFP-tagged CNGA3. Oocyte lysates were prepared as previously described (47, 53, 54). Briefly, oocytes were placed in lysis buffer containing 20 mM Hepes (pH = 7.5), 150 mM NaCl, 5 mM EDTA, 0.5% Triton X-100 (Surfact-Amps X-100, Pierce, Rockford, IL) and a

protease inhibitor cocktail (Roche Applied Science, Indianapolis, IN). Oocytes were subjected to trituration followed by cup sonication, repeated a total of three times. The soluble cell lysate was then separated from yolk and other insoluble material by centrifugation at 20,000 g and 4 °C for 10 min, repeated three times. Lysate representing approximately one oocyte per lane was loaded and separated by SDS-PAGE using NuPage 4–12% Tris acetate gels (Invitrogen, Carlsbad, CA). Proteins were then transferred to nitrocellulose membrane using the NuPage transfer buffer system (Invitrogen). Immunoblots were blocked by 5% nonfat dry milk in TTBS buffer (Tris-buffered saline with 0.1% Tween-20 (BIO-RAD)) for 2 hours, and then probed with anti-GFP *Aequorea victoria* peptide polyclonal antibody (Clontech, Palo Alto, CA) at a concentration of 1:2500 in TTBS buffer with 1% nonfat dry milk. GFP-tagged channel subunits were visualized using SuperSignal West Dura substrate (Pierce) and autoradiography film (Kodak X-Omat Blue XB-1, Eastman Kodak Co.). The approximate molecular weights of the GFP-tagged subunits were estimated using protein standards (SeeBlue Plus2, Invitrogen). The relative amounts of CNGA3 protein (band density) for all GFP-A3 immunoreactive bands (glycosylated and unglycosylated) were estimated using NIH ImageJ software. To verify that approximately equal amounts of total protein were loaded per lane, the same blots were probed with MAB1501 pan-actin antibody (Chemicon International, Temecula, CA). The variation in actin signal between lanes, determined by densitometry, was less than ± 10% (n = 4 immunoblots).

RESULTS

Functional Expression and Plasma Membrane Targeting of Mutant Human CNGA3 Subunit

To investigate the effect of progressive cone dystrophy-associated mutations on plasma membrane localization of homomeric and heteromeric channels, we introduced these mutations into cDNA encoding GFP tagged human CNGA3 subunits (71) and expressed mutant or wild type CNGA3 subunits alone or together with the human CNGB3 subunits (31, 47, 60) in *Xenopus* oocytes.

Surface membrane fluorescence levels in oocytes were determined by confocal microscopy after 4 days of incubation. Figure 1B and C show representative confocal images and relative surface membrane fluorescence levels (F) normalized to that of wild type homomeric CNGA3 channels. For both homomeric and heteromeric channels, cell surface expression levels were significantly reduced ($p < 0.01$) for R277C ($F_{homo} = 0.06 \pm 0.01$, n = 39; $F_{hetero} = 0.04 \pm 0.01$, n = 26) and R563H ($F_{homo} = 0.15 \pm 0.04$, n = 42; $F_{hetero} = 0.12 \pm 0.02$, n = 26) (Fig. 1B, C) compared to the corresponding wild-type channels. Surprisingly, N471S did not interfere with plasma membrane localization of homomeric or heteromeric channels. Maximum patch current (I_{max}) levels, determined by patch-clamp recording at a saturating concentration of cGMP (1 mM), were consistent with the observed plasma membrane fluorescence levels (Fig. 1C). Compared to wild-type channels, mean I_{max} for both homomeric and heteromeric channels was reduced for R563H-containing channels (n = 12 to 13, $p < 0.01$) but not changed significantly for N471S-containing channels. No current was elicited by a saturating concentration of cGMP for R277C-containing channels. These results suggest that R277C and R563H mutations impaired the

plasma membrane expression of cone CNG channel subunits.

Cone dystrophy mutations altered CNG channel protein processing

There are two possible explanations for the reduced plasma-membrane localization observed for R277C and R563H subunits. One is that protein folding and/or stability are impaired by the mutations. Another possibility is that the channel proteins are not properly assembled and/or targeted to the plasma membrane. To address these possibilities, we conducted Western blot analysis of oocyte lysates. Immunoblots revealed a reduction in overall protein amount and a change in the processing and maturation of R277C subunits (Fig. 2A, B). The reduced protein levels for R277C compared to wild-type subunits (Fig. 2A, B) indicate that the mutation disrupted channel biogenesis and/or stability, which likely accounts for much of the reduction in cell-surface expression of these subunits (Fig. 1). In contrast, R563H subunits exhibited only a slight reduction in protein levels (that was not statistically significant), suggesting that this mutation primarily impaired plasma membrane targeting of CNGA3 subunits. Confocal images of intact oocytes display GFP-tagged subunits located at the surface membrane but not the fraction of subunits that remain intracellular (see ref (75)). Thus, compared to wild-type and N471S subunits, there is a much larger fraction of R563H subunits that are retained intracellularly and/or retrieved to intracellular compartments.

In addition to the overall reduction in amount of CNGA3 protein for R277C (Fig. 2A, B), the upper molecular weight bands evident for wild-type subunits were also reduced or absent. As shown previously, the generation of mature channels by bovine CNGA1 or CNGA3 subunits is associated with a series of post-translational modifications involving glycosylation (13, 53).

To confirm that the upper molecular weight bands observed here represented glycosylated CNGA3 subunits, oocytes expressing wild type homomeric and heteromeric CNG channels were treated with tunicamycin, a known *N*-acetylglucosaminase inhibitor that prevents protein glycosylation (56) (Fig. 2C). As anticipated, tunicamycin-treated groups lacked the upper molecular weight bands evident in non-treated groups, indicating that these upper molecular weight bands represented N-glycosylated subunits. Impaired N–glycosylation of mutant CNGA3 subunits suggests that the cone dystrophy-associated R277C mutation disrupted CNG channel post-translational processing and maturation.

Altered gating properties of homomeric CNGA3 channels

The electrophysiological properties of the channels were investigated using patch-clamp recording. Since CNGA3 subunits can form functional homomeric channels when expressed alone, we first examined the effect of these three mutations on the behavior of homomeric channels. Expression of R277C subunits alone did not give rise to cyclic nucleotide-dependent currents even after application of a saturating concentration of cGMP, suggesting that R277C subunits did not form functional CNG channels. Homomeric channels containing N471S or R563H mutations exhibited cyclic nucleotide-activated currents (Fig. 3A) with properties that differed from wild-type channels. Cyclic AMP is a partial agonist for recombinant and native rod and cone photoreceptor CNG channels, exhibiting a lower efficacy compared to cGMP (29). The initial binding of cAMP is comparable to that of cGMP, but cAMP is much less capable of promoting channel opening once bound (23). For both mutant channels, the relative agonist efficacy for channel activation by a saturating concentration of cAMP compared with maximal

activation by cGMP ($I_{max,\ cAMP}/I_{max,\ cGMP}$) was increased significantly (N471S: 0.35 ± 0. 12, n = 18, $p < 0.01$; R563H: 0.64 ± 0.20, n = 12, $p < 0.01$) compared to wild-type channels (0.12 ± 0.01, $n = 23$) (Fig. 3A, B). Furthermore, we calculated the apparent ligand affinity ($K_{1/2}$) for cGMP and cAMP by fitting the Hill equation to the dose-response relationships for activation of channels formed by wild type or mutant subunits (Fig. 3C). The results demonstrated a significant increase in apparent affinity for both cGMP and cAMP with R563H ($K_{1/2,\ cGMP}$ = 3.28 ± 0.63 μM, h = 1.7 ± 0.2; $K_{1/2,\ cAMP}$ = 0.64 ± 0.09 mM, h = 1.1 ± 0.2; $n = 13$, $p < 0.01$) and an increase in the apparent affinity for cGMP with N471S ($K_{1/2,\ cGMP}$ = 5.76 ± 1.66 μM, h = 2.0 ± 0.3, $n = 19$, $p < 0.01$) compared with activation of wild type homomeric channels ($K_{1/2,\ cGMP}$ = 9.26 ± 1.77 μM, h = 1.9 ± 0.06; $K_{1/2,\ cAMP}$ = 1.07 ± 0.27 mM h = 1.0 ± 0.2; $n = 18$) (Fig. 3D, E). The Hill coefficients (h) showed no significant change compared to that of wild-type channels. These results suggest that the N471S and R563H mutations made the channel more sensitive to activation by cyclic nucleotide.

The observed increase in ligand sensitivity for mutant channels might result from an increase in the channel's ability to bind ligand (affinity), or an increased ability to couple ligand binding to the allosteric conformational change associated with channel opening (efficacy), or both. To quantify the altered gating properties of mutant homomeric channels, we applied the local anesthetic tetracaine, a known closed-state blocker of CNG channels (17, 18), in the presence of a saturating concentration of cGMP (fully ligand-bound state). Channels that are less sensitive to tetracaine block spend more time in the open state. Under these conditions, we calculated the equilibrium constant for the allosteric transition associated with channel opening

(L) and for the initial binding of ligand (K) using a simple allosteric model (18, 23, 36) described in the methods. Consistent with this model and similar to previous results for CNGA1, CNGA2 and A1/A2 chimeric channels (18), wild type and mutant CNGA3 channels (particularly with mutations outside the cyclic nucleotide-binding domain) exhibit an inverse relationship between cGMP apparent affinity and tetracaine apparent affinity (data not shown).

Figure 4A illustrates block of wild type and mutant CNG channels (in 1 mM cGMP) by 50 μM tetracaine. We calculated tetracaine apparent affinity ($K_{1/2,\ tetracaine}$) by fitting the dose-response relationships with a modified Hill equation as described in the methods (Fig. 4B). Compared to wild type homomeric channels ($K_{1/2,\ tetracaine}$ = 55.2 ± 5.3 μM, n = 6), N471S exhibited a statistically significant decrease in tetracaine apparent affinity ($K_{1/2,\ tetracaine}$ = 102.4 ± 12 μM, n = 8, $p < 0.05$), suggesting that this mutant subunit generated channels that spent more time in the open state compared to wild-type channels. R563H-containing channels also exhibited an decrease in tetracaine apparent affinity ($K_{1/2,\ tetracaine}$ = 76 ± 9.6 μM, n = 5), but this change was not statistically significant ($p = 0.078$).

Figure 5 summarizes the changes in free energy difference ($\Delta\Delta G = \Delta G_{mutant} - \Delta G_{wt}$), determined for the equilibrium constants K and L, relative to those of the wild-type channels ($\Delta G_{L,\ cGMP}$ = -3.42 ± 0.2 kcal/mol, $\Delta G_{L,\ cAMP}$ = 1.09 ± 0.4 kcal/mol; $\Delta G_{K,\ cGMP}$ = -5.03 ± 0.1 kcal/mol, $\Delta G_{K,\ cAMP}$ = -4.50 ± 0.2 kcal/mol, n = 6). A significant decrease ($p < 0.05$ or $p < 0.01$) in the free energy difference of the allosteric transition promoted by cyclic nucleotides ($\Delta\Delta G_L <$ 0) was observed for both N471S and R563H compared to wild type channels (Fig. 5B). The effect of N471S on L was largely independent of which ligand was bound (no significant

difference between $\Delta\Delta G_L$ for cGMP and cAMP, $p = 0.911$), consistent with a change in the intrinsic gating properties of the channels (9). The free energy difference of initial ligand binding (ΔG_K) was not significantly changed for N471S compared to wild type ($p = 0.76$ for cGMP and $p = 0.18$ for cAMP, Fig. 5C), as expected for a mutation located outside of the ligand binding domain (discussed by Colquhoun (9); but see also (45)). In contrast, R563H, which is located within the ligand binding domain, exhibited a ligand-specific effect on the free energy difference for L ($p < 0.01$, comparing $\Delta\Delta G_L$ for cGMP and cAMP): R563H significantly decreased ΔG_L for cAMP-bound channels, yet had no significant effect on cGMP-bound channels ($p = 0.073$ compared to wild type) (Fig. 5B). R563H also exhibited a ligand-specific change in ΔG_K ($p < 0.01$ comparing $\Delta\Delta G_K$ for cGMP and cAMP): a significant decrease for cGMP ($p < 0.01$), and no significant effect for cAMP ($p = 0.76$) compared to wild type (Fig. 5C). Thus, initial ligand binding of cGMP to the channels was enhanced by R563H. The decreased free energy difference for the initial ligand binding step and/or the allosteric transition is consistent with the view that both N471S and R563H mutations make channel opening more favorable.

Effect of cone dystrophy mutations on the gating properties of heteromeric channels

While the CNGA3 subunit itself can form functional homomeric channels, native CNG channels in cone photoreceptors are thought to be heteromeric proteins composed of CNGA3 and CNGB3 subunits. To investigate the possible functional consequences of these mutations in heteromeric channels, we co-expressed mutant CNGA3 subunits with CNGB3 subunits in oocytes. To confirm that mutant CNGA3 subunits can form functional heteromeric channels, we

used the channel blocker L-*cis*-diltiazem. For recombinant CNG channels, sensitivity to block by L-*cis*-diltiazem depends on the presence of CNGB3 or CNGB1 subunits (6, 21, 34, 47). L-*cis*-diltiazem sensitivity was determined by comparing currents elicited by a saturating concentration of cGMP in the presence or absence of L-*cis*-diltiazem ($I_{diltiazem}/I$). Consistent with previous studies (47), currents for wild type heteromeric channels were blocked by 25 μM L-*cis*-diltiazem ($I_{diltiazem}/I$ = 0.43 ± 0.06, n = 8) while wild type homomeric channels were insensitive ($I_{diltiazem}/I$ = 0.95 ± 0.01, n = 6) (Fig. 6). Both N471S and R563H-containing heteromeric channels were sensitive to L-*cis*-diltiazem block (for N471S, $I_{diltiazem}/I$ = 0.45 ± 0.17, n = 7, $p < 0.01$; for R563H, $I_{diltiazem}/I$ = 0.46 ± 0.1, n = 12, $p < 0.01$), indicating that these mutant CNGA3 subunits can form functional heteromeric channels when co-expressed with CNGB3 subunits. Similar to experiments performed with homomeric channels, R277C-containing CNGA3 subunits did not generate cyclic nucleotide-dependent currents following application of 1 mM cGMP when co-expressed with CNGB3, indicating that R277C subunits cannot form functional heteromeric channels (Fig. 1C).

Electrophysiological measurements demonstrated that R563H containing heteromeric channels exhibited a significant increase in the relative agonist efficacy of cAMP ($I_{max\ cAMP}/I_{max\ cGMP}$ = 0.79 ± 0.15, n = 12, $p < 0.01$) compared to wild type heteromeric channel ($I_{max\ cAMP}/I_{max\ cGMP}$ = 0.39 ±0.07, n = 8) (Fig. 7A, B). An increase in apparent affinity for cGMP was also observed for both mutant channel subunits (N471S: $K_{1/2,\ cGMP}$ = 12.6 ± 1.5 μM, n = 7, $p < 0.01$; R563H: $K_{1/2,\ cGMP}$ = 9.44 ± 3.8 μM, n = 11, $p < 0.01$) (Fig. 7C, D) compared to wild-type channels ($K_{1/2,\ cGMP}$ = 15.4 ± 1.5 μM, n = 9). Heteromeric channels containing N471S did not

show a significant change in relative agonist efficacy or in apparent affinity for cAMP compared to the wild-type channels, suggesting partial functional rescue when co-assembled with CNGB3 subunits. These results indicate that the cone dystrophy-associated mutations N471S and R563H altered the gating properties of the heteromeric channels when co-assembled with CNGB3 subunits. The altered gating properties of the heteromeric channels, which more closely resemble the native condition, provide further evidence supporting the pathogenicity of these mutations.

DISCUSSION

We have functionally characterized severe progressive cone dystrophy-associated mutations in the gene encoding the human CNGA3 subunit (R277C, N471S and R563H) and have identified changes in the cell surface expression levels and the gating properties of mutant channels. CNGA3 subunits with N471S and R563H mutations formed functional homomeric and heteromeric channels with altered gating properties, displaying increased apparent affinity for cyclic nucleotide and increased relative agonist efficacy for cAMP compared to cGMP. In contrast, R277C subunits did not form functional homomeric or heteromeric channels. Our studies are the first functional characterization of *CNGA3* mutations linked to progressive cone dystrophy. Most of the disease-associated mutations identified so far in *CNGA3* (40 out of 51) are missense mutations at positions that are highly conserved among orthologous sequences (27, 32, 68). It seems that there is little tolerance for structural changes at these positions in the subunits.

Loss of function phenotype

Previous studies indicate that a lack of functional CNG channels in the photoreceptor outer segment might contribute to cell degeneration. In this regard, animal models provide a useful tool for investigating the molecular mechanisms of photoreceptor degeneration. CNGA3 knockout mice exhibit a progressive loss of cone photoresponse and cone photoreceptor degeneration with intact rod function (1). This animal model closely resembles human progressive cone dystrophy. Recent studies in CNGA3/Rho double-knockout mice demonstrate normal retinal morphology and photoresponse in neonatal mice, yet rod and cone photoreceptor

degeneration is observed after four weeks and progresses to almost complete loss of photoreceptors by three months (8). In addition to CNGA3-deficient mice, constitutive closure of CNG channels in continuous light resembles a loss-of-function phenotype. Progressive photoreceptor degeneration is evident in this model as well (15). Functional studies of disease-associated mutations also provide evidence that the lack of functional CNG channels in the photoreceptor outer segment might contribute to photoreceptor degeneration. Five mutations in the gene encoding the rod channel CNGA1 subunit have been linked to autosomal recessive retinitis pigmentosa (arRP), a disease characterized by impaired rod function and rod degeneration (12). Three of the five mutations are null mutations, which result in the synthesis of non-functional channel proteins lacking the transmembrane domain and the pore forming region (E76stop and K139stop) or no protein synthesis in the case of complete gene deletion (12). The other two mutations (S316F and frame shift R654 (1-bp del)) are thought to encode functional channels with impaired targeting to the plasma membrane (12, 40, 61).

In the present study, R277C and R563H mutations significantly reduced the availability of functional CNG channels at the cell surface, resembling a "loss of function" phenotype. R277C, which is also a common mutation in patients with complete achromatopsia, did not form functional homomeric or heteromeric channels. This result can be accounted for primarily by a reduction in overall protein levels and in subunit maturation. Recently, several mutations in the S4 domain of bovine CNGA3 subunits also have been shown to impair subunit stability and/or processing (13). R563H subunits exhibited decreased plasma membrane localization as well, but without a significant reduction in CNGA3 protein levels or maturation. The functional

consequences of these mutations *in vitro* suggest that high-level expression of working CNG channels in the outer segment is critical for photoreceptor survival.

There are various mechanisms by which disease-associated mutations can impair channel protein expression at the plasma membrane, chief among these are mutations in the channel subunits that may disturb protein folding or assembly, destabilize synthesized proteins, and/or disrupt targeting to the plasma membrane. The precise cellular mechanisms involved in photoreceptor degeneration for loss-of-function phenotypes remain to be determined. It has been shown previously that the survival of central nervous system neurons, including retinal ganglion cells, depends on physiological levels of electrical activity (42). Does the decrease or absence of functional CNG channel expression at the plasma membrane lead to a lack of proper levels of electrical activity, thus resulting in photoreceptor degeneration? Further work needs to be done to address these questions.

Gain of function phenotype

Functional characterization of cone CNG channels containing mutations N471S or R563H in the CNGA3 subunits revealed an increase in apparent ligand affinity and in relative agonist efficacy of cAMP compared to cGMP, consistent with a "gain-of-function" phenotype. A similar gain-of-function phenotype has been found for an achromatopsia-associated mutation in CNGB3 subunits (S435F) that alters the gating properties of heteromeric channels when co-expressed with CNGA3 subunits (48). CNGB3 S435F containing heteromeric channels exhibit a greater than 4-fold increase in cAMP sensitivity and a modest increase in apparent affinity for cGMP. In addition, single channel recordings reveal an increase in open probability, in the

presence of saturating concentration of cGMP or cAMP, for mutant heteromeric channels (48). In the present study, the increased ligand sensitivity and efficacy suggests that in cone photoreceptors of patients with progressive cone dystrophy, CNG channels may fail to close appropriately as intracellular cGMP (or cAMP) levels fall in response to light stimulation.

What is the likely relationship between the altered gating properties of the mutant channels in the native cone outer segment membrane and cone photoreceptor degeneration? Under physiological conditions, the free intracellular cGMP level is estimated to be about 2-4 μM (50, 51), which is well below the concentration of cGMP expected to elicit half-maximal activation of the channels ($K_{1/2}$). This cGMP concentration is sufficient to keep only a small fraction (less than 10%) of the channels in the open state in the absence of light (51). A light induced rapid decrease (10-20 fold) of intracellular cGMP thus results in closure of nearly all of the channels (51). Because the sensitivity of channels to cGMP is so steep, even slight alterations in apparent ligand affinity may be detrimental to normal physiological function. For example, if the apparent affinity of the channels for cGMP changes (e.g., the $K_{1/2}$ decreases from ~15 μM (wild-type channel) to ~9 μM (mutant channel)) (see Fig. 7C), nearly ten-fold more channels may be open in the absence of light and/or channels may not close properly in response to the fall in cGMP levels after light activation. Similar gain-of-function phenotypes have been discovered for mutations in the genes encoding other critical proteins involved in phototransduction, adaptation and recovery processes. Recent evidence indicates that mutations which produce constitutively active guanylyl cyclase (30, 46, 62), or loss of rod cGMP PDE activity (10, 26, 63), result in increased intracellular cGMP levels. Increased intracellular cGMP, similar to an

increase in channel sensitivity to cGMP, might lead to inappropriate opening of the channels. Thus, more Ca^{2+} will enter the photoreceptors through the CNG channels.

We hypothesize that "calcium overload" might explain photoreceptor degeneration with gain of function mutations in cone CNG channels. One important aspect of CNG channel function is that it is the major pathway for Ca^{2+} entry into the outer segment of photoreceptors (16). It is possible that sustained opening of CNG channels, resulting from increased ligand affinity, may lead to abnormally high levels of intracellular Ca^{2+}. Calcium is a critical second messenger that participates in several intracellular signaling pathways. Numerous studies have reported that a sustained elevation of intracellular Ca^{2+} could result in apoptotic cell death (reviewed by Choi (7) and Leist & Nicotera (43)). In the retina, for example, sustained elevation of intracellular Ca^{2+} has been shown to trigger rod photoreceptor apoptosis and retinal degeneration (19). This general mechanism may underlie other photoreceptor degenerative diseases such as progressive cone dystrophy. At the same time, it has been suggested recently that apoptosis may be triggered by a sustained decrease in intracellular Ca^{2+} levels in rod photoreceptors (reviewed in (35)), as is expected for rod channel mutations presenting loss-of-function phenotypes. Consistent with this hypothesis, Rpe65-knockout mice, which exhibit impaired synthesis of the opsin chromophore ligand 11-cis-retinal, display light-independent signaling by unliganded opsin, diminished intracellular calcium in photoreceptors and progressive photoreceptor degeneration (69). Furthermore, mutations in Rpe65 have been linked to Leber congenital amaurosis (LCA), a severe, early-onset retinal dystrophy (41).

For the cone dystrophy-associated mutations characterized in the present study, both loss-

of-function and gain-of-function effects were observed. For example, R563H produced both a reduction in channel cell surface expression levels and an increase in ligand sensitivity. The profound decrease in functional expression for R563H, however, suggests that loss-of-function might play a greater part in the pathogenicity of the disease in these patients than the change in channel gating.

Assembly of N471S containing CNGA3 subunits with wild type CNGB3 subunits rescued most functional properties associated with wild type heteromeric channels, with the exception of increased apparent cGMP affinity. The discrepancy between the mild functional change for N471S-containing heteromeric channels and the severe cone degeneration typically exhibited by patients with this disease implies that an additional, as yet unidentified mutation is necessary for disease progression (68). This additional mutation may be present in a non-coding region of *CNGA3*, in *CNGB3,* or in some other allele or modifying gene. Thus, further mutation screening is needed to address the possible phenotype-genotype inconsistency indicated here.

Overall, our results suggest that complex effects may arise from the progressive cone dystrophy-associated mutations in CNGA3 subunits, including a decrease in plasma membrane localization of the channels, a disruption of channel protein biogenesis, processing and/or stability, and an increase in ligand sensitivity and/or efficacy. These results provide insight into the molecular pathophysiology and possible cellular mechanisms underlying cone photoreceptor degenerative disease. How these mutations affect cone photoreceptor function and survival *in vivo* remains an important yet unanswered question that needs to be addressed using animal models.

ACKNOWLEDGEMENTS

We thank E. Rich for expert technical support, and C. Peng, S. Bright, and E. Rich for critical comments on the manuscript. We are also grateful to Prof. K.-W. Yau for providing the cDNA clone for human CNGA3.

GRANTS

This work was supported by a grant from NIH/NEI (R01-EY12836) to MDV.

REFERENCES

1. **Biel M, Seeliger M, Pfeifer A, Kohler K, Gerstner A, Ludwig A, Jaissle G, Fauser S, Zrenner E, and Hofmann F.** Selective loss of cone function in mice lacking the cyclic nucleotide-gated channel CNG3. *Proc Natl Acad Sci U S A* 96: 7553-7557., 1999.
2. **Bonigk W, Altenhofen W, Muller F, Dose A, Illing M, Molday RS, and Kaupp UB.** Rod and cone photoreceptor cells express distinct genes for cGMP-gated channels. *Neuron* 10: 865-877, 1993.
3. **Bonigk W, Bradley J, Muller F, Sesti F, Boekhoff I, Ronnett GV, Kaupp UB, and Frings S.** The native rat olfactory cyclic nucleotide-gated channel is composed of three distinct subunits. *J Neurosci* 19: 5332-5347, 1999.
4. **Bradley J, Li J, Davidson N, Lester HA, and Zinn K.** Heteromeric olfactory cyclic nucleotide-gated channels: a subunit that confers increased sensitivity to cAMP. *Proc Natl Acad Sci U S A* 91: 8890-8894, 1994.
5. **Bradley J, Reuter D, and Frings S.** Facilitation of calmodulin-mediated odor adaptation by cAMP-gated channel subunits. *Science* 294: 2176-2178, 2001.
6. **Chen TY, Peng YW, Dhallan RS, Ahamed B, Reed RR, and Yau KW.** A new subunit of the cyclic nucleotide-gated cation channel in retinal rods. *Nature* 362: 764-767, 1993.
7. **Choi DW.** Calcium and excitotoxic neuronal injury. *Ann N Y Acad Sci* 747: 162-171, 1994.
8. **Claes E, Seeliger M, Michalakis S, Biel M, Humphries P, and Haverkamp S.** Morphological characterization of the retina of the CNGA3(-/-)Rho(-/-) mutant mouse lacking functional cones and rods. *Invest Ophthalmol Vis Sci* 45: 2039-2048, 2004.
9. **Colquhoun D.** Binding, gating, affinity and efficacy: the interpretation of structure-activity relationships for agonists and of the effects of mutating receptors. *Br J Pharmacol* 125: 924-947, 1998.
10. **Danciger M, Heilbron V, Gao YQ, Zhao DY, Jacobson SG, and Farber DB.** A homozygous PDE6B mutation in a family with autosomal recessive retinitis pigmentosa. *Mol Vis* 2: 10, 1996.
11. **Dhallan RS, Yau KW, Schrader KA, and Reed RR.** Primary structure and functional expression of a cyclic nucleotide-activated channel from olfactory neurons. *Nature* 347: 184-187, 1990.
12. **Dryja TP, Finn JT, Peng YW, McGee TL, Berson EL, and Yau KW.** Mutations in the gene encoding the alpha subunit of the rod cGMP-gated channel in autosomal recessive retinitis pigmentosa. *Proc Natl Acad Sci U S A* 92: 10177-10181, 1995.
13. **Faillace MP, Bernabeu RO, and Korenbrot JI.** Cellular Processing of Cone Photoreceptor Cyclic GMP-gated Ion Channels: A ROLE FOR THE S4 STRUCTURAL MOTIF. *J Biol Chem* 279: 22643-22653, 2004.
14. **Fain GL.** Dark adaptation. *Prog Brain Res* 131: 383-394, 2001.

15. **Fain GL and Lisman JE.** Light, Ca2+, and photoreceptor death: new evidence for the equivalent-light hypothesis from arrestin knockout mice. *Invest Ophthalmol Vis Sci* 40: 2770-2772, 1999.
16. **Finn JT, Grunwald ME, and Yau KW.** Cyclic nucleotide-gated ion channels: an extended family with diverse functions. *Annu Rev Physiol* 58: 395-426, 1996.
17. **Fodor AA, Black KD, and Zagotta WN.** Tetracaine reports a conformational change in the pore of cyclic nucleotide-gated channels. *J Gen Physiol* 110: 591-600, 1997.
18. **Fodor AF, Gordon SE, and Zagotta WN.** Mechanism of tetracaine block of cyclic nucleotide-gated channels. *J Gen Physiol* 109: 3-14, 1997.
19. **Fox DA, Poblenz AT, and He L.** Calcium overload triggers rod photoreceptor apoptotic cell death in chemical-induced and inherited retinal degenerations. *Ann N Y Acad Sci* 893: 282-285, 1999.
20. **Gegenfurtner KR and Kiper DC.** Color vision. *Annu Rev Neurosci* 26: 181-206, 2003.
21. **Gerstner A, Zong X, Hofmann F, and Biel M.** Molecular cloning and functional characterization of a new modulatory cyclic nucleotide-gated channel subunit from mouse retina. *J Neurosci* 20: 1324-1332, 2000.
22. **Gordon SE and Zagotta WN.** A histidine residue associated with the gate of the cyclic nucleotide-activated channels in rod photoreceptors. *Neuron* 14: 177-183, 1995.
23. **Gordon SE and Zagotta WN.** Localization of regions affecting an allosteric transition in cyclic nucleotide-activated channels. *Neuron* 14: 857-864, 1995.
24. **Gray-Keller MP and Detwiler PB.** The calcium feedback signal in the phototransduction cascade of vertebrate rods. *Neuron* 13: 849-861, 1994.
25. **Ho SN, Hunt HD, Horton RM, Pullen JK, and Pease LR.** Site-directed mutagenesis by overlap extension using the polymerase chain reaction. *Gene* 77: 51-59, 1989.
26. **Huang SH, Pittler SJ, Huang X, Oliveira L, Berson EL, and Dryja TP.** Autosomal recessive retinitis pigmentosa caused by mutations in the alpha subunit of rod cGMP phosphodiesterase. *Nat Genet* 11: 468-471, 1995.
27. **Johnson S, Michaelides M, Aligianis IA, Ainsworth JR, Mollon JD, Maher ER, Moore AT, and Hunt DM.** Achromatopsia caused by novel mutations in both CNGA3 and CNGB3. *J Med Genet* 41: e20, 2004.
28. **Kaupp UB, Niidome T, Tanabe T, Terada S, Bonigk W, Stuhmer W, Cook NJ, Kangawa K, Matsuo H, and Hirose T.** Primary structure and functional expression from complementary DNA of the rod photoreceptor cyclic GMP-gated channel. *Nature* 342: 762-766, 1989.
29. **Kaupp UB and Seifert R.** Cyclic nucleotide-gated ion channels. *Physiol Rev* 82: 769-824, 2002.
30. **Kelsell RE, Gregory-Evans K, Payne AM, Perrault I, Kaplan J, Yang RB, Garbers DL, Bird AC, Moore AT, and Hunt DM.** Mutations in the retinal guanylate cyclase (RETGC-1) gene in dominant cone-rod dystrophy. *Hum Mol Genet* 7: 1179-1184, 1998.
31. **Kohl S, Baumann B, Broghammer M, Jagle H, Sieving P, Kellner U, Spegal R, Anastasi M, Zrenner E, Sharpe LT, and Wissinger B.** Mutations in the CNGB3 gene

encoding the beta-subunit of the cone photoreceptor cGMP-gated channel are responsible for achromatopsia (ACHM3) linked to chromosome 8q21. *Hum Mol Genet* 9: 2107-2116., 2000.

32. **Kohl S, Marx T, Giddings I, Jagle H, Jacobson SG, Apfelstedt-Sylla E, Zrenner E, Sharpe LT, and Wissinger B.** Total colourblindness is caused by mutations in the gene encoding the alpha-subunit of the cone photoreceptor cGMP-gated cation channel. *Nat Genet* 19: 257-259, 1998.
33. **Korenbrot JI and Rebrik TI.** Tuning outer segment Ca2+ homeostasis to phototransduction in rods and cones. *Adv Exp Med Biol* 514: 179-203., 2002.
34. **Korschen HG, Illing M, Selfert R, Sesti F, Williams A, Gotzes S, Colville C, Muller F, Dose A, Godde M, Molday L, Kaupp UB, and Molday RS.** A 240 kDa protein represents the complete β subunit of the cyclic nucleotide-gated channel from rod photoreceptor. *Neuron* 15: 627-636, 1995.
35. **Lem J and Fain GL.** Constitutive opsin signaling: night blindness or retinal degeneration? *Trends Mol Med* 10: 150-157, 2004.
36. **Li J, Zagotta WN, and Lester HA.** Cyclic nucleotide-gated channels: structural basis of ligand efficacy and allosteric modulation. *Q Rev Biophys* 30: 177-193, 1997.
37. **Liman ER and Buck LB.** A second subunit of the olfactory cyclic nucleotide-gated channel confers high sensitivity to cAMP. *Neuron* 13: 611-621, 1994.
38. **Liman ER, Tytgat J, and Hess P.** Subunit stoichiometry of a mammalian K+ channel determined by construction of multimeric cDNAs. *Neuron* 9: 861-871, 1992.
39. **Liu DT, Tibbs GR, and Siegelbaum SA.** Subunit stoichiometry of cyclic nucleotide-gated channels and effects on Subunit Order on Channel Function. *Neuron* 16: 983-990, 1996.
40. **Mallouk N, Ildefonse M, Pages F, Ragno M, and Bennett N.** Basis for intracellular retention of a human mutant of the retinal rod channel alpha subunit. *J Membr Biol* 185: 129-136, 2002.
41. **Marlhens F, Bareil C, Griffoin JM, Zrenner E, Amalric P, Eliaou C, Liu SY, Harris E, Redmond TM, Arnaud B, Claustres M, and Hamel CP.** Mutations in RPE65 cause Leber's congenital amaurosis. *Nat Genet* 17: 139-141., 1997.
42. **Meyer-Franke A, Kaplan MR, Pfrieger FW, and Barres BA.** Characterization of the signaling interactions that promote the survival and growth of developing retinal ganglion cells in culture. *Neuron* 15: 805-819, 1995.
43. **Nicotera P and Orrenius S.** The role of calcium in apoptosis. *Cell Calcium* 23: 173-180, 1998.
44. **Okada A, Ueyama H, Toyoda F, Oda S, Ding WG, Tanabe S, Yamade S, Matsuura H, Ohkubo I, and Kani K.** Functional role of hCngb3 in regulation of human cone cng channel: effect of rod monochromacy-associated mutations in hCNGB3 on channel function. *Invest Ophthalmol Vis Sci* 45: 2324-2332, 2004.

45. **Paoletti P, Young EC, and Siegelbaum SA.** C-Linker of Cyclic Nucleotide-gated Channels Controls Coupling of Ligand Binding to Channel Gating. *J Gen Physiol* 113: 17-34, 1999.
46. **Payne AM, Downes SM, Bessant DA, Taylor R, Holder GE, Warren MJ, Bird AC, and Bhattacharya SS.** A mutation in guanylate cyclase activator 1A (GUCA1A) in an autosomal dominant cone dystrophy pedigree mapping to a new locus on chromosome 6p21.1. *Hum Mol Genet* 7: 273-277, 1998.
47. **Peng C, Rich ED, Thor CA, and Varnum MD.** Functionally important calmodulin binding sites in both N- and C-terminal regions of the cone photoreceptor cyclic nucleotide-gated channel CNGB3 subunit. *J Biol Chem* 278: 24617-24623, 2003.
48. **Peng C, Rich ED, and Varnum MD.** Achromatopsia-associated mutation in the human cone photoreceptor cyclic nucleotide-gated channel CNGB3 subunit alters the ligand sensitivity and pore properties of heteromeric channels. *J Biol Chem* 278: 34533-34540, 2003.
49. **Peng C, Rich ED, and Varnum MD.** Subunit configuration of heteromeric cone cyclic nucleotide-gated channels. *Neuron* 42: 401-410, 2004.
50. **Pugh ENJ and Lamb TD.** Amplification and kinetics of the activation steps in phototransduction. *Biochim Biophys Acta* 1141: 111-149, 1993.
51. **Pugh ENJ and Lamb TD.** Cyclic GMP and calcium: the internal messengers of excitation and adaptation in vertebrate photoreceptors. *Vision Res* 30: 1923-1948, 1990.
52. **Rattner A, Sun H, and Nathans J.** Molecular genetics of human retinal disease. *Annu Rev Genet* 33: 89-131, 1999.
53. **Rho S, Lee HM, Lee K, and Park C.** Effects of mutation at a conserved N-glycosylation site in the bovine retinal cyclic nucleotide-gated ion channel. *FEBS Lett* 478: 246-252, 2000.
54. **Rosenbaum T and Gordon SE.** Dissecting intersubunit contacts in cyclic nucleotide-gated ion channels. *Neuron* 33: 703-713, 2002.
55. **Sambrook J, Fritsch EF, and Maniatis T.** *Molecular Cloning: A Laboratory Manual*: Cold Spring Harbor Laboratory Press, 1989.
56. **Santacruz-Toloza L, Huang Y, John SA, and Papazian DM.** Glycosylation of shaker potassium channel protein in insect cell culture and in Xenopus oocytes. *Biochemistry* 33: 5607-5613, 1994.
57. **Sautter A, Zong X, Hofmann F, and Biel M.** An isoform of the rod photoreceptor cyclic nucleotide-gated channel beta subunit expressed in olfactory neurons. *Proc Natl Acad Sci U S A* 95: 4696-4701, 1998.
58. **Simunovic MP and Moore AT.** The cone dystrophies. *Eye* 12: 553-565., 1998.
59. **Sloan LL and Feiock K.** Selective impairment of cone function. Perimetric techniques for its detection. *Mod Probl Ophthalmol* 11: 50-62, 1972.
60. **Sundin OH, Yang JM, Li Y, Zhu D, Hurd JN, Mitchell TN, Silva ED, and Maumenee IH.** Genetic basis of total colourblindness among the Pingelapese islanders. *Nat Genet* 25: 289-293, 2000.

61. **Trudeau MC and Zagotta WN.** An intersubunit interaction regulates trafficking of rod cyclic nucleotide-gated channels and is disrupted in an inherited form of blindness. *Neuron* 34: 197-207, 2002.
62. **Tucker CL, Woodcock SC, Kelsell RE, Ramamurthy V, Hunt DM, and Hurley JB.** Biochemical analysis of a dimerization domain mutation in RetGC-1 associated with dominant cone-rod dystrophy. *Proc Natl Acad Sci U S A* 96: 9039-9044, 1999.
63. **Valverde D, Solans T, Grinberg D, Balcells S, Vilageliu L, Bayes M, Chivelet P, Besmond C, Goossens M, Gonzalez-Duarte R, and Baiget M.** A novel mutation in exon 17 of the beta-subunit of rod phosphodiesterase in two RP sisters of a consanguineous family. *Hum Genet* 97: 35-38, 1996.
64. **Varnum MD, Black KD, and Zagotta WN.** Molecular mechanism for ligand discrimination of cyclic nucleotide-gated channels. *Neuron* 15: 619-625, 1995.
65. **Varnum MD and Zagotta WN.** Subunit interactions in the activation of cyclic nucleotide-gated channels. *Biophysical Journal* 70: 2667-2679, 1996.
66. **Weitz D, Ficek N, Kremmer E, Bauer PJ, and Kaupp UB.** Subunit Stoichiometry of the CNG Channel of Rod Photoreceptors. *Neuron* 36: 881-889, 2002.
67. **Weyand I, Godde M, Frings S, Weiner J, Muller F, Altenhofen W, Hatt H, and Kaupp UB.** Cloning and functional expression of a cyclic-nucleotide-gated channel from mammalian sperm. *Nature* 368: 859-863, 1994.
68. **Wissinger B, Gamer D, Jagle H, Giorda R, Marx T, Mayer S, Tippmann S, Broghammer M, Jurklies B, Rosenberg T, Jacobson SG, Sener EC, Tatlipinar S, Hoyng CB, Castellan C, Bitoun P, Andreasson S, Rudolph G, Kellner U, Lorenz B, Wolff G, Verellen-Dumoulin C, Schwartz M, Cremers FP, Apfelstedt-Sylla E, Zrenner E, Salati R, Sharpe LT, and Kohl S.** CNGA3 mutations in hereditary cone photoreceptor disorders. *Am J Hum Genet* 69: 722-737, 2001.
69. **Woodruff ML, Wang Z, Chung HY, Redmond TM, Fain GL, and Lem J.** Spontaneous activity of opsin apoprotein is a cause of Leber congenital amaurosis. *Nat Genet* 35: 158-164, 2003.
70. **Yau KW and Baylor DA.** Cyclic GMP-activated conductance of retinal photoreceptor cells. *Annu Rev Neurosci* 12: 289-327, 1989.
71. **Yu WP, Grunwald ME, and Yau KW.** Molecular cloning, functional expression and chromosomal localization of a human homolog of the cyclic nucleotide-gated ion channel of retinal cone photoreceptors. *FEBS Lett* 393: 211-215, 1996.
72. **Zagotta WN, Hoshi T, and Aldrich RW.** Gating of single Shaker potassium channels in Drosophila muscle and in Xenopus oocytes injected with Shaker mRNA. *Proc Natl Acad Sci U S A* 86: 7243-7247, 1989.
73. **Zagotta WN and Siegelbaum SA.** Structure and Function of Cyclic Nucleotide-Gated Channels. *Annu Rev Neurosci* 19: 235-263, 1996.
74. **Zheng J, Trudeau MC, and Zagotta WN.** Rod Cyclic Nucleotide-Gated Channels Have a Stoichiometry of Three CNGA1 Subunits and One CNGB1 Subunit. *Neuron* 36: 891-896, 2002.

75. **Zheng J and Zagotta WN.** Stoichiometry and assembly of olfactory cyclic nucleotide-gated channels. *Neuron* 42: 411-421., 2004.
76. **Zhong H, Molday LL, Molday RS, and Yau KW.** The heteromeric cyclic nucleotide-gated channel adopts a 3A:1B stoichiometry. *Nature* 420: 193-198, 2002.

Figure 1

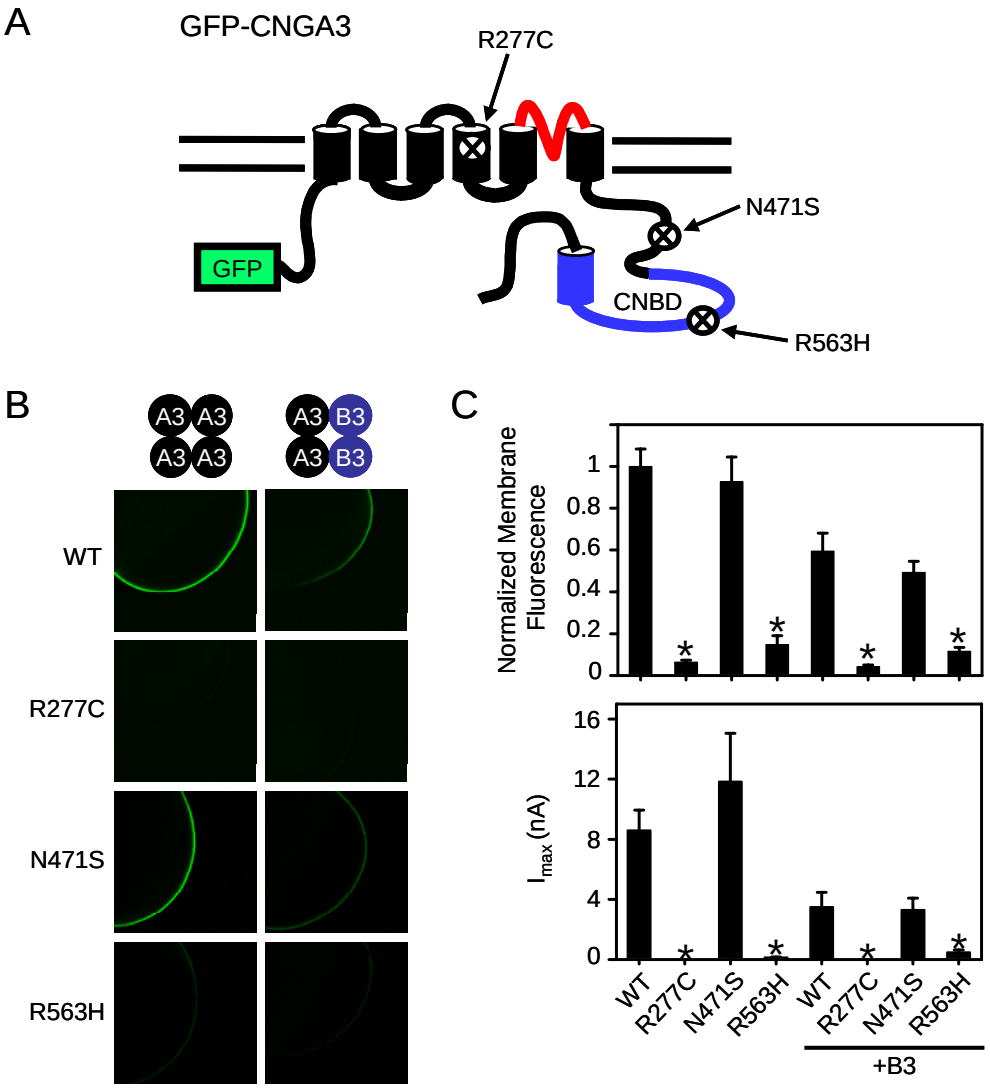
A
GFP-CNGA3
R277C
N471S
GFP
CNBD
R563H
B
A3 A3
A3 A3
A3 B3
A3 B3
WT
R277C
N471S
R563H
C
Normalized Membrane Fluorescence
1
0.8
0.6
0.4
0.2
0
I_{max} (nA)
16
12
8
4
0
WT
R277C
N471S
R563H
WT
R277C
N471S
R563H
+B3

Figure 2

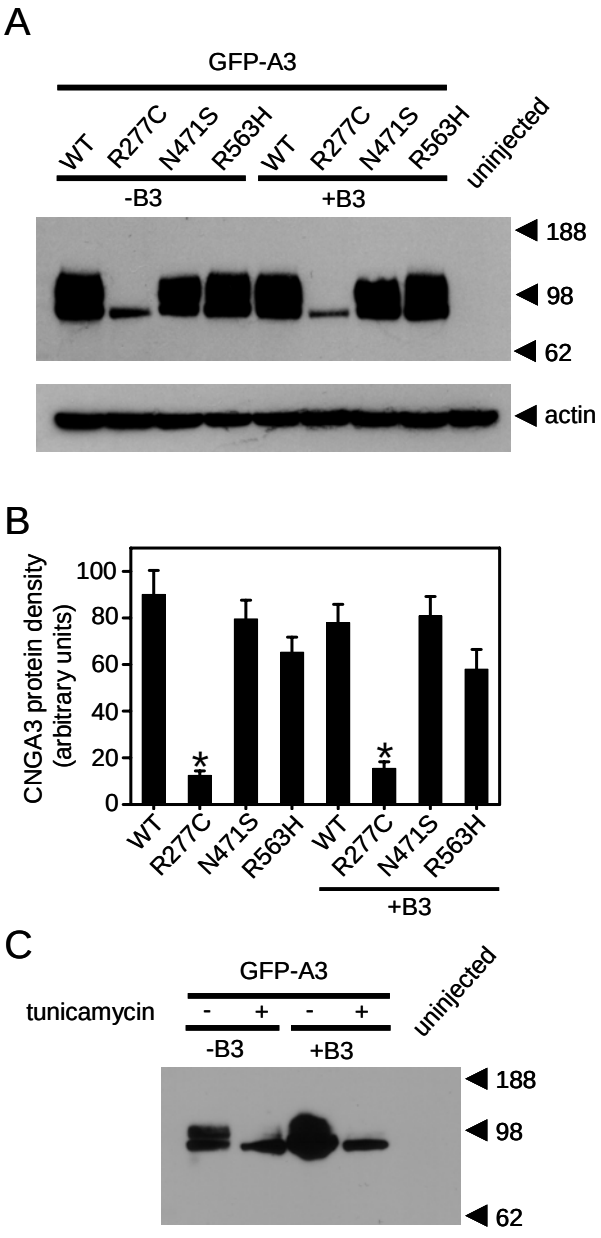
A
GFP-A3
WT
R277C
N471S
R563H
WT
R277C
N471S
R563H
uninjected
-B3
+B3
188
98
62
actin
B
CNGA3 protein density (arbitrary units)
100
80
60
40
20
0
*
*
WT
R277C
N471S
R563H
WT
R277C
N471S
R563H
+B3
C
GFP-A3
tunicamycin
-
+
-
+
uninjected
-B3
+B3
188
98
62

Figure 3

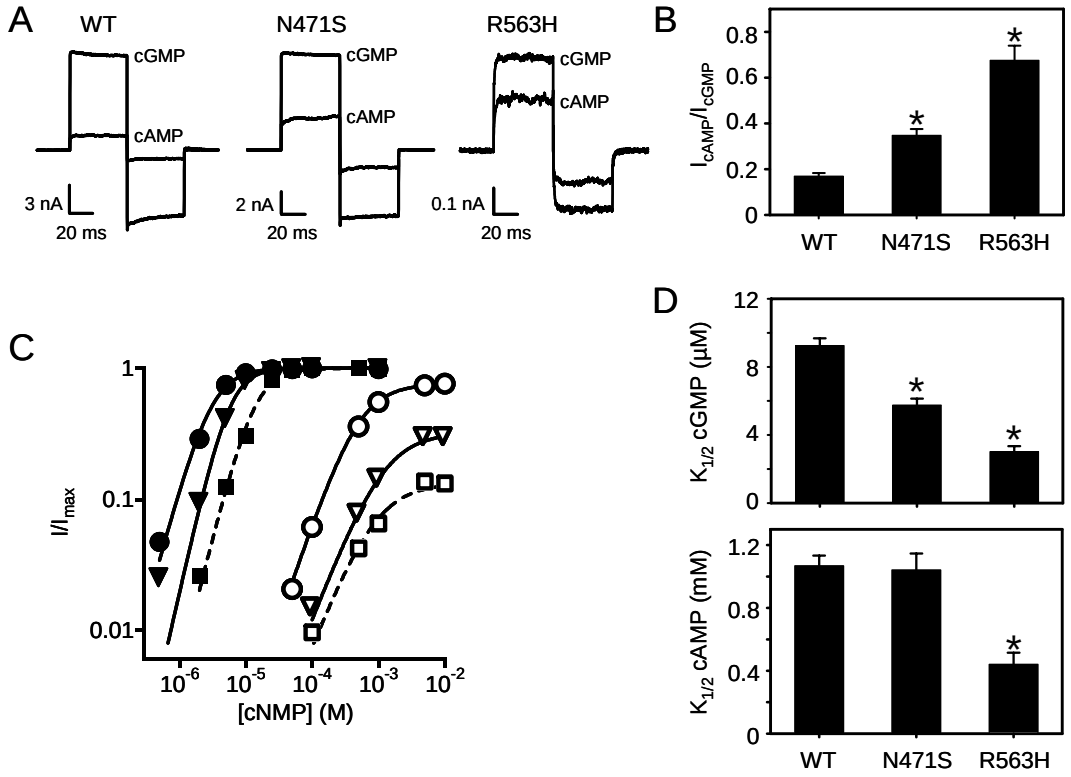
A
WT
N471S
R563H
cGMP
cAMP
3 nA
20 ms
2 nA
20 ms
0.1 nA
20 ms
B
I_{cAMP}/I_{cGMP}
0.8
0.6
0.4
0.2
0
WT
N471S
R563H
C
I/I_{max}
1
0.1
0.01
10^{-6}
10^{-5}
10^{-4}
10^{-3}
10^{-2}
[cNMP] (M)
D
$K_{1/2}$ cGMP (µM)
12
8
4
0
$K_{1/2}$ cAMP (mM)
1.2
0.8
0.4
0
WT
N471S
R563H

Figure 4

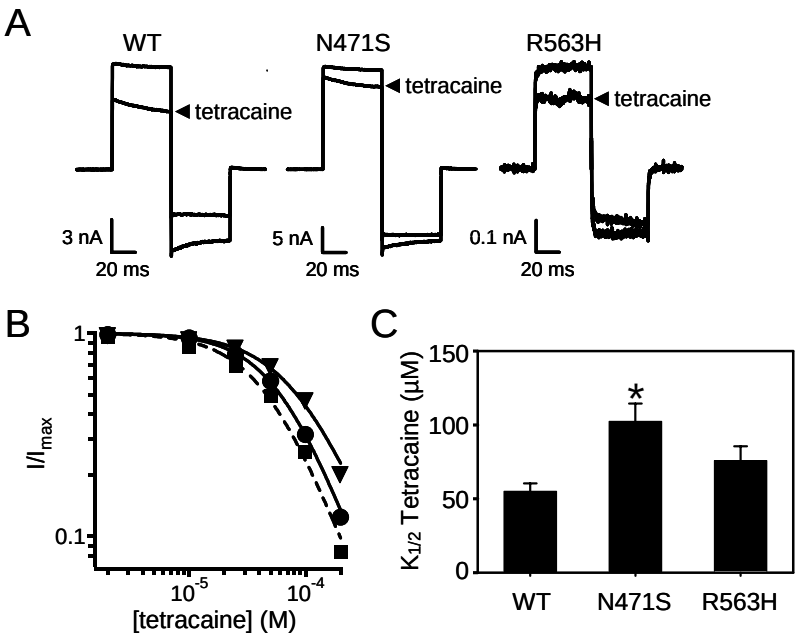
A
WT
N471S
R563H
tetracaine
tetracaine
tetracaine
3 nA
20 ms
5 nA
20 ms
0.1 nA
20 ms
B
1
0.1
I/I_max
10^-5
10^-4
[tetracaine] (M)
C
150
100
50
0
K1/2 Tetracaine (μM)
*
WT
N471S
R563H

Figure 5

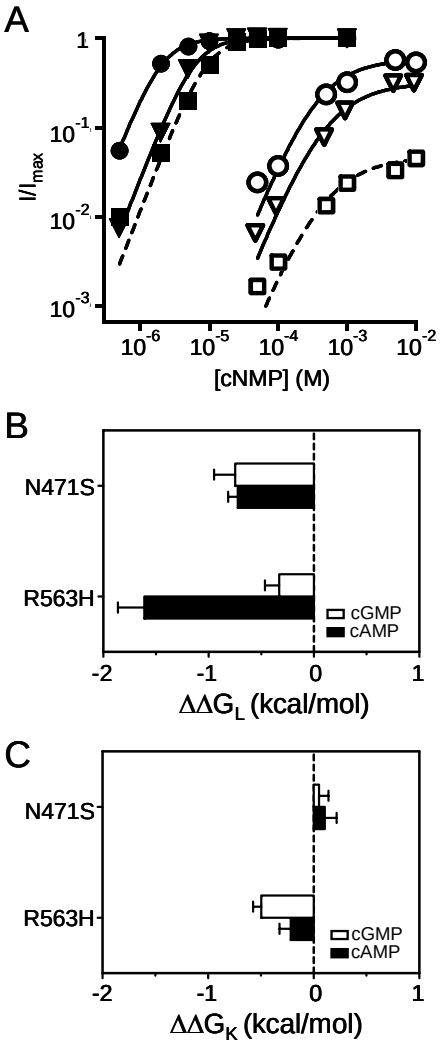
A
1
10-1
10-2
10-3
I/Imax
10-6
10-5
10-4
10-3
10-2
[cNMP] (M)
B
N471S
R563H
cGMP
cAMP
-2
-1
0
1
ΔΔGL (kcal/mol)
C
N471S
R563H
cGMP
cAMP
-2
-1
0
1
ΔΔGK (kcal/mol)

Figure 6


A
A3 (WT)
diltiazem
5 nA
20 ms
WT+B3
diltiazem
3 nA
20 ms
N471S+B3
diltiazem
3 nA
20 ms
R563H+B3
diltiazem
0.2 nA
20 ms
B
I diltiazem /I
1
0.8
0.6
0.4
0.2
0
*
*
*
A3 WT WT N471S R563H
B3 - + + +

Figure 7

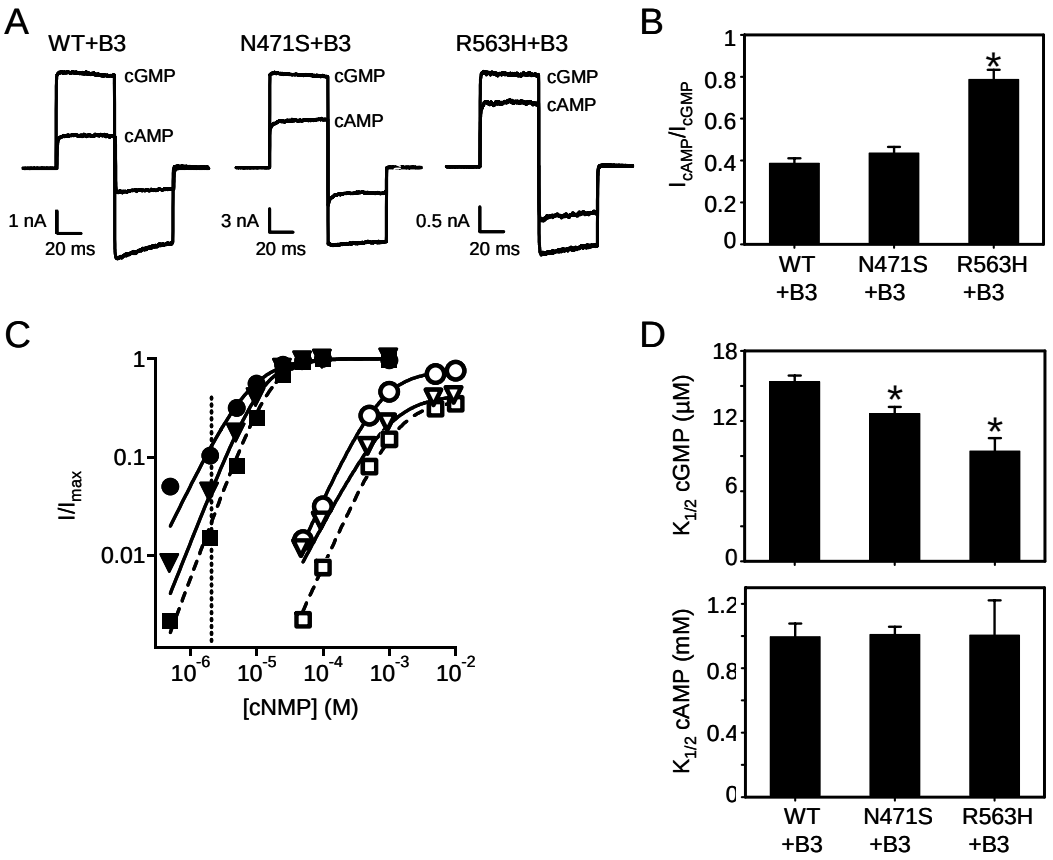
A
WT+B3
N471S+B3
R563H+B3
cGMP
cAMP
1 nA
20 ms
3 nA
20 ms
0.5 nA
20 ms
B
I_{cAMP}/I_{cGMP}
WT +B3
N471S +B3
R563H +B3
C
I/I_{max}
[cNMP] (M)
D
$K_{1/2}$ cGMP (μM)
$K_{1/2}$ cAMP (mM)
WT +B3
N471S +B3
R563H +B3

FIGURE LEGENDS

Fig. 1. Cone dystrophy-associated mutations impaired functional expression and plasma membrane localization of CNGA3 channel subunits. *A*: cartoon showing the transmembrane topology of green fluorescent protein (GFP)-tagged CNGA3 subunit, indicating the general location of progressive cone dystrophy-associated mutations (×) described in this study: R277C (in the S4 domain), N471S (in C-linker region) and R563H (in the cyclic nucleotide-binding domain, CNBD). *B*: confocal images of *Xenopus* oocytes injected with mRNA encoding wild type (WT) or mutant GFP-tagged CNGA3 (A3) subunits alone or together with non-tagged CNGB3 (B3) subunits. The amount of A3 mRNA was held constant, and for co-injection the ratio of A3 to B3 mRNA was 1:5, a ratio that is effective for the formation of heteromeric channels (49). *C*: bar graph of surface fluorescence (upper graph, n = 25 to 50) and maximum patch current in 1 mM cGMP (lower graph, n = 7 to 19). The * indicates a statistically significant difference compared to WT homomeric (left) or heteromeric (right) channels ($p < 0.01$). The fluorescent signal was normalized to the mean surface fluorescence of oocytes expressing GFP-A3 alone from the same experimental group. For R277C, no cyclic nucleotide-dependent current was elicited by a saturating concentration of cGMP in the absence or presence of B3 subunits.

Fig. 2. Cone dystrophy-associated mutations reduced protein levels and impaired post-translational processing of A3 subunits. *A*: Western blot of protein lysates from oocytes

expressing GFP-A3 (WT or mutant) subunits alone or together with B3 subunits, probed with anti-GFP antibody (upper blot). Lysate from uninjected oocytes is shown at right. The same blot was probed with anti-actin antibody, demonstrating that similar amount of protein were loaded per lane (lower blot). *B*: bar graph showing the relative density of CNGA3 protein bands (mature plus immature) determined by densitometry analysis (n = 6). The * indicates a statistically significant difference compared to WT homomeric (left) or heteromeric (right) channels ($p < 0.01$). *C*: Western blot, using anti-GFP antibody, of protein lysates from oocytes expressing WT homomeric or heteromeric channels after three day incubation in the absence or presence of 5 μM tunicamycin.

Fig. 3. Cone dystrophy-associated mutations altered the gating properties of homomeric channels. *A*: representative current traces are shown for homomeric (A3) CNG channels after activation by saturating concentrations of cGMP (1 mM) or cAMP (10 mM). Current traces were elicited by the voltage protocol described in methods. *B*: bar graph for the relative agonist efficacy of cAMP compared to cGMP (n = 12 to 18, * indicates $p < 0.01$ compared to WT). *C*: representative dose-response relationships for activation of WT (squares), N471S (triangles) or R563H (circles) homomeric A3 channels by cGMP (closed symbols) or cAMP (open symbols). Currents were normalized to the maximum cGMP current. Continuous curves (dashed line for wild type) represent fits of the dose-response relation to the Hill equation as indicated in the methods. Parameters for each patch shown here were as followed: for wild type, $K_{1/2,\ cGMP}$ = 13.6 μM, h = 2.02; $K_{1/2,\ cAMP}$ = 1.0 mM, h = 1.33; for N471S, $K_{1/2,\ cGMP}$ = 5.72 μM, h = 2.05; $K_{1/2,}$

$_{cAMP}$ = 1.10 mM, h = 1.31; for R563H, $K_{1/2, cGMP}$ = 3.01 μM, h = 1.86; $K_{1/2, cAMP}$ = 0.57 mM, h = 1.49. *D*: bar graphs showing the apparent ligand affinity ($K_{1/2}$) for cGMP (upper graph) and cAMP (lower graph), determined from fits of the dose-response relation to the Hill equation. Compared to WT A3 channels, both N471S and R563H exhibited a statistically significant increase in apparent cGMP affinity (n = 13 to 19, * represents $p < 0.01$ compared to WT). R563H also exhibited a statistically significant increase in apparent affinity for cAMP (n = 7 to 12, * represents $p < 0.01$ compared to WT).

Fig. 4. Cone dystrophy-associated mutations in homomeric channels altered sensitivity to tetracaine block. *A*: representative currents activated by 1 mM cGMP in the absence or presence of 50 μM tetracaine for A3 channels. *B*: representative dose-response relationships for tetracaine block of wild type (squares), N471S (triangles) or R563H (circles) homomeric A3 channels. Currents were normalized to the maximum cGMP current. Continuous curves represent fits of the dose-response relation to the modified Hill equation as indicated in the methods. Parameters for each patch shown here were as followed: $K_{1/2, wt}$ = 51.9 μM, h = 1.51; $K_{1/2, N471S}$ = 83.7 μM, h = 1.50; $K_{1/2, R563H}$ = 60.4 μM, h = 1.56. *C*: bar graph of the apparent affinity ($K_{1/2}$) for tetracaine block determined from fits of the dose-response relation to the modified Hill equation. Compared to wild type A3 channels, N471S exhibited a statistically significant decrease in $K_{1/2}$ for tetracaine (n = 5 to 11, * indicates $p < 0.05$).

Fig. 5. Cone dystrophy-associated mutations altered the free energy difference for channel

activation. *A*: representative dose-response relationships for activation of homomeric wild type (squares), N471S (triangles) or R563H (circles) channels by cGMP (open symbols) and cAMP (closed symbols). Currents were normalized to the maximum cGMP current. Continuous curves represent fits of the dose-response relationships with the simple allosteric model described in the methods. *B, C*: bar graphs are shown for the changes in the free energy difference by N471S (n = 8) and R563H (n = 5) compared to that of WT channels, of the allosteric transition (L) and the initial ligand binding step (K) for channel activation by cGMP (open bar) or cAMP (filled bar).

Fig. 6. Mutant A3 subunits formed functional heteromeric channels when co-expressed with B3 subunits. *A*: representative currents elicited by 1 mM cGMP in the absence or presence of 25 μM L-*cis*-diltiazem for homomeric or heteromeric channels. Sensitivity to block by L-*cis*-diltiazem indicates functional assembly with B3 subunits. *B*: bar graph showing the ratio of the currents activated by 1 mM cGMP in the presence and absence of L-*cis*-diltiazem (n = 5 to 11, * indicates $p < 0.01$ compared to WT homomeric A3 channels).

Fig. 7. Cone dystrophy-associated mutations altered the gating properties of heteromeric channels. *A*: representative current traces for heteromeric A3+B3 channels activated by 1 mM cGMP or 10 mM cAMP. Traces were elicited by the voltage protocol described in the methods. *B*: bar graph for the relative agonist efficacy of cAMP compared to cGMP (n = 7 to 12, * indicates $p < 0.01$ compared to WT channels). *C*: representative dose-response relationships for wild type (squares), N471S (triangles) or R563H (circles) containing heteromeric channels

activated by cGMP (closed symbols) or cAMP (open symbols). Currents were normalized to the maximum cGMP current. Continuous curves (dashed line for wild type) represent fits of the dose-response relation to the Hill equation as indicated in the methods. Vertical dotted line indicates approximate physiological intracellular cGMP concentration in the dark, about 2 μM (50). Parameters for each patch shown here were as followed: for wild type, $K_{1/2,\ cGMP}$ = 17.3 μM, h = 1.89; $K_{1/2,\ cAMP}$ = 1.35 mM, h = 1.31; for N471S, $K_{1/2,\ cGMP}$ = 12.7 μM, h = 1.67; $K_{1/2,\ cAMP}$ = 1.07 mM, h = 1.18; for R563H, $K_{1/2,\ cGMP}$ = 8.18 μM, h = 1.40; $K_{1/2,\ cAMP}$ = 0.67 mM, h = 1.48. *D*: bar graphs of the apparent ligand affinity ($K_{1/2}$) for cGMP (upper graph) and cAMP (lower graph), determined from the fits of the dose-response relation to the Hill equation (n = 7 to 11, * indicates $p < 0.01$ compared to WT channels).

CHAPTER TWO

Disease-associated mutations in CNGB3 promote cytotoxicity in photoreceptor derived 661W cells

Chunming Liu[1,2] and Michael D. Varnum[1,2,3]

From the [1]Department of Veterinary and Comparative Anatomy, Pharmacology and Physiology, [2]Program in Neuroscience and [3]Center for Integrative Biotechnology, Washington State University, Pullman, WA

Corresponding Author: Michael D. Varnum, Department of Veterinary and Comparative Anatomy, Pharmacology and Physiology, Washington State University, Box 646520, Pullman, WA 99164; varnum@wsu.edu.

Abbreviations: CNG, cyclic nucleotide-gated; CNBD, cyclic nucleotide binding domain; CPT-cGMP, 8-(4-chlorophenylthio) guanosine 3', 5'-cyclic monophosphate; CPT-cAMP, 8-(4-chlorophenylthio) adenosine 3', 5'-cyclic monophosphate; LDH, lactate dehydrogenase.

Word count: 4,293

Supported by grants from the National Institutes of Health (EY12836) and the Adler Foundation (to MDV), and by a Poncin Award (to CL).

Running Title: CNGB3 mutations promote cytotoxicity in photoreceptor-derived cells

PURPOSE. To determine if achromatopsia associated F525N and T383fsX mutations in the CNGB3 subunit of cone photoreceptor cyclic nucleotide-gated (CNG) channels increase susceptibility to cell death in photoreceptor derived 661W cells.

METHODS. 661W cells were transfected with cDNA encoding wild type (WT) CNGA3 subunits plus WT or mutant CNGB3 subunits, and incubated with membrane permeable CNG channel activators 8-(4-chlorophenylthio) guanosine 3', 5'-cyclic monophosphate (CPT-cGMP) or 8-(4-chlorophenylthio) adenosine 3', 5'-cyclic monophosphate (CPT-cAMP). Cell viability under these conditions was determined by measuring lactate dehydrogenase (LDH) release. Channel ligand sensitivity was calibrated by patch-clamp recording after expression of WT or mutant channels in *Xenopus* oocytes.

RESULTS. Co-expression of CNGA3 with CNGB3 subunits containing F525N or T383fsX mutations produced channels exhibiting increased apparent affinity for CPT-cGMP compared to WT channels. Consistent with these effects, cytotoxicity in the presence of 0.1 μM CPT-cGMP was enhanced relative to WT channels, and the increase in cell death was more pronounced for the mutation having the largest gain-of-function effect on channel gating, F525N. Increased susceptibility to cell death was prevented by application of CNG channel blockers L-*cis*-diltiazem (10 μM) or tetracaine (10 μM). The increased cytotoxicity was also found to be dependent on the presence of extracellular calcium.

CONCLUSIONS. These results indicate a connection between disease-associated mutations in cone CNG channel subunits, altered CNG channel-activation properties, and photoreceptor cytotoxicity. Rescue of cell viability via CNG channel block or removal of extracellular calcium

suggests that cytotoxicity in this model depends on calcium entry through hyperactive CNG channels.

Rod and cone photoreceptor cells are highly specialized to carry out their primary task: transforming absorbed light into electrical responses that can be processed and understood as vision by the central nervous system. Long-term perturbations in components of the signal transduction cascade, energy metabolism, or structural integrity within the photoreceptors or their supporting cells can increase the risk of photoreceptor cell death (see review in [1], [2] and [3]). The resulting loss of vision is one of the most common causes of disability. However, the exact cellular and molecular mechanisms by which mutations lead to photoreceptor cell death are not completely understood.

One critical component of the phototransduction cascade is the cyclic nucleotide-gated (CNG) channels in the outer segment plasma membrane of rods and cones. Closure of these channels converts the chemical signal (a fall in intracellular cGMP concentration) that is initiated by light absorption, into membrane hyperpolarization and decreased neurotransmitter release onto second order cells (reviewed in [4]). The specialized CNG channels of cone photoreceptors are composed of CNGA3 and CNGB3 subunits in a two plus two configuration around the central pore [5]. Mutations in the genes encoding these subunits have been linked to complete and incomplete achromatopsia [6-16], progressive cone dystrophy [10, 17], macular degeneration and macular malfunction [13]. Recent studies have determined how several disease-associated mutations in CNGA3 [14, 18-21] and CNGB3 [22-24] subunits alter the functional properties of recombinant cone CNG channels. Surprisingly, several mutations in CNGB3 have gain-of-function effects on channel gating [22, 23], producing CNG channels that are more sensitive to cGMP. How these gain-

of-function changes in CNG channel gating may lead to cone dysfunction and degeneration is a question that has not yet been addressed.

Since CNG channels are the main pathway for Ca^{2+} entry into the outer segment of photoreceptors [25, 26], we hypothesize that gain-of-function mutations in CNGB3 increase susceptibility to cell death via a Ca^{2+} overload mechanism. To address this issue we have utilized 661W cells as an *in vitro* model to investigate the effect of CNG channel mutations on cell viability. These cells exhibit many of the cellular and biochemical features of cone photoreceptor cells [27-29], but are reported to lack endogenous CNGA3 subunits [30]. In this study, we have found that two mutations in CNGB3 linked previously to achromatopsia, progressive cone dystrophy and/or macular degeneration increased susceptibility to cell death in the presence of a physiologically relevant concentration of channel activator. The increase in cytotoxicity associated with activation of mutant CNG channels was alleviated by application of CNG channel blockers or by removal of extracellular Ca^{2+}. This implies a connection between the altered gating properties of mutant CNG channels and photoreceptor cell death, providing insight into the cellular and molecular mechanisms underlying inherited retinal degeneration.

MATERIALS AND METHORDS:

Molecular biology. pGEMHE vector containing the coding sequence for WT or mutant human CNGA3 and CNGB3 subunits were obtained from previous studies [22, 23]. For expression in the mammalian cell line, cDNAs for CNGA3 and CNGB3 were subcloned into pOPRSVI vector using unique restriction enzymes. QuikChange Site-Directed Mutagenesis Kit (Stratagene) was then used to generate point mutations in CNGB3. All mutations were confirmed by DNA sequencing.

Functional expression in *Xenopus laevis* oocytes. For heterologous expression in *Xenopus laevis* oocytes, identical amounts of cDNA were linearized using *Sph*I or *Nhe*I, and capped mRNA was transcribed *in vitro* using the T-7 RNA polymerase mMessage mMachine kit (Ambion, Austin, TX). mRNA concentrations and relative amounts were determined by denaturing gel electrophoresis and 1D image analysis software (Kodak, NY), and spectrophotometry. Oocytes were isolated as previously described [31, 32] and microinjected with a fixed amount of mRNA for all constructs (approximately 5 ng of CNGA3 and 20 ng CNGB3, a ratio confirmed to efficiently generate heteromeric channels [5]). Oocytes were incubated in ND96 (96 mM NaCl, 2mM KCl, 1.8 mM $CaCl_2$, 1 mM $MgCl_2$, and 5 mM HEPES, pH 7.6, supplemented with 10 μg/ml gentamycin).

Electrophysiology. Two to seven days after microinjection of mRNA, patch-clamp experiments were performed in the inside-out configuration with an Axopatch 200B amplifier (Axon

Instruments, Foster City, CA). Recordings were made at 20–23 °C. Data were acquired using Pulse software (HEKA Elektronik, Lambrecht, Germany). Current traces were elicited by voltage steps from a holding potential of 0 mV to +80 mV, then to -80 mV and back to 0 mV. Initial pipette resistances were 0.4–0.8 megaohms. Intracellular and extracellular solutions contained 130 mM NaCl, 0.2 mM EDTA, and 3 mM HEPES (pH 7.2). Intracellular solutions were changed using an RSC-160 rapid solution changer (Molecular Kinetics, Pullman, WA). Currents in the absence of cyclic nucleotide were subtracted. For channel activation by CPT-cGMP or CPT-cAMP, dose-response data were fitted to the Hill equation, $I/I_{max} = ([cNMP]^h/(K_{1/2}{}^h + [cNMP]^h))$, where I is the current amplitude, I_{max} is the maximum current elicited by saturating concentration of ligand, [cNMP] is the ligand concentration, $K_{1/2}$ is the apparent ligand affinity, and h is the Hill slope. We measured sensitivity to block by tetracaine and L-*cis*-diltiazem (RBI, Natick, MA) applied to the intracellular face of the patch in the presence of 0.1 μM CPT-cGMP. Data were fitted with a modified Hill equation in the form $I_{blocker}/I = (K_{1/2}{}^h/(K_{1/2}{}^h + [blocker]^h))$. Data were analyzed using Igor (Wavemetrics, Lake Oswego, OR), SigmaPlot, and SigmaStat (SPSS Inc.). All values are reported as the mean ± S.E. of n experiments (patches) unless otherwise indicated. Statistical significance was determined using a Student's t test or Mann-Whitney rank sum test, and a p value of < 0.05 was considered significant.

Cell culture and transfection of complementary DNAs: The mouse 661W photoreceptor cell line used in this study was a generous gift from Dr. Al-Ubaidi (U of Oklahoma). 661W cells

were routinely maintained in Dulbecco's modified Eagle's medium (DMEM) supplemented with 10% fetal bovine serum (FBS) and 1% penicillin/streptomycin at 37°C in a humidified atmosphere of 5% CO2 and 95% air, and subcultured every 3–5 days. 661W cells were transfected with pOPRSVI plasmids encoding human cone CNG channel subunits using LipofectAMINE 2000 (Invitrogen Corp., Carlsbad, California). A reporter plasmid, a green fluorescent protein-expressing vector under a constitutive promoter, was transfected with the same condition each time to assess the transfection efficiency, and the pOPRSVI plasmid were transfected each time as control. The amounts of each vector were as follows (μg/10 cm^2 culture surface): 2 FLAG/GFP-hCNGA3 and 2 FLAG-hCNGB3 (or FLAG-hCNGB3-T383fsX, FLAG-hCNGB3-F525N), 4 GFP, 4 pOPRSVI.

Cell viability assays. For most of the studies, the lactate dehydrogenase (LDH) Cytotoxicity Detection Kit (Roche Applied Science, Indianapolis, IN) was used as per the manufacturer's protocol (see also [33]). Briefly, cultured 661W cells were transfected with desired plasmid constructs as described above and then plated in 96-well tissue culture plates at a density of approximately $8x10^3$ cells/well. 48 hours after transfection, cells were treated with various concentrations of CPT-cGMP (Sigma) and/or CPT-cAMP (Biolog, Germany), alone or together with tetracaine (Sigma) or L-*cis*-diltiazem (Sigma) in DMEM medium supplemented with 1% FBS for 24 hours in 37°C. Following treatment, half of the culture medium was transferred to another 96-well plate and LDH released into the culture medium was measured to assess the amount of damaged/dead cells. Cells in the original plate were then lysed and the total amount

of cellular LDH was assessed. Percentage of cytotoxicity was then calculated from the above measurements. For each of the experiment, results were normalized to the percentage of cytotoxicity in the untreated cells transfected with control pOPRSVI plasmid only.

The viability of 661W cells transfected with WT or mutant CNG channels was also assessed using the LIVE/DEAD Viability/Cytotoxicity Kit (Invitrogen) according to the manufacturer's protocol. Briefly, cells were transfected under the conditions described above and plated into 4-well multi-chamber glass slides (LabTek Inc, Campbell, California). At the end of cyclic nucleotide treatment, cells were washed with PBS three times and stained with 2 μM calcein AM and 4 μM ethidium homodimer-1 solution at room temperature for 30 minutes. Fluorescence confocal microscopy was then performed to visualize the live and dead cells.

Fluorescence confocal microscopy: Confocal microscopy of cells expressing CNG channel subunits was carried out at the Washington State University Franceschi Microscopy and Imaging Center. Images were obtained using a 10x objective on an Axiovert 200M inverted microscope equipped with a Zeiss LSM 510 confocal laser-scanning system and a krypton-argon laser. Fluorescence was measured using an excitation wavelength of 488 nm, and a 522 DF 32 emission filter for green fluorescence and 635 DF 32 emission filter for red fluorescence.

RESULTS

Disease-associated mutations in CNGB3 increase ligand sensitivity of channels.

Disease-associated mutations in the CNGB3 subunit of cone CNG channels have been shown previously to produce channels with gain-of-function changes in gating properties [22, 23]. Here we determined whether co-expression of mutant F525N or T383fsX CNGB3 subunits with WT CNGA3 subunits altered the sensitivity of the resulting channels to membrane-permeable analogues of cGMP and cAMP, 8-(4-chlorophenylthio) guanosine 3', 5'-cyclic monophosphate (CPT-cGMP) and 8-(4-chlorophenylthio) adenosine 3', 5'-cyclic monophosphate (CPT-cAMP), respectively. FLAG-tagged WT or mutant CNGB3 subunits were heterologously expressed together with human CNGA3 subunits in *Xenopus laevis* oocytes. Patch-clamp recordings were performed with excised membrane patches using the inside-out configuration; channels were activated by application of cyclic nucleotide-containing solutions to the intracellular face of the patch membrane (Fig. 1A). Maximum patch current density (I_{max} /area), determined at a saturating concentration of CPT-cGMP (4 μM), was not significantly altered by the mutations (WT: 55.1 ± 10.9 pA/μm^2, n = 13; T383fsX: 86.6 ± 17.0 pA/μm^2, n = 9; F525N: 80.3 ± 18.6 pA/μm^2, n = 15). This indicates that the amount of functional CNG channels at the plasma membrane was not reduced by these mutations.

The apparent CPT-cGMP affinity ($K_{1/2,\ CPT\text{-}cGMP}$) of WT and mutant heteromeric channels was determined by fits of the Hill equation to the dose-response relationships for channel activation. Compared to WT heteromeric channels ($K_{1/2,\ CPT\text{-}cGMP}$ = 254.0 ± 18.1 nM, h = 1.5 ± 0.05, n = 13),

channels formed after expression of CNGB3 T383fsX with CNGA3 subunits were more sensitive to ligand ($K_{1/2,\ CPT\text{-}cGMP}$ = 105.1 ± 7.3 nM, h = 2.2 ± 0.1, n = 8; $p < 0.01$) (Fig.1B). T383fsX likely represents a CNGB3 null mutation, producing only homomeric CNGA3 channels at the plasma membrane [23]. Consistent with this idea, homomeric CNGA3-only channels exhibited a similar apparent affinity for CPT-cGMP ($K_{1/2,\ CPT\text{-}cGMP}$ = 113.9 ± 7.9 nM, h = 2.2 ± 0.1, n = 9; data not shown). Channels containing CNGB3-F525N exhibited a larger increase in apparent ligand affinity ($K_{1/2,\ CPT\text{-}cGMP}$ = 86.8 ± 10.6 nM, h = 1.8 ± 0.04; $p < 0.01$) (Fig.1B), in agreement with previous studies using unmodified cGMP [22]. Overall, 8-pCPT modified cGMP was 80-100 fold more potent than unmodified cGMP [18, 23] for activation of cone CNG channels, similar to its increased potency with rod CNGA1 channels [34]. These results illustrate the functional disturbances produced by F525N or T383fsX mutations, and help calibrate the physiologically appropriate CPT-cGMP concentration range for cone CNG channel activation.

Disease-associated mutations in CNGB3 subunits increased susceptibility to cell death in photoreceptor-derived cell line.

We used a cone photoreceptor derived cell line (661W) to investigate the possible effects of mutant CNG channels on cell viability. 661W cells are a well-established model for photoreceptor viability studies [28, 35-38], and have been shown to express several markers characteristic of cone but not rod photoreceptors [27]. 661W cells were transiently transfected with WT or mutant CNGB3 subunits together with CNGA3 subunits, and treated with CPT-cGMP for 24 hours at concentrations ranging from 0.01 μM to 10 μM. An LDH-release assay was then

performed to assess cytotoxicity induced by activation of CNG channels. Results within each experiment were expressed as relative cytotoxicity calculated from normalization to percent cytotoxicity of untreated cells transfected with the pOPRSVI vector control alone. As summarized in Figure 2A, incubation of 0.1 μM CPT-cGMP with 661W cells expressing mutant CNG channels produced a significant increase in relative cytotoxicity (T383fsX: 1.26 ± 0.05, $p < 0.05$; F525N: 1.59 ± 0.05, $p < 0.01$) compared to WT channels (1.11 ± 0.04). The size of increase in relative cytotoxicity for the different channel mutations was in the same rank order as the increase in channel ligand sensitivity. In the absence of CPT-cGMP treatment, cells expressing channels with the F525N mutation also exhibited a slight increase in relative cytotoxicity (1.21 ± 0.03) compared to WT channels under these conditions (1.05 ± 0.03; $p < 0.01$), suggesting that activation of F525N-containing channels by endogenous cGMP increased susceptibility to cell death. No increase in relative cytotoxicity was observed at CPT-cGMP concentrations of 1 μM or greater (data not shown). Together, these results suggest a correlation between CNG channel activity and cell death.

To confirm the effects of mutant CNG channel subunits on photoreceptor viability, we also used an alternate assay (LIVE/DEAD Viability/Cytotoxicity Kit) to label live and dead cells. Cells were transfected with mutant or WT channels as described above; fluorescence microscopy was performed after 0.1 μM CPT-cGMP treatment and calcein AM and ethidium homodimer-1 staining of the transfected cells. As shown in Figure 3, CPT-cGMP treated cells expressing CNG channels with the F525N mutation exhibited more damaged/dead cells (red fluorescence)

and less intact/viable cells (green fluorescence) compared to cells expressing WT channels or untreated F525N-expressing cells. In addition, a decrease in overall cell number was observed for CNGB3 F525N-expressing cells (Fig. 3).

Disease-associated mutations in CNGB3 subunits alter channel sensitivity to CPT-cAMP. Although cGMP is the primary natural agonist for CNG channels in photoreceptors, both cAMP and cGMP co-exist under physiological conditions. The level of intracellular cAMP also changes with illumination (see review in [39]). In addition, cAMP levels are controlled in a circadian manner, with higher levels at night [40]. We found that the F525N mutation produced a significant increase in apparent affinity for CPT-cAMP ($K_{1/2,\ CPT\text{-}cAMP}$ = 13.8 ± 1.4 μM, h = 1.4 ± 0.08; n = 15) compared to WT channels ($K_{1/2,\ CPT\text{-}cAMP}$ = 28.1 ± 2.6 μM, h = 1.7 ± 0.1; n = 10, $p < 0.01$), while the T383fsX mutation produced no significant change in CPT-cAMP sensitivity ($K_{1/2,\ CPT\text{-}cAMP}$ = 29.8 ± 1.9 μM, h = 1.8 ± 0.1; n = 9) (Fig. 4A).

We also determined the relative agonist efficacy for channel activation by a saturating concentration of CPT-cAMP compared with maximal activation by CPT-cGMP ($I_{max,\ CPT\text{-}cAMP}/I_{max,\ CPT\text{-}cGMP}$). For cone photoreceptor CNG channels, cAMP is a partial agonist (reviewed in [41]). CNG channels containing the F525N mutation exhibited a significant increase in CPT-cAMP efficacy ($I_{max,\ CPT\text{-}cAMP}/I_{max,\ CPT\text{-}cGMP}$ = 0.49 ± 0.04, n = 15) compared to that of WT heteromeric channels ($I_{max,\ CPT\text{-}cAMP}/I_{max,\ CPT\text{-}cGMP}$ = 0.25 ± 0.03, n = 10; p = 0.001); channels formed after expression of CNGB3 T383fsX with CNGA3 showed a significant decrease in CPT-cAMP efficacy ($I_{max,\ CPT\text{-}cAMP}/I_{max,\ CPT\text{-}cGMP}$ = 0.07 ± 0.01, n = 8; $p < 0.001$) (Fig. 1A).

Reduced CPT-cAMP efficacy reflects the generation of homomeric CNGA3-only channels with co-expression of CNGB3 T383fsX. For F525N-containing channels, increased CPT-cAMP efficacy combined with increased CPT-cGMP and CPT-cAMP apparent affinity is consistent with hyperactive CNG channels.

Low concentrations of CPT-cAMP had a protective effect for cell viability.

Because CNG channels containing F525N exhibited a two-fold increase in apparent cAMP affinity compared to WT channels (Fig. 4A), we hypothesized that activation of mutant channels by CPT-cAMP might also enhance cytotoxicity. Surprisingly, treatment of transfected 661W cells with CPT-cAMP (at concentrations ranging from 0.1 – 10 µM) produced no significant increase in relative cytotoxicity (data not shown).

It has been shown previously that cAMP and cGMP can have synergistic effects on CNG channel activation [42, 43]. We applied CPT-cAMP and CPT-cGMP together to investigate the potential effect of this combination on cell viability. Co-application of 1 µM CPT-cAMP with 0.1 µM CPT-cGMP attenuated the increased relative cytotoxicity induced by CPT-cGMP alone for F525N-containing channels (CPT-cGMP alone: 1.59 ± 0.05; CPT-cGMP with CPT-cAMP: 1.31 ± 0.06, $p < 0.01$) (Fig. 4B); differences in the relative cytotoxicity between WT (0.98 ± 0.03) and mutant channels under these conditions remained statistically significant ($p < 0.01$). Treatment with a higher concentration of CPT-cAMP (10 µM) combined with CPT-cGMP (0.1 µM) produced increased cytotoxicity for mutant channels comparable to that of 0.1 µM CPT-

cGMP treatment alone (T383fsX: 1.30 ± 0.05, $p < 0.01$; F525N: 1.67 ± 0.08; $p < 0.01$ compared to WT channels).

Protective effects of CNG channel blockers or removal of extracellular Ca^{2+}.

L-*cis*-diltiazem and tetracaine are known CNG channel blockers that have been used extensively to dissect the properties of the native and heterologously expressed CNG channels [18, 44-48]. Since increased cytotoxicity described above for CNGB3 mutations may be related to enhanced channel activity, we hypothesized that application of CNG channel blockers would exert a rescuing effect. We used patch-clamp recordings to determine the sensitivity of WT and mutant channels to block by L-*cis*-diltiazem and tetracaine in the presence of 0.1 µM CPT-cGMP. Figure 5A illustrates block of WT and mutant CNG channels (activated with 0.1 µM CPT-cGMP) by 10 µM L-*cis*-diltiazem. The apparent affinity for L-*cis*-diltiazem ($K_{1/2,\ \text{L-}cis\text{-dilt.}}$) was calculated by fitting the dose-response relationships for channel block with a modified Hill equation as described in the methods (Fig. 5B). Compared to WT heteromeric channels ($K_{1/2,\ \text{L-}cis\text{-dilt.}}$ = 4.06 ± 1.0 µM, n = 5), F525N exhibited no significant change in apparent affinity for L-*cis*-diltiazem ($K_{1/2,\ \text{L-}cis\text{-dilt.}}$ = 3.03 ± 0.75 µM, n = 5). In contrast, T383fsX exhibited a statistically significant decrease in diltiazem apparent affinity ($K_{1/2,\ \text{L-}cis\text{-dilt.}}$ = 77.9 ± 23.1 µM, n = 4, $p < 0.01$). Reduced sensitivity to block by diltiazem was in agreement with the previous finding that T383fsX likely represents a CNGB3 null mutation, preventing the formation of functional heteromeric channels with CNGA3 subunits [23]. Sensitivity to block by 10 µM tetracaine in the presence of 0.1 µM CPT-cGMP is depicted in Figure 6A. Compared to WT ($K_{1/2,\ \text{tetracaine}}$ = 1.03

± 0.17 μM, n = 5) and F525N ($K_{1/2,\ tetracaine}$ = 2.05 ± 0. 24 μM, n = 5) channels, channels formed after co-expression of CNGA3 with CNGB3 T383fsX exhibited greater sensitivity to tetracaine block ($K_{1/2,\ tetracaine}$ = 0.321 ± 0.014 μM, n = 4, $p < 0.01$) (Fig. 5B). The trend in decreased sensitivity to block by tetracaine for F525N-containing channels, although not significantly different from WT channels (p = 0.117), was consistent with their greater sensitivity to CPT-cGMP, since tetracaine is known to be less effective in blocking CNG channels when they are in the open state [18, 48].

We next examined the functional effects of CNG channel blockers on cell viability by applying L-*cis*-diltiazem or tetracaine, in the presence of 0.1 μM CPT-cGMP, to transfected 661W cells. Figures 5C and 6C demonstrate that application of 10 μM L-*cis*-diltiazem (Fig. 5C) or 10 μM tetracaine (Fig. 6C) effectively rescued cells from the increased cytotoxicity elicited by F525N mutant channel activation. The rescuing effect of channel blockers was somewhat ambiguous for T383fsX mutant group. Despite the reduced sensitivity to block by L-*cis*-diltiazem, the CPT-cGMP-induced increase in cytotoxicity is attenuated compared to no diltiazem treatment (Fig. 5C). On the other hand, no protective effect was observed with tetracaine treatment (Fig. 6C). These results suggest that other mechanisms might be involved in the T383fsX-related increase in cytotoxicity.

Calcium overload is thought to serve as an important trigger for photoreceptor cell degeneration. CNG channel mutations that increase ligand sensitivity are expected to increase calcium entry through the hyperactive, calcium-permeable channels. Thus, we hypothesized that the increased

cytotoxicity observed with CNGB3-F525N and -T383fsX mutations would depend on extracellular calcium. To test this prediction, we assessed the relative cytotoxicity of transfected 661W cells maintained in normal or Ca^{2+} -free media during CPT-cGMP treatment. As shown in Figure 7, removal of extracellular Ca^{2+} effectively attenuated the increased relative cytotoxicity elicited by F525N mutant channel activation compared to WT channel activation ($p < 0.01$). Absence of extracellular Ca^{2+}, however, had no significant effect on the relative cytotoxicity of cells expressing T383fsX subunits. Interestingly, removal of extracellular Ca^{2+} for cells expressing WT channels caused a mild increase in cytotoxicity ($p = 0.0115$).

DISCUSSION

We have examined the cellular consequences of two different *CNGB3* mutations linked to achromatopsia in humans. Our results indicate that expression of CNGB3 subunits containing F525N or T383fsX mutations significantly increased susceptibility to cell death compared to WT channels, in the presence of a low, physiologically relevant concentration of membrane permeable channel activator. Importantly, the concentration of channel activator producing this difference in cytotoxicity was within the concentration range showing the greatest difference in channel activation of mutant versus WT channels. This concentration of channel activator also mimics the low level of channel ligand and corresponding low level of channel activity existing in the photoreceptor outer segment in the dark [49-51]. Higher levels of CPT-cGMP are expected to activate other cellular pathways, including those known to be neuroprotective [52]. In addition, increased susceptibility to cell death was prevented by CNG channel blockers or by removal of extracellular calcium, consistent with the idea that photoreceptor death can arise via excess calcium entry through hyperactive CNG channels. These results are important because they begin to establish a connection between mutations in cone CNG channels, altered channel-activation properties, and cell death.

We expect that in native photoreceptors of patients having gain of function CNG channel mutations such as F525N, the channels will have a higher open probability in the dark and fail to close appropriately during light stimulation. Because CNG channels are the main entryway for calcium into the photoreceptor outer segment [25], hyperactive channels are expected to disturb

calcium homeostasis in these cells. We hypothesize that abnormally high levels of calcium under these circumstances will lead to photoreceptor death. Similar cellular mechanisms have been described for mutations in genes encoding other critical proteins involved in phototransduction, adaptation and recovery processes. Mutations that produce constitutively active guanylyl cyclase [53-55] or loss of cGMP-PDE activity [56-58] result in increased intracellular cGMP levels. Increased intracellular cGMP, similar to an increase in channel sensitivity to cGMP, is expected to lead to inappropriate opening of the channels with more Ca^{2+} entering the photoreceptor. Numerous studies have reported that a sustained elevation of intracellular Ca^{2+} can result in apoptotic cell death (reviewed by Choi [59] and Leist & Nicotera [60]). In the retina, for example, sustained elevation of intracellular Ca^{2+} has been shown to trigger rod photoreceptor apoptosis and retinal degeneration [61]. Some of the Ca^{2+}-dependent pathways producing photoreceptor degeneration are thought to involve caspase and/or calpain activation as a central mechanism [62, 63], but some diversity of cell death mechanisms, including autophagy, has been uncovered [64-66]. The precise pathways involved in photoreceptor degeneration caused by cone CNG channel mutations remains to be determined.

With the F525N mutation, our results strongly suggest that channel hyperactivity and subsequent Ca^{2+} overload is likely to contribute to increased cell death. However, the effect of T383fsX is more difficult to interpret. This frame shift is effectively a null mutation producing a truncated CNGB3 subunit that does not combine with CNGA3 subunits to form functional heteromeric channels at the plasma membrane [23]. Channels resulting from expression of mutant T383fsX subunits closely resemble homomeric CNGA3 channels. Homomeric CNGA3 channels exhibit

greater apparent affinity for cGMP compared to heteromeric channels, a gain-of-function phenotype. Also, homomeric CNGA3 channels are insensitive to down-regulation by Ca^{2+}/calmodulin [67] and phosphoinositides such as PIP_3 [68]. It is possible that lack of feedback control of channels by Ca^{2+}/calmodulin may contribute to enhanced channel activity and increased susceptibility to cell death. In addition, improperly localized [67] or misfolded CNGB3-T383fsX subunits may produce ER stress and the UPR, subsequently leading to cell death (see review in [69]). Consistent with this idea, removal of extracellular Ca^{2+} did not significantly reduce the effect of T383fsX on cell viability. It is also possible that the premature stop codon upstream of intronic sequence induces nonsense mediated mRNA decay during processing of the CNGB3 T383fsX message *in vivo*. Further studies are needed to address these alternative mechanisms.

Acknowledgments

The authors thank E. Rich for expert technical support, and C. Peng, D. Duricka, and E. Rich for helpful comments. The authors are also grateful to Prof. M. R. Al-Ubaidi for kindly providing the 661W cell line, and to Prof. K.-W. Yau for sharing the cDNA clone for human CNGA3.

References

1. Travis GH. Mechanisms of cell death in the inherited retinal degenerations. *Am J Hum Genet* 1998;62:503-508.
2. Rattner A, Sun H, Nathans J. Molecular genetics of human retinal disease. *Annu Rev Genet* 1999;33:89-131.
3. Pierce EA. Pathways to photoreceptor cell death in inherited retinal degenerations. *Bioessays* 2001;23:605-618.
4. Burns ME, Baylor DA. Activation, deactivation, and adaptation in vertebrate photoreceptor cells. *Annu Rev Neurosci* 2001;24:779-805.
5. Peng C, Rich ED, Varnum MD. Subunit configuration of heteromeric cone cyclic nucleotide-gated channels. *Neuron* 2004;42:401-410.
6. Kohl S, Baumann B, Broghammer M, et al. Mutations in the CNGB3 gene encoding the beta-subunit of the cone photoreceptor cGMP-gated channel are responsible for achromatopsia (ACHM3) linked to chromosome 8q21. *Hum Mol Genet* 2000;9:2107-2116.
7. Goto-Omoto S, Hayashi T, Gekka T, Kubo A, Takeuchi T, Kitahara K. Compound heterozygous CNGA3 mutations (R436W, L633P) in a Japanese patient with congenital achromatopsia. *Vis Neurosci* 2006;23:395-402.
8. Johnson S, Michaelides M, Aligianis IA, et al. Achromatopsia caused by novel mutations in both CNGA3 and CNGB3. *J Med Genet* 2004;41:e20.
9. Sundin OH, Yang JM, Li Y, et al. Genetic basis of total colourblindness among the Pingelapese islanders. *Nature genetics* 2000;25:289-293.
10. Wissinger B, Gamer D, Jagle H, et al. CNGA3 mutations in hereditary cone photoreceptor disorders. *Am J Hum Genet* 2001;69:722-737.
11. Kohl S, Marx T, Giddings I, et al. Total colourblindness is caused by mutations in the gene encoding the alpha-subunit of the cone photoreceptor cGMP-gated cation channel. *Nature genetics* 1998;19:257-259.
12. Kohl S, Varsanyi B, Antunes GA, et al. CNGB3 mutations account for 50% of all cases with autosomal recessive achromatopsia. *Eur J Hum Genet* 2005;13:302-308.
13. Nishiguchi KM, Sandberg MA, Gorji N, Berson EL, Dryja TP. Cone cGMP-gated channel mutations and clinical findings in patients with achromatopsia, macular degeneration, and other hereditary cone diseases. *Hum Mutat* 2005;25:248-258.
14. Trankner D, Jagle H, Kohl S, et al. Molecular basis of an inherited form of incomplete achromatopsia. *J Neurosci* 2004;24:138-147.
15. Rojas CV, Maria LS, Santos JL, Cortes F, Alliende MA. A frameshift insertion in the cone cyclic nucleotide gated cation channel causes complete achromatopsia in a consanguineous family from a rural isolate. *Eur J Hum Genet* 2002;10:638-642.
16. Wiszniewski W, Lewis RA, Lupski JR. Achromatopsia: the CNGB3 p.T383fsX mutation results from a founder effect and is responsible for the visual phenotype in the original report of uniparental disomy 14. *Hum Genet* 2007;121:433-439.

17. Michaelides M, Aligianis IA, Ainsworth JR, et al. Progressive cone dystrophy associated with mutation in CNGB3. *Invest Ophthalmol Vis Sci* 2004;45:1975-1982.
18. Liu C, Varnum MD. Functional consequences of progressive cone dystrophy-associated mutations in the human cone photoreceptor cyclic nucleotide-gated channel CNGA3 subunit. *Am J Physiol Cell Physiol* 2005;289:C187-198.
19. Patel KA BK, Fandino RA, Ngatchou AN, Woch G, Carey J, Tanaka JC. Transmembrane S1 mutations in CNGA3 from achromatopsia 2 patients cause loss of function and impaired cellular trafficking of the cone CNG channel. *Invest Ophthalmol Vis Sci* 2005;46:2282-2290.
20. Muraki-Oda S, Toyoda F, Okada A, et al. Functional analysis of rod monochromacy-associated missense mutations in the CNGA3 subunit of the cone photoreceptor cGMP-gated channel. *Biochem Biophys Res Commun* 2007;362:88-93.
21. Faillace MP, Bernabeu RO, Korenbrot JI. Cellular Processing of Cone Photoreceptor Cyclic GMP-gated Ion Channels: A ROLE FOR THE S4 STRUCTURAL MOTIF. *J Biol Chem* 2004;279:22643-22653.
22. Bright SR, Brown TE, Varnum MD. Disease-associated mutations in CNGB3 produce gain of function alterations in cone cyclic nucleotide-gated channels. *Molecular vision* 2005;11:1141-1150.
23. Peng C, Rich ED, Varnum MD. Achromatopsia-associated mutation in the human cone photoreceptor cyclic nucleotide-gated channel CNGB3 subunit alters the ligand sensitivity and pore properties of heteromeric channels. *J Biol Chem* 2003;278:34533-34540.
24. Okada A, Ueyama H, Toyoda F, et al. Functional role of hCNGB3 in regulation of human cone CNG channel: effect of rod monochromacy-associated mutations in hCNGB3 on channel function. *Invest Ophthalmol Vis Sci* 2004;45:2324-2332.
25. Fain GL, Matthews HR, Cornwall MC, Koutalos Y. Adaptation in vertebrate photoreceptors. *Physiol Rev* 2001;81:117-151.
26. Korenbrot JI, Rebrik TI. Tuning outer segment Ca2+ homeostasis to phototransduction in rods and cones. *Adv Exp Med Biol* 2002;514:179-203.
27. Tan E, Ding XQ, Saadi A, Agarwal N, Naash MI, Al-Ubaidi MR. Expression of cone-photoreceptor-specific antigens in a cell line derived from retinal tumors in transgenic mice. *Invest Ophthalmol Vis Sci* 2004;45:764-768.
28. Krishnamoorthy RR, Crawford MJ, Chaturvedi MM, et al. Photo-oxidative stress down-modulates the activity of nuclear factor-kappaB via involvement of caspase-1, leading to apoptosis of photoreceptor cells. *J Biol Chem* 1999;274:3734-3743.
29. Crawford MJ, Krishnamoorthy RR, Rudick VL, et al. Bcl-2 overexpression protects photooxidative stress-induced apoptosis of photoreceptor cells via NF-kappaB preservation. *Biochem Biophys Res Commun* 2001;281:1304-1312.
30. Fitzgerald JB, Malykhina AP, Al-Ubaidi MR, Ding XQ. Functional expression of cone cyclic nucleotide-gated channel in cone photoreceptor-derived 661W cells. *Adv Exp Med Biol* 2008;613:327-334.

31. Varnum MD, Black KD, Zagotta WN. Molecular mechanism for ligand discrimination of cyclic nucleotide-gated channels. *Neuron* 1995;15:619-625.
32. Zagotta WN, Hoshi T, Aldrich RW. Gating of single Shaker potassium channels in Drosophila muscle and in Xenopus oocytes injected with Shaker mRNA. *Proceedings of the National Academy of Sciences of the United States of America* 1989;86:7243-7247.
33. Wang WZ, Chu XP, Li MH, Seeds J, Simon RP, Xiong ZG. Modulation of acid-sensing ion channel currents, acid-induced increase of intracellular Ca2+, and acidosis-mediated neuronal injury by intracellular pH. *J Biol Chem* 2006;281:29369-29378.
34. Wei JY, Cohen ED, Genieser HG, Barnstable CJ. Substituted cGMP analogs can act as selective agonists of the rod photoreceptor cGMP-gated cation channel. *J Mol Neurosci* 1998;10:53-64.
35. Gomez-Vicente V, Doonan F, Donovan M, Cotter TG. Induction of BIM(EL) following growth factor withdrawal is a key event in caspase-dependent apoptosis of 661W photoreceptor cells. *Eur J Neurosci* 2006;24:981-990.
36. Sharma AK, Rohrer B. Calcium-induced calpain mediates apoptosis via caspase-3 in a mouse photoreceptor cell line. *J Biol Chem* 2004;279:35564-35572.
37. Tuohy G, Millington-Ward S, Kenna PF, Humphries P, Farrar GJ. Sensitivity of photoreceptor-derived cell line (661W) to baculoviral p35, Z-VAD.FMK, and Fas-associated death domain. *Invest Ophthalmol Vis Sci* 2002;43:3583-3589.
38. Gomez-Vicente V, Donovan M, Cotter TG. Multiple death pathways in retina-derived 661W cells following growth factor deprivation: crosstalk between caspases and calpains. *Cell Death Differ* 2005;12:796-804.
39. Iuvone PM. Cell biology and metabolic activity of photoreceptor cells: light-evoked and circadian regulation. *Neurobiology and clinical aspects of the outer retina (Djamgoz MBA, Archer S, Vallerga S, eds, London: Chapman and Hall)* 1995;25-55.
40. Ivanova TN, Iuvone PM. Circadian rhythm and photic control of cAMP level in chick retinal cell cultures: a mechanism for coupling the circadian oscillator to the melatonin-synthesizing enzyme, arylalkylamine N-acetyltransferase, in photoreceptor cells. *Brain Res* 2003;991:96-103.
41. Kaupp UB, Seifert R. Cyclic nucleotide-gated ion channels. *Physiol Rev* 2002;82:769-824.
42. Furman RE, Tanaka JC. Photoreceptor channel activation: interaction between cAMP and cGMP. *Biochemistry* 1989;28:2785-2788.
43. Tanaka JC, Eccleston JF, Furman RE. Photoreceptor channel activation by nucleotide derivatives. *Biochemistry* 1989;28:2776-2784.
44. Haynes LW. Block of the cyclic GMP-gated channel of vertebrate rod and cone photoreceptors by l-cis-diltiazem. *J Gen Physiol* 1992;100:783-801.
45. Chen TY, Peng YW, Dhallan RS, Ahamed B, Reed RR, Yau KW. A new subunit of the cyclic nucleotide-gated cation channel in retinal rods. *Nature* 1993;362:764-767.

46. Gerstner A, Zong X, Hofmann F, Biel M. Molecular cloning and functional characterization of a new modulatory cyclic nucleotide-gated channel subunit from mouse retina. *J Neurosci* 2000;20:1324-1332.
47. McLatchie LM, Matthews HR. Voltage-dependent block by L-cis-diltiazem of the cyclic GMP-activated conductance of salamander rods. *Proc R Soc Lond B Biol Sci* 1992;247:113-119.
48. Fodor AF, Gordon SE, Zagotta WN. Mechanism of tetracaine block of cyclic nucleotide-gated channels. *J Gen Physiol* 1997;109:3-14.
49. Pugh ENJ, Lamb TD. Cyclic GMP and calcium: the internal messengers of excitation and adaptation in vertebrate photoreceptors. *Vision Res* 1990;30:1923-1948.
50. Rebrik TI, Korenbrot JI. In intact mammalian photoreceptors, Ca2+-dependent modulation of cGMP-gated ion channels is detectable in cones but not in rods. *J Gen Physiol* 2004;123:63-75.
51. Soo FS, Detwiler PB, Rieke F. Light adaptation in salamander L-cone photoreceptors. *J Neurosci* 2008;28:1331-1342.
52. Nakamizo T, Kawamata J, Yoshida K, et al. Phosphodiesterase inhibitors are neuroprotective to cultured spinal motor neurons. *J Neurosci Res* 2003;71:485-495.
53. Tucker CL, Woodcock SC, Kelsell RE, Ramamurthy V, Hunt DM, Hurley JB. Biochemical analysis of a dimerization domain mutation in RetGC-1 associated with dominant cone-rod dystrophy. *Proceedings of the National Academy of Sciences of the United States of America* 1999;96:9039-9044.
54. Payne AM, Downes SM, Bessant DA, et al. A mutation in guanylate cyclase activator 1A (GUCA1A) in an autosomal dominant cone dystrophy pedigree mapping to a new locus on chromosome 6p21.1. *Hum Mol Genet* 1998;7:273-277.
55. Kelsell RE, Gregory-Evans K, Payne AM, et al. Mutations in the retinal guanylate cyclase (RETGC-1) gene in dominant cone-rod dystrophy. *Hum Mol Genet* 1998;7:1179-1184.
56. Huang SH, Pittler SJ, Huang X, Oliveira L, Berson EL, Dryja TP. Autosomal recessive retinitis pigmentosa caused by mutations in the alpha subunit of rod cGMP phosphodiesterase. *Nature genetics* 1995;11:468-471.
57. Danciger M, Heilbron V, Gao YQ, Zhao DY, Jacobson SG, Farber DB. A homozygous PDE6B mutation in a family with autosomal recessive retinitis pigmentosa. *Molecular vision* 1996;2:10.
58. Valverde D, Solans T, Grinberg D, et al. A novel mutation in exon 17 of the beta-subunit of rod phosphodiesterase in two RP sisters of a consanguineous family. *Hum Genet* 1996;97:35-38.
59. Choi DW. Calcium and excitotoxic neuronal injury. *Ann N Y Acad Sci* 1994;747:162-171.
60. Nicotera P, Orrenius S. The role of calcium in apoptosis. *Cell Calcium* 1998;23:173-180.
61. Fox DA, Poblenz AT, He L. Calcium overload triggers rod photoreceptor apoptotic cell death in chemical-induced and inherited retinal degenerations. *Ann N Y Acad Sci* 1999;893:282-285.

62. Azuma M, Sakamoto-Mizutani K, Nakajima T, Kanaami-Daibo S, Tamada Y, Shearer TR. Involvement of calpain isoforms in retinal degeneration in WBN/Kob rats. *Comp Med* 2004;54:533-542.
63. Paquet-Durand F, Azadi S, Hauck SM, Ueffing M, van Veen T, Ekstrom P. Calpain is activated in degenerating photoreceptors in the rd1 mouse. *J Neurochem* 2006;96:802-814.
64. Doonan F, Donovan M, Cotter TG. Caspase-independent photoreceptor apoptosis in mouse models of retinal degeneration. *J Neurosci* 2003;23:5723-5731.
65. Rohrer B, Pinto FR, Hulse KE, Lohr HR, Zhang L, Almeida JS. Multidestructive pathways triggered in photoreceptor cell death of the rd mouse as determined through gene expression profiling. *J Biol Chem* 2004;279:41903-41910.
66. Yoshimura N. [Retinal neuronal cell death: molecular mechanism and neuroprotection]. *Nippon Ganka Gakkai Zasshi* 2001;105:884-902.
67. Peng C, Rich ED, Thor CA, Varnum MD. Functionally important calmodulin binding sites in both N- and C-terminal regions of the cone photoreceptor cyclic nucleotide-gated channel CNGB3 subunit. *J Biol Chem* 2003;278:24617-24623.
68. Brady JD, Rich ED, Martens JR, Karpen JW, Varnum MD, Brown RL. Interplay between PIP3 and calmodulin regulation of olfactory cyclic nucleotide-gated channels. *Proceedings of the National Academy of Sciences of the United States of America* 2006;103:15635-15640.
69. Zhang K, Kaufman RJ. Protein folding in the endoplasmic reticulum and the unfolded protein response. *Handb Exp Pharmacol* 2006;69-91.

Figure 1

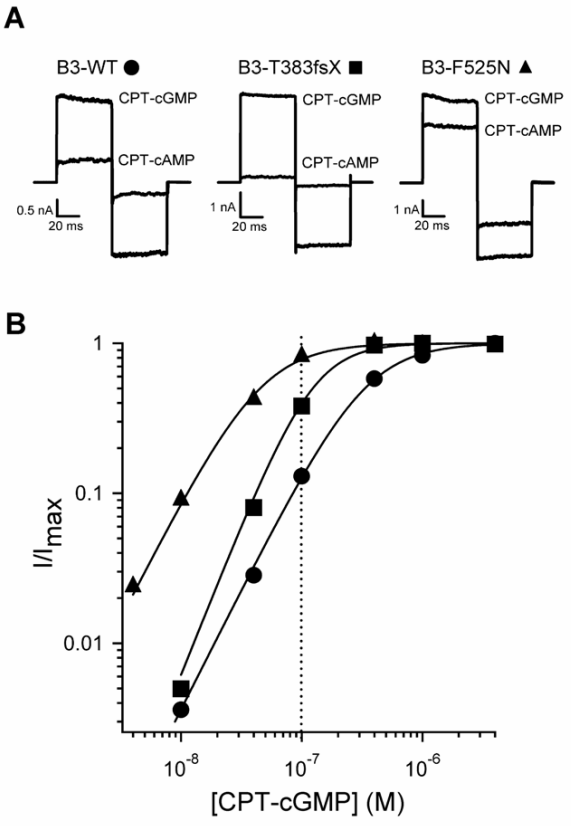
A
B3-WT ●
B3-T383fsX ■
B3-F525N ▲
CPT-cGMP
CPT-cAMP
0.5 nA
20 ms
1 nA
20 ms
1 nA
20 ms
B
1
0.1
0.01
I/Imax
10-8
10-7
10-6
[CPT-cGMP] (M)

Figure 2

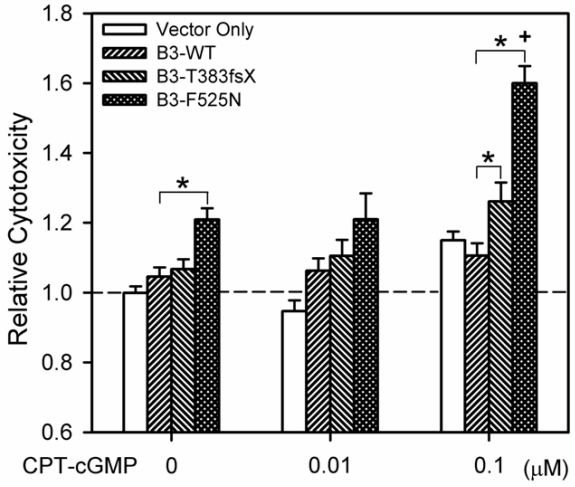
Vector Only
B3-WT
B3-T383fsX
B3-F525N
Relative Cytotoxicity
1.8
1.6
1.4
1.2
1.0
0.8
0.6
*
*
*
+
CPT-cGMP
0
0.01
0.1
(μM)

Figure 3

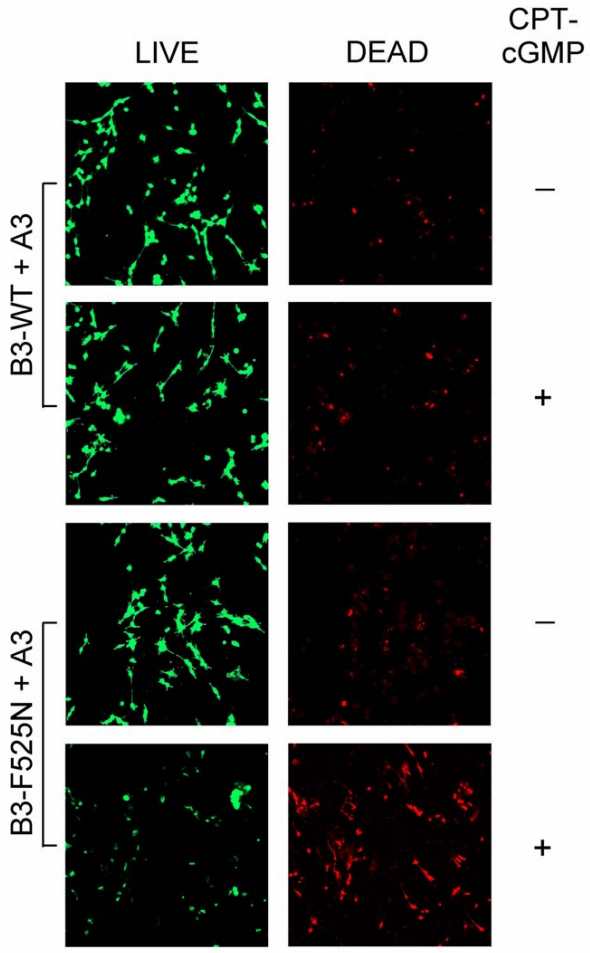

Figure 5

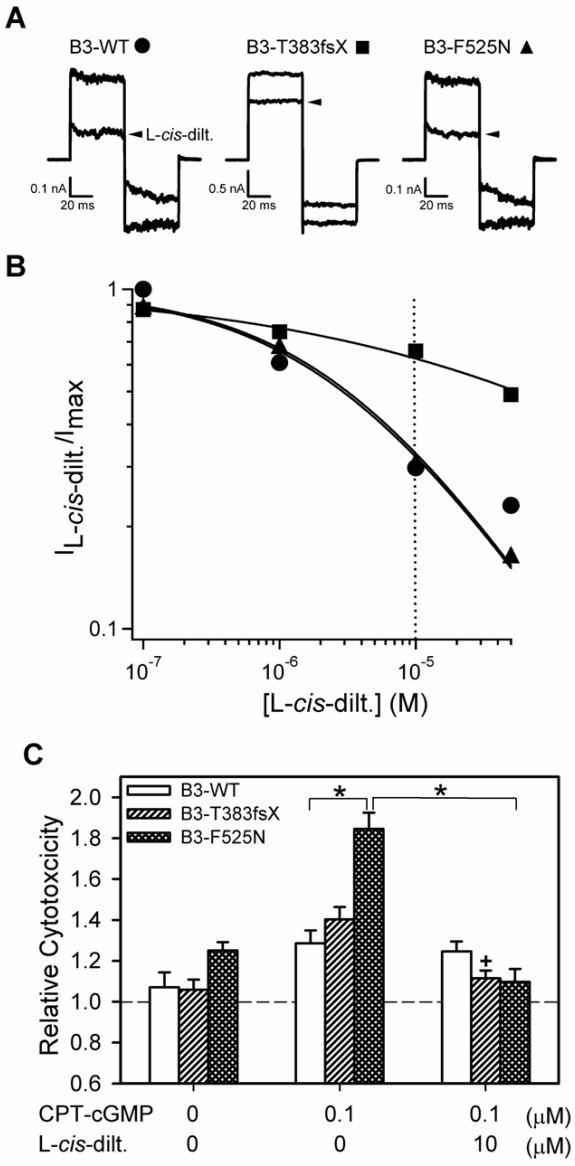
A
B3-WT ●
B3-T383fsX ■
B3-F525N ▲
L-cis-dilt.
0.1 nA
20 ms
0.5 nA
20 ms
0.1 nA
20 ms
B
1
0.1
I L-cis-dilt./I max
10-7
10-6
10-5
[L-cis-dilt.] (M)
C
B3-WT
B3-T383fsX
B3-F525N
Relative Cytotoxcicity
2.0
1.8
1.6
1.4
1.2
1.0
0.8
0.6
*
*
+
CPT-cGMP 0 0.1 0.1 (μM)
L-cis-dilt. 0 0 10 (μM)

Figure 6

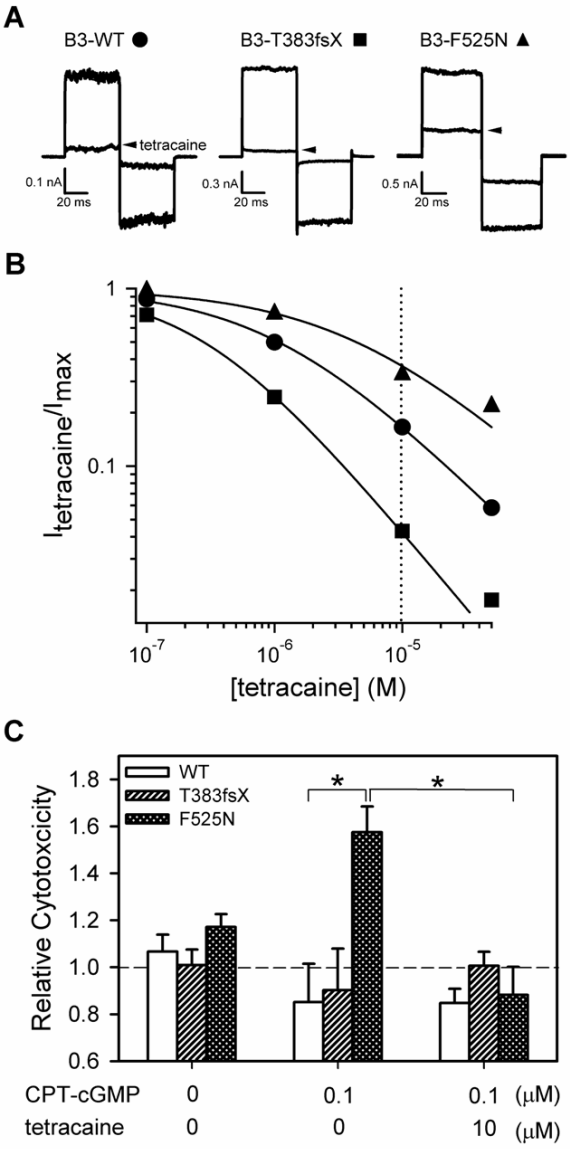
A
B3-WT ●
B3-T383fsX ■
B3-F525N ▲
tetracaine
0.1 nA
20 ms
0.3 nA
20 ms
0.5 nA
20 ms
B
1
0.1
$I_{tetracaine}/I_{max}$
10^{-7}
10^{-6}
10^{-5}
[tetracaine] (M)
C
WT
T383fsX
F525N
*
*
Relative Cytotoxcicity
1.8
1.6
1.4
1.2
1.0
0.8
0.6
CPT-cGMP 0 0.1 0.1 (μM)
tetracaine 0 0 10 (μM)

Figure 7

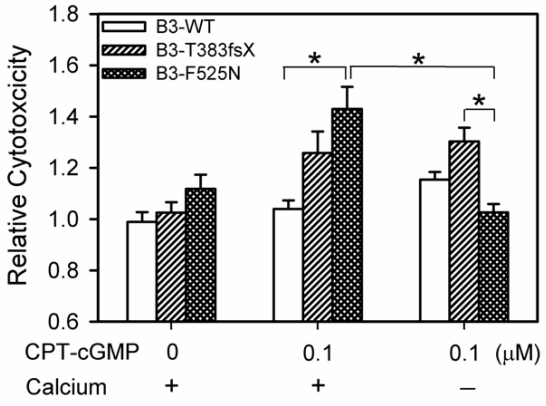
B3-WT
B3-T383fsX
B3-F525N
Relative Cytotoxcicity
1.8
1.6
1.4
1.2
1.0
0.8
0.6
*
*
*
CPT-cGMP 0 0.1 0.1 (μM)
Calcium + + –

FIGURE LEGENDS

Figure 1. Disease-associated mutations in CNGB3 altered the gating properties of heteromeric channels. (A) Representative current traces are shown for CNGA3 plus CNGB3 channels after activation by saturating concentrations of CPT-cGMP (4 μM) or CPT-cAMP (100 μM). Current traces were elicited by the voltage protocol described in methods. (B) Representative dose-response relationships for CPT-cGMP activation of CNG channels, after expression of CNGA3 plus CNGB3-WT (circles), -T383fsX (squares) or -F525N (triangles) subunits. Currents were normalized to the maximum cGMP current. Continuous curves represent fits of the dose-response relationship to the Hill equation as described in the methods. Parameters for each patch were as follows: for WT, $K_{1/2,\ \text{CPT-cGMP}}$ = 333.8 nM, h = 1.6; for T383fsX, $K_{1/2,\ \text{cGMP}}$ = 122.3 nM, h = 2.1; for F525N, $K_{1/2,\ \text{CPT-cGMP}}$ = 45.3 nM, h = 1.7. Dotted line represents CPT-cGMP concentration used in subsequent experiments (0.1 μM).

Figure 2. Disease-associated mutations in CNGB3 increase cytotoxicity in 661W cells expressing CNG channels. Bar graph shows cytotoxicity (calculated as described in Methods) for CNG channel-expressing cells exposed to various concentrations of CPT-cGMP for 24 hours (n = 46 to 48); cytotoxicity was normalized to that of negative control cells transfected with pOPRSVI vector alone. *, significant difference between groups indicated by the bracket ($p < 0.05$); +, significant difference between F525N groups with or without 0.1 μM CPT-cGMP treatment ($p < 0.01$).

Figure 3. F525N mutation in CNGB3 reduced cell viability with CPT-cGMP

treatment compared to WT channels. Transfected 661W cells were treated with or without 0.1 μM CPT-cGMP for 24 hours. After treatment, cells were labeled according to the Live/Dead assay protocol: vital cells were stained by calcein AM and show green fluorescence; damaged cells were penetrated by ethidium homodimer and show red fluorescent nuclei. Fluorescent images were obtained using a Zeiss LSM 510 confocal laser-scanning system as described in methods.

Figure 4. Heteromeric channels containing disease-associated mutations in CNGB3 exhibited an increased sensitivity to CPT-cAMP and elevated relative cytotoxicity after combined treatment of CPT-cGMP and CPT-cAMP. (A) Representative dose-response relationships for CPT-cAMP activation of CNG channels, after co-expression of CNGA3 with CNGB3-WT (circles), -T383fsX (squares) or -F525N (triangles) subunits (same representative patches as in Figure 1B). Currents were normalized to the maximum CPT-cGMP current. Continuous curves represent fits of the dose-response relationship to the Hill equation. Parameters for each patch shown here were as followed: for WT, $K_{1/2,\ \text{CPT-cAMP}}$ = 38.1 μM, h = 2.0; for T383fsX, $K_{1/2,\ \text{cAMP}}$ = 32.8 μM, h = 2.1; for F525N, $K_{1/2,\ \text{CPT-cAMP}}$ = 7.5 μM, h = 1.4. (B) Bar graph of the relative cytotoxicity for channel expressing cells exposed to various concentrations of CPT-cAMP plus 0.1 μM CPT-cGMP (n = 12). Dashed line represents the percentage of cell death in the vector only control group without treatment. * indicates statistical significance between groups indicated by bracket ($p < 0.05$); + represents statistical significance between F525N group treated with 10 μM CPT-cAMP together with 0.1 μM CPT-cGMP and F525N group without treatment ($p < 0.01$).

Figure 5. Block of CNG channels by L-*cis*-diltiazem increased viability of cells expressing disease-associated mutations. (A) Representative current traces elicited by 0.1 μM CPT-cGMP in the absence or presence (arrow) of 10 μM L-*cis*-diltiazem for CNG channels expressed in *Xenopus* oocytes. Current traces were elicited by the voltage protocol described in methods. (B) Dose-response relationships for block by L-*cis*-diltiazem in the presence of 0.1μM CPT-cGMP in heteromeric CNG channels containing CNGB3-WT (circles), -T383fsX (squares) or -F525N (triangles) subunits. Currents were normalized to the current elicited by 0.1 μM CPT-cGMP in the absence of L-*cis*-diltiazem. Continuous curves represent fits of the dose-response relation to the modified Hill equation described in the methods. Parameters for each patch shown here were as followed: WT channels: $K_{1/2,\ \text{L-}cis\text{-dilt.}}$ = 3.14 μM, and h = 0.6; T383fsX: $K_{1/2,\ \text{L-}cis\text{-dilt.}}$ = 57.4 μM, and h = 0.3; F525N: $K_{1/2,\ \text{L-}cis\text{-dilt.}}$ = 2.90 μM, and h = 0.6. Dotted line represents L-*cis*-diltiazem concentration used in subsequent experiments (10 μM). (C) Bar graph of the relative cytotoxicity for channel expressing 661Wcells with or without 10 μM L-*cis*-diltiazem in the presence of 0.1 μM CPT-cGMP treatment (n = 12). Dashed line indicates the extent of cell death in vector only control cells without treatment. Significant differences were observed between groups indicated by brackets (*, $p < 0.05$); + indicates significant difference between T383fsX groups treated with or without channel blocker ($p < 0.01$)).

Figure 6. Block of heteromeric CNG channels by tetracaine increased viability of cells expressing disease-associated mutations. (A) Representative current traces elicited

by 0.1 μM CPT-cGMP in the absence or presence (arrow) of 10 μM tetracaine for CNG channels expressed in *Xenopus* oocytes. (B) Dose-response relationships for CNG channel block by tetracaine in the presence of 0.1μM CPT-cGMP, for channels generated by co-expression of CNGA3 with CNGB3-WT (circles), -T383fsX (squares) or -F525N (triangles) subunits. Currents were normalized to the current elicited by 0.1 μM CPT-cGMP in the absence of tetracaine. Continuous curves represent fits of the dose-response relationship to the modified Hill equation described in the methods. Parameters for each patch were as follows: WT channels: $K_{1/2,\ tetracaine}$ = 1.07 μM, and h = 0.7; T383fsX: $K_{1/2,\ tetracaine}$ = 0.278 μM, and h = 0.9; F525N: $K_{1/2,\ tetracaine}$ = 2.19 μM, and h = 0.5. Dotted line represents tetracaine concentration used in subsequent experiments (10 μM). (C) Bar graph of relative cytotoxicity for channel expressing 661W cells with or without 10 μM tetracaine in the presence of 0.1 μM CPT-cGMP (n = 12; *, $p < 0.05$). Dashed line indicates the extent of cell death in vector only control without treatment.

Figure 7. Removal of extracellular Ca^{2+} from culture media prevented the increase in cytotoxicity for cells expressing CNGB3 F525N. Bar graph of the relative cytotoxicity for channel expressing 661W cells treated with 0.1 μM CPT-cGMP in normal or Ca^{2+}-free DMEM media (n = 12; *, $p < 0.05$). Dashed line indicates the level of cytotoxicity in control cells expressing pOPRSVI plasmid alone cultured in normal media without treatment.

DISCUSSION

Inherited photoreceptor degenerative diseases, such as retinitis pigmentosa, achromatopsia and cone dystrophy, are major causes of visual impairment and disability. Various mutations in CNG channel subunits have been linked to this group of diseases, yet relatively little research has been conducted to examine the molecular and cellular mechanisms underlying the demise of photoreceptor cells, particularly cone photoreceptors. Since the cloning of cone specific CNG channel subunits, CNGA3 in 1993 (6) and CNGB3 in 2000 (58), our laboratory has focused research efforts on understanding the function and dysfunction of cone CNG channels, and were the first to determine the molecular characteristics of recombinant human cone CNG channels via heterologous expression studies. The research presented within this thesis represents a continuation toward this research goal. Studies in this thesis focused on functionally characterizing disease-associated mutations in CNG channel subunits and determining the underlying molecular mechanisms of cone photoreceptor degeneration induced by altered channel properties.

In Chapter One of this thesis we determined the functional consequences of three PCD-associated mutations in CNGA3 subunits (R277C, N471S and R563H) using a heterologous expression system. Two major effects, both “loss-of-function” and “gain-of-function”, were identified in channels containing these mutations. The loss-of-function changes were evident in channels containing R277C or R563H mutations, represented by impaired plasma membrane localization and disrupted channel protein processing and maturation. Such loss-of-function

effects are thought to be predominant for *CNGA3* mutations, since most *CNGA3* mutations characterized so far (32 out of 39) do not form functional channels at the plasma membrane (118, 127). Similar to CNGA3 mutations, several RP-associated mutations in rod CNGA1 are null mutations or mutations that disrupt plasma membrane targeting of channel subunits (33, 107, 177). Interestingly, one CNGA3 mutation (E593K) expressed in HEK293 cells produced functional homomeric channels with lowered apparent affinity for cGMP (118). Such gating changes represent another type of loss-of-function phenotype.

In Chapter One, we also reported gain-of-function changes in channel gating properties, represented by an increase in ligand sensitivity and/or relative agonist efficacy in channels containing mutant CNGA3 subunits (N471S or R563H). The increased apparent affinity for cGMP had also been reported in another CNGA3 mutation (T656M) (118). In contrast to most CNGA3 mutations, disease-associated mutations in CNGB3 characterized to date were found to produce gain-of-function changes in channel gating properties (13, 121, 132). Recent studies carried out in our lab also suggested that the severity of the alterations in channel gating properties, i.e. the extent of the gain-of-function, partially correlated with the severity of the disease linked to the mutation (13). Together, these results indicate that proper channel function is critical for the viability of photoreceptor cells. Any perturbation, whether it results in gain or loss of channel function, may trigger photoreceptor degeneration associated with inherited photoreceptor degenerative diseases.

It remains unclear how altered channel properties are linked to photoreceptor cell death. Thus, elucidating the exact cellular and molecular mechanisms underlying inherited

photoreceptor degenerative diseases is one of the main research goals in our lab. The *CNGA3* knockout mouse model, similar to the loss-of-function changes described in Chapter One, showed progressive degeneration of cone photoreceptors, with rod function relatively intact (5). Apoptotic cell death was observed in CNGA3$^{-/-}$ cones (115). A double knockout mouse model (CNGA3$^{-/-}$/Rho$^{-/-}$) showed similar progressiveness in photoreceptor degeneration. Double knockout CNGA3$^{-/-}$/Rho$^{-/-}$ mice exhibited more visual function at birth; however photoreceptor degeneration and visual impairment started at 4 weeks of age and progressed to almost complete loss by 3 months (22). In addition, targeting of cone opsins and the expression of other visual transduction proteins had been shown to be impaired in CNGA3 deficient mice, suggesting that CNGA3 is essential for the routing of transduction proteins into the outer segments or necessary for the structural integrity of the outer segment (115). It has been proposed that the "equivalent light" hypothesis might be one possible explanation for initiating cell death in these situations (102). Continuous light stimulation was thought to induce permanent closure of the CNG channels, resulting in lowered intracellular Ca^{2+} and increased reactive oxygen species (38, 39, 102, 136). Similarly, mutations in rhodopsin, rhodopsin kinase and arrestin, which resulted in constitutively active phototransduction signaling, induce rod photoreceptor degeneration (56, 64, 190). Constantly active phototransduction mimics prolonged light exposure, supporting the "equivalent light" hypothesis. However, Donovan and coworkers have reported an increase in intracellular Ca^{2+} after extensive light exposure, possibly resulting from activated guanylyl cyclase by NO and increased CNG activity (29). Thus, the "equivalent light" hypothesis seems unlikely to be the explanatory underlying mechanism for photoreceptor degeneration with loss-

of-function CNG channel mutations. Some loss-of-function mutations in CNGA1 subunits lead to accumulation of misfolded protein in intracellular compartments (33, 177). Massive opsin accumulation in the ER also has been observed in CNGA3 knockout mice (115), suggesting the involvement of ER stress and the UPR in photoreceptor cell degeneration. Further experiments are needed to examine this hypothesis.

Compared with loss-of-function mutations, it is relatively easier to understand how gain-of-function mutations initiate photoreceptor degeneration. Since Ca^{2+} enters the photoreceptor outer segment mainly through CNG channels, heightened channel activity may result in sustained elevation of intracellular Ca^{2+}. It is proposed that Ca^{2+}-overload may trigger rod photoreceptor apoptotic cell death (52). We hypothesized that Ca^{2+}-overload might be the underlying mechanism by which channel mutations eventually induced cone photoreceptor cell death. This hypothesis was tested by a series of experiments and the results were presented in Chapter Two of this thesis.

In Chapter Two of this thesis we reached two major conclusions about disease-associated, gain-of-function mutations in the CNGB3 subunit. First, gain-of-function mutations in CNGB3 increased susceptibility to cell death in photoreceptor derived 661W cells. Second, the increased susceptibility to cell death appeared to arise via a Ca^{2+}-overload mechanism, and could be partially rescued by CNG channel blockers or by removing extracellular Ca^{2+}.

Two previously characterized mutations in CNGB3 (T383fsX and F525N), both of which produced gain-of-function phenotypes (13, 132), were tested in an immortalized cell line derived from retinal tumors of a transgenic mouse. These 661W cells exhibit cellular and biochemical

characteristics of cone photoreceptor cells (174), and also exhibit an absence of endogenous CNGA3 subunit expression and only weak expression of CNGB3 (47). These cells thus provide a good *in vitro* model for studying cone cell biology and cone channel function (24, 60, 92, 147, 152, 157, 174, 179). Consistent with previous studies, mutant channels exhibited increased ligand sensitivity and/or relative agonist efficacy after activation by membrane permeable cyclic nucleotide derivative 8-(4-chlorophenylthio) guanosine 3', 5'-cyclic monophosphate (CPT-cGMP) and 8-(4-chlorophenylthio) adenosine 3', 5'-cyclic monophosphate (CPT-cAMP). Application of a physiological low concentration of CPT-cGMP, or combined CPT-cGMP and CPT-cAMP treatment, increased cell death in 661W cells expressing mutant channels compared to expression of wild type channels.

It has been proposed previously that increased intracellular cGMP levels are related to photoreceptor degeneration. In support of this idea, treatment of 661W cells with the PDE inhibitor IBMX, which resulted in elevated cGMP levels, increased apoptotic cell death (158),. However, cGMP is a universal second messenger that is involved in multiple cellular pathways. It is presumptuous to only consider its effect on CNG channel when cGMP is introduced into cells. In a previous study, 1 mM 8-Br-cGMP, another membrane permeable cGMP derivative, had been shown to induce 661W cell apoptosis (157). Although increased Ca^{2+} was also observed in this model, indicating the probable involvement of CNG channel activation, such high concentrations of cGMP would be likely to activate other molecular pathways, potentially masking the channel effect. What would be an appropriate concentration for CPT-cGMP treatment that maximizes the effect of differences in channel gating alteration, which at the same

time elicits minimum nonspecific effect? Under physiological conditions in the absence of light, the endogenous cGMP concentration in photoreceptor outer segment is predicted to keep only a small fraction (less than 10%) of the channels in the open state (140, 141, 167). The low concentration of CPT-cGMP we used (0.1 μM) is sufficient to keep about 10% of wild type channels open (Chapter 2, Fig. 1), mimicking the native situation. Yet an almost 5-fold increase in channel opening was observed in F525N mutant channels exposed to this concentration of CPT-cGMP. Maximum increase in relative cytotoxicity was also apparent under this low CPT-cGMP treatment.

Consistent with our hypothesis that enhanced channel activity initiates cell death, the greatest increase in relative cell death was observed for the F525N group, which also showed the greatest increase in apparent affinity for CPT-cGMP compared to wild type channels. On the other hand, the T383fsX mutation induced a relatively smaller change in channel gating properties compared with that of the F525N group. In accordance with this, only a modest increase in CPT-cyclic nucleotide induced cell death was observed in 661W cells expressing this mutation. These results suggest a strong link between mutant channel activity and photoreceptor viability.

The involvement of Ca^{2+}-overload induced by hyperactive channels in triggering 661W cell death was supported by the protective effect of CNG channel blockers, L-*cis*-diltiazem and tetracaine. A number of organic compounds, including L-*cis*-diltiazem (20, 46, 69, 103, 110) and tetracaine (48, 49, 155), have been reported to block current through CNG channels. L-*cis*-diltiazem is thought to block the CNG channels from the cytoplasmic face in a voltage-dependent

manner (69, 110, 142). It is unclear how well the membrane is permeable to L-*cis*-diltiazem. Although Haynes and coworkers reported that L-*cis*-diltiazem can cross the membrane (69), extracellular application of L-*cis*-diltiazem is known to be much less effective (144, 169). D-*cis*-diltiazem, which is more selective for blocking L-type Ca^{2+} channels, has been shown to have weak effect on blocking CNG channels (74, 85). Previous experiments have been carried out to test whether application of D-*cis*- or L-*cis*-diltiazem had a protective effect against photoreceptor degeneration. The results were somewhat controversial. Rod photoreceptor apoptosis was attenuated by D-*cis*-diltiazem in $Pde6b^{rd1}$ mice (30, 54). But other reports suggested no rescuing effect with same treatment using the same or different animal models, including $Pde6b^{rd1}$ mice (128), dogs with a similar PDE mutation (130) or rats with the Pro23His rhodopsin mutation (16). In contrast, Fox and coworkers reported that blockage of Ca^{2+} influx through CNG channels with L-*cis*-diltiazem partially rescue rod degeneration in $Pde6b^{rd1}$ mice (53). Our results showing that both L-*cis*-diltiazem and tetracaine exerted a rescuing effect against gain-of-function mutation induced cytotoxicity strongly suggest that hyperactive channels are responsible for initiating cell degeneration. Also consistent with our hypothesis, removal of extracellular Ca^{2+} produced a rescuing effect for F525N expressing 661W cells. The linkage between abnormally high channel activity, Ca^{2+} influx and increased cell degeneration was evident with this disease-associated mutation.

Compared to F525N, rescuing effects were somewhat ambiguous for T383fsX-expressing cells. Removing extracellular Ca^{2+} did not produce a protective effect for the CPT-cGMP-induced increase in relative cell death, indicating that mechanisms other than Ca^{2+}-overload might be

important for this mutation. Heterologous expression of this mutant channel subunit, in *Xenopus* oocytes (132) and 661W cells (data not published), revealed an increase in the amount of truncated protein compared with wild type subunits. It is possible that accumulation of immature or misfolded T383fsX subunits may trigger ER stress and the subsequent UPR, initiating apoptotic cell death in photoreceptor cells. Evidence has emerged recently suggesting the involvement of ER stress in photoreceptor degenerative diseases. Yang and coworker reported that ER stress marker proteins were significantly up-regulated in both light-induced photoreceptor degeneration and the *rd1* mouse model of degenerating photoreceptor cells (192, 193). The accumulation of misfolded rhodopsin and subsequent ER stress was also observed in apoptotic photoreceptor degeneration in a *Drosophila* model for autosomal recessive form of RP (150). It is highly probable that complex changes might occur concomitantly in the process of initiating photoreceptor degeneration by T383fsX mutation. Addition experiments are needed to address this question.

CONCLUSIONS

We have functionally characterized three progressive cone dystrophy-associated mutations in CNGA3 subunits and identified both loss-of-function and gain-of-function effects induced by channel mutations, supporting the pathogenicity of these mutations. The changes were evident as impairment of plasma membrane localization of channel subunits and alterations in channel gating properties. These results suggest that survivability of cone photoreceptor cells depends on proper functioning of CNG channel in the outer segment membrane. Complex effects of different PCD-related mutations indicate heterogeneity of this group of diseases. How different alterations in channel function lead to the same ultimate result--photoreceptor degeneration--remain unclear. It is possible that multiple cellular pathways are involved in triggering cell death, including disruptions of intracellular Ca^{2+} homeostasis, impaired protein metabolism, and ER stress. We have discovered here a significant increase in susceptibility to cell death that correlates with altered channel function. The increase in cell death elicited by disease-associated mutations was Ca^{2+}-dependent, supporting our hypothesis that Ca^{2+}-overload mechanisms are be involved in initiating photoreceptor degeneration. How loss-of-function changes in mutant channels trigger photoreceptor degeneration remains an unanswered question that must be addressed with additional experiments. Application of CNG channel blockers exerted a protective effect against the increased cell death, shedding light on possible viable therapeutic strategies for inherited photoreceptor degenerative diseases. Our studies provide the first link between altered channel function due to disease-associated mutations and photoreceptor

degeneration. Further studies are needed to identify the exact cellular and molecular pathways of photoreceptor cell pathogenesis.

BIBLIOGRAPHY

1. **Adamus G, Machnicki M, Elerding H, Sugden B, Blocker YS, and Fox DA**. Antibodies to recoverin induce apoptosis of photoreceptor and bipolar cells in vivo. *J Autoimmun* 11: 523-533, 1998.

2. **Azuma M, Sakamoto-Mizutani K, Nakajima T, Kanaami-Daibo S, Tamada Y, and Shearer TR**. Involvement of calpain isoforms in retinal degeneration in WBN/Kob rats. *Comp Med* 54: 533-542, 2004.

3. **Berridge MJ, Bootman MD, and Lipp P**. Calcium--a life and death signal. *Nature* 395: 645-648, 1998.

4. **Biel M, and Michalakis S**. Function and dysfunction of CNG channels: insights from channelopathies and mouse models. *Mol Neurobiol* 35: 266-277, 2007.

5. **Biel M, Seeliger M, Pfeifer A, Kohler K, Gerstner A, Ludwig A, Jaissle G, Fauser S, Zrenner E, and Hofmann F**. Selective loss of cone function in mice lacking the cyclic nucleotide-gated channel CNG3. *Proc Natl Acad Sci U S A* 96: 7553-7557., 1999.

6. **Bonigk W, Altenhofen W, Muller F, Dose A, Illing M, Molday RS, and Kaupp UB**. Rod and cone photoreceptor cells express distinct genes for cGMP-gated channels. *Neuron* 10: 865-877, 1993.

7. **Bonigk W, Bradley J, Muller F, Sesti F, Boekhoff I, Ronnett GV, Kaupp UB, and Frings S**. The native rat olfactory cyclic nucleotide-gated channel is composed of three distinct subunits. *J Neurosci* 19: 5332-5347, 1999.

8. **Bowes C, Li T, Danciger M, Baxter LC, Applebury ML, and Farber DB**. Retinal degeneration in the rd mouse is caused by a defect in the beta subunit of rod cGMP-phosphodiesterase. *Nature* 347: 677-680, 1990.

9. **Bradley J, Li J, Davidson N, Lester HA, and Zinn K**. Heteromeric olfactory cyclic nucleotide-gated channels: a subunit that confers increased sensitivity to cAMP. *Proc Natl Acad Sci U S A* 91: 8890-8894, 1994.

10. **Bradley J, Reuter D, and Frings S**. Facilitation of calmodulin-mediated odor adaptation by cAMP-gated channel subunits. *Science* 294: 2176-2178, 2001.

11. **Brady JD, Rich ED, Martens JR, Karpen JW, Varnum MD, and Brown RL**. Interplay between PIP3 and calmodulin regulation of olfactory cyclic nucleotide-gated

channels. *Proc Natl Acad Sci U S A* 103: 15635-15640, 2006.

12. **Bredesen DE, Rao RV, and Mehlen P**. Cell death in the nervous system. *Nature* 443: 796-802, 2006.

13. **Bright SR, Brown TE, and Varnum MD**. Disease-associated mutations in CNGB3 produce gain of function alterations in cone cyclic nucleotide-gated channels. *Mol Vis* 11: 1141-1150, 2005.

14. **Buchi ER**. Cell death in the rat retina after a pressure-induced ischaemia-reperfusion insult: an electron microscopic study. I. Ganglion cell layer and inner nuclear layer. *Exp Eye Res* 55: 605-613, 1992.

15. **Burns ME, and Baylor DA**. Activation, deactivation, and adaptation in vertebrate photoreceptor cells. *Annu Rev Neurosci* 24: 779-805., 2001.

16. **Bush RA, Kononen L, Machida S, and Sieving PA**. The effect of calcium channel blocker diltiazem on photoreceptor degeneration in the rhodopsin Pro213His rat. *Invest Ophthalmol Vis Sci* 41: 2697-2701, 2000.

17. **Chang B, Hawes NL, Hurd RE, Davisson MT, Nusinowitz S, and Heckenlively JR**. Retinal degeneration mutants in the mouse. *Vision Res* 42: 517-525, 2002.

18. **Chang B, Hawes NL, Pardue MT, German AM, Hurd RE, Davisson MT, Nusinowitz S, Rengarajan K, Boyd AP, Sidney SS, Phillips MJ, Stewart RE, Chaudhury R, Nickerson JM, Heckenlively JR, and Boatright JH**. Two mouse retinal degenerations caused by missense mutations in the beta-subunit of rod cGMP phosphodiesterase gene. *Vision Res* 47: 624-633, 2007.

19. **Chang GQ HY, Wong F.** Apoptosis: final common pathway of photoreceptor death in rd, rds, and rhodopsin mutant mice. *Neuron* 11: 595-605, 1993.

20. **Chen TY, Peng YW, Dhallan RS, Ahamed B, Reed RR, and Yau KW**. A new subunit of the cyclic nucleotide-gated cation channel in retinal rods. *Nature* 362: 764-767, 1993.

21. **Choi DW**. Calcium and excitotoxic neuronal injury. *Ann N Y Acad Sci* 747: 162-171, 1994.

22. **Claes E, Seeliger M, Michalakis S, Biel M, Humphries P, and Haverkamp S**. Morphological characterization of the retina of the CNGA3(-/-)Rho(-/-) mutant mouse lacking functional cones and rods. *Invest Ophthalmol Vis Sci* 45: 2039-2048, 2004.

23. **Colley NJ, Cassill JA, Baker EK, and Zuker CS**. Defective intracellular transport is the molecular basis of rhodopsin-dependent dominant retinal degeneration. *Proc Natl Acad Sci U S A* 92: 3070-3074, 1995.

24. **Crawford MJ, Krishnamoorthy RR, Rudick VL, Collier RJ, Kapin M, Aggarwal BB, Al-Ubaidi MR, and Agarwal N**. Bcl-2 overexpression protects photooxidative stress-induced apoptosis of photoreceptor cells via NF-kappaB preservation. *Biochem Biophys Res Commun* 281: 1304-1312, 2001.

25. **Crosson CE, Willis JA, and Potter DE**. Effect of the calcium antagonist, nifedipine, on ischemic retinal dysfunction. *J Ocul Pharmacol* 6: 293-299, 1990.

26. **Deeb SS**. Molecular genetics of color-vision deficiencies. *Vis Neurosci* 21: 191-196, 2004.

27. **Detwiler P**. Open the loop: dissecting feedback regulation of a second messenger transduction cascade. *Neuron* 36: 3-4, 2002.

28. **Dizhoor AM, Boikov SG, and Olshevskaya EV**. Constitutive activation of photoreceptor guanylate cyclase by Y99C mutant of GCAP-1. Possible role in causing human autosomal dominant cone degeneration. *J Biol Chem* 273: 17311-17314, 1998.

29. **Donovan M, Carmody RJ, and Cotter TG**. Light-induced photoreceptor apoptosis in vivo requires neuronal nitric-oxide synthase and guanylate cyclase activity and is caspase-3-independent. *J Biol Chem* 276: 23000-23008, 2001.

30. **Donovan M, and Cotter TG**. Caspase-independent photoreceptor apoptosis in vivo and differential expression of apoptotic protease activating factor-1 and caspase-3 during retinal development. *Cell Death Differ* 9: 1220-1231, 2002.

31. **Doonan F, Donovan M, and Cotter TG**. Activation of multiple pathways during photoreceptor apoptosis in the rd mouse. *Invest Ophthalmol Vis Sci* 46: 3530-3538, 2005.

32. **Doonan F, Donovan M, and Cotter TG**. Caspase-independent photoreceptor apoptosis in mouse models of retinal degeneration. *J Neurosci* 23: 5723-5731, 2003.

33. **Dryja TP, Finn JT, Peng YW, McGee TL, Berson EL, and Yau KW**. Mutations in the gene encoding the alpha subunit of the rod cGMP-gated channel in autosomal recessive retinitis pigmentosa. *Proc Natl Acad Sci U S A* 92: 10177-10181, 1995.

34. **Dunaief JL, Dentchev T, Ying GS, and Milam AH**. The role of apoptosis in age-related

macular degeneration. *Arch Ophthalmol* 120: 1435-1442, 2002.

35. **Edward DP, Lam TT, Shahinfar S, Li J, and Tso MO**. Amelioration of light-induced retinal degeneration by a calcium overload blocker. Flunarizine. *Arch Ophthalmol* 109: 554-562, 1991.

36. **Faillace MP, Bernabeu RO, and Korenbrot JI**. Cellular Processing of Cone Photoreceptor Cyclic GMP-gated Ion Channels: A ROLE FOR THE S4 STRUCTURAL MOTIF. *J Biol Chem* 279: 22643-22653, 2004.

37. **Fain GL**. Dark adaptation. *Prog Brain Res* 131: 383-394, 2001.

38. **Fain GL**. Why photoreceptors die (and why they don't). *Bioessays* 28: 344-354, 2006.

39. **Fain GL, and Lisman JE**. Light, Ca2+, and photoreceptor death: new evidence for the equivalent-light hypothesis from arrestin knockout mice. *Invest Ophthalmol Vis Sci* 40: 2770-2772, 1999.

40. **Fain GL, Matthews HR, Cornwall MC, and Koutalos Y**. Adaptation in vertebrate photoreceptors. *Physiol Rev* 81: 117-151, 2001.

41. **Farber DB**. From mice to men: the cyclic GMP phosphodiesterase gene in vision and disease. The Proctor Lecture. *Invest Ophthalmol Vis Sci* 36: 263-275, 1995.

42. **Farber DB, Flannery JG, Bird AC, Shuster T, and Bok D**. Histopathological and biochemical studies on donor eyes affected with retinitis pigmentosa. *Prog Clin Biol Res* 247: 53-67, 1987.

43. **Farber DB, and Lolley RN**. Cyclic guanosine monophosphate: elevation in degenerating photoreceptor cells of the C3H mouse retina. *Science* 186: 449-451, 1974.

44. **Fesenko EE, Kolesnikov SS, and Lyubarsky AL**. Induction by cyclic GMP of cationic conductance in plasma membrane of retinal rod outer segment. *Nature* 313: 310-313, 1985.

45. **Finn JT, Grunwald ME, and Yau KW**. Cyclic nucleotide-gated ion channels: an extended family with diverse functions. *Annu Rev Physiol* 58: 395-426, 1996.

46. **Finn JT, Xiong WH, Solessio EC, and Yau KW**. A cGMP-gated cation channel and phototransduction in depolarizing photoreceptors of the lizard parietal eye. *Vision Res* 38: 1353-1357, 1998.

47. **Fitzgerald JB, Malykhina AP, Al-Ubaidi MR, and Ding XQ**. Functional expression of cone cyclic nucleotide-gated channel in cone photoreceptor-derived 661W cells. *Adv Exp Med Biol* 613: 327-334, 2008.

48. **Fodor AA, Black KD, and Zagotta WN**. Tetracaine reports a conformational change in the pore of cyclic nucleotide-gated channels. *J Gen Physiol* 110: 591-600, 1997.

49. **Fodor AF, Gordon SE, and Zagotta WN**. Mechanism of tetracaine block of cyclic nucleotide-gated channels. *J Gen Physiol* 109: 3-14, 1997.

50. **Fox DA, Campbell ML, and Blocker YS**. Functional alterations and apoptotic cell death in the retina following developmental or adult lead exposure. *Neurotoxicology* 18: 645-664, 1997.

51. **Fox DA, and Chu LW**. Rods are selectively altered by lead: II. Ultrastructure and quantitative histology. *Exp Eye Res* 46: 613-625, 1988.

52. **Fox DA, Poblenz AT, and He L**. Calcium overload triggers rod photoreceptor apoptotic cell death in chemical-induced and inherited retinal degenerations. *Ann N Y Acad Sci* 893: 282-285, 1999.

53. **Fox DA, Poblenz AT, He L, Harris JB, and Medrano CJ**. Pharmacological strategies to block rod photoreceptor apoptosis caused by calcium overload: a mechanistic target-site approach to neuroprotection. *Eur J Ophthalmol* 13 Suppl 3: S44-56, 2003.

54. **Frasson M, Sahel JA, Fabre M, Simonutti M, Dreyfus H, and Picaud S**. Retinitis pigmentosa: rod photoreceptor rescue by a calcium-channel blocker in the rd mouse. *Nat Med* 5: 1183-1187, 1999.

55. **Frins S, Bonigk W, Muller F, Kellner R, and Koch KW**. Functional characterization of a guanylyl cyclase-activating protein from vertebrate rods. Cloning, heterologous expression, and localization. *J Biol Chem* 271: 8022-8027, 1996.

56. **Fuchs S, Nakazawa M, Maw M, Tamai M, Oguchi Y, and Gal A**. A homozygous 1-base pair deletion in the arrestin gene is a frequent cause of Oguchi disease in Japanese. *Nat Genet* 10: 360-362, 1995.

57. **Gegenfurtner KR, and Kiper DC**. Color vision. *Annu Rev Neurosci* 26: 181-206, 2003.

58. **Gerstner A, Zong X, Hofmann F, and Biel M**. Molecular cloning and functional characterization of a new modulatory cyclic nucleotide-gated channel subunit from

mouse retina. *J Neurosci* 20: 1324-1332, 2000.

59. **Goll DE, Thompson VF, Li H, Wei W, and Cong J**. The calpain system. *Physiol Rev* 83: 731-801, 2003.

60. **Gomez-Vicente V, Donovan M, and Cotter TG**. Multiple death pathways in retina-derived 661W cells following growth factor deprivation: crosstalk between caspases and calpains. *Cell Death Differ* 12: 796-804, 2005.

61. **Gordon SE, and Zagotta WN**. A histidine residue associated with the gate of the cyclic nucleotide-activated channels in rod photoreceptors. *Neuron* 14: 177-183, 1995.

62. **Goto-Omoto S, Hayashi T, Gekka T, Kubo A, Takeuchi T, and Kitahara K**. Compound heterozygous CNGA3 mutations (R436W, L633P) in a Japanese patient with congenital achromatopsia. *Vis Neurosci* 23: 395-402, 2006.

63. **Gray-Keller MP, and Detwiler PB**. The calcium feedback signal in the phototransduction cascade of vertebrate rods. *Neuron* 13: 849-861, 1994.

64. **Gross AK, Rao VR, and Oprian DD**. Characterization of rhodopsin congenital night blindness mutant T94I. *Biochemistry* 42: 2009-2015, 2003.

65. **Gu Y, Oberwinkler J, Postma M, and Hardie RC**. Mechanisms of light adaptation in Drosophila photoreceptors. *Curr Biol* 15: 1228-1234, 2005.

66. **Hardie RC, and Minke B**. Novel Ca2+ channels underlying transduction in Drosophila photoreceptors: implications for phosphoinositide-mediated Ca2+ mobilization. *Trends Neurosci* 16: 371-376, 1993.

67. **Hartong DT, Berson EL, and Dryja TP**. Retinitis pigmentosa. *Lancet* 368: 1795-1809, 2006.

68. **Haynes L, and Yau KW**. Cyclic GMP-sensitive conductance in outer segment membrane of catfish cones. *Nature* 317: 61-64, 1985.

69. **Haynes LW**. Block of the cyclic GMP-gated channel of vertebrate rod and cone photoreceptors by l-cis-diltiazem. *J Gen Physiol* 100: 783-801, 1992.

70. **He L, Poblenz AT, Medrano CJ, and Fox DA**. Lead and calcium produce rod photoreceptor cell apoptosis by opening the mitochondrial permeability transition pore. *J Biol Chem* 275: 12175-12184, 2000.

71. **Hsu YT, and Molday RS**. Interaction of calmodulin with the cyclic GMP-gated channel of rod photoreceptor cells. Modulation of activity, affinity purification, and localization. *J Biol Chem* 269: 29765-29770, 1994.

72. **Hsu YT, and Molday RS**. Modulation of the cGMP-gated channel of rod photoreceptor cells by calmodulin. *Nature* 361: 76-79, 1993.

73. **Huttl S, Michalakis S, Seeliger M, Luo DG, Acar N, Geiger H, Hudl K, Mader R, Haverkamp S, Moser M, Pfeifer A, Gerstner A, Yau KW, and Biel M**. Impaired channel targeting and retinal degeneration in mice lacking the cyclic nucleotide-gated channel subunit CNGB1. *J Neurosci* 25: 130-138, 2005.

74. **Ikeda S, Oka J, and Nagao T**. Effects of four diltiazem stereoisomers on binding of d-cis-[3H]diltiazem and (+)-[3H]PN200-110 to rabbit T-tubule calcium channels. *Eur J Pharmacol* 208: 199-205, 1991.

75. **Illing ME, Rajan RS, Bence NF, and Kopito RR**. A rhodopsin mutant linked to autosomal dominant retinitis pigmentosa is prone to aggregate and interacts with the ubiquitin proteasome system. *J Biol Chem* 277: 34150-34160, 2002.

76. **Isacoff EY, Jan YN, and Jan LY**. Putative receptor for the cytoplasmic inactivation gate in the Shaker K+ channel. *Nature* 353: 86-90, 1991.

77. **Johnson S, Michaelides M, Aligianis IA, Ainsworth JR, Mollon JD, Maher ER, Moore AT, and Hunt DM**. Achromatopsia caused by novel mutations in both CNGA3 and CNGB3. *J Med Genet* 41: e20, 2004.

78. **Kalloniatis M, and Fletcher EL**. Retinitis pigmentosa: understanding the clinical presentation, mechanisms and treatment options. *Clin Exp Optom* 87: 65-80, 2004.

79. **Kanan Y, Moiseyev G, Agarwal N, Ma JX, and Al-Ubaidi MR**. Light induces programmed cell death by activating multiple independent proteases in a cone photoreceptor cell line. *Invest Ophthalmol Vis Sci* 48: 40-51, 2007.

80. **Kaupp UB, and Seifert R**. Cyclic nucleotide-gated ion channels. *Physiol Rev* 82: 769-824, 2002.

81. **Kaushal S, Ridge KD, and Khorana HG**. Structure and function in rhodopsin: the role of asparagine-linked glycosylation. *Proc Natl Acad Sci U S A* 91: 4024-4028, 1994.

82. **Khan NW, Wissinger B, Kohl S, and Sieving PA**. CNGB3 achromatopsia with

progressive loss of residual cone function and impaired rod-mediated function. *Invest Ophthalmol Vis Sci* 48: 3864-3871, 2007.

83. **Klionsky DJ**. Autophagy. *Curr Biol* 15: R282-283, 2005.
84. **Koch KW**. Biochemical mechanism of light adaptation in vertebrate photoreceptors. *Trends Biochem Sci* 17: 307-311, 1992.

85. **Koch KW, and Kaupp UB**. Cyclic GMP directly regulates a cation conductance in membranes of bovine rods by a cooperative mechanism. *J Biol Chem* 260: 6788-6800, 1985.

86. **Kohl S, Baumann B, Broghammer M, Jagle H, Sieving P, Kellner U, Spegal R, Anastasi M, Zrenner E, Sharpe LT, and Wissinger B**. Mutations in the CNGB3 gene encoding the beta-subunit of the cone photoreceptor cGMP-gated channel are responsible for achromatopsia (ACHM3) linked to chromosome 8q21. *Hum Mol Genet* 9: 2107-2116., 2000.

87. **Kohl S, Baumann B, Rosenberg T, Kellner U, Lorenz B, Vadala M, Jacobson SG, and Wissinger B**. Mutations in the cone photoreceptor G-protein alpha-subunit gene GNAT2 in patients with achromatopsia. *Am J Hum Genet* 71: 422-425., 2002.

88. **Kohl S, Marx T, Giddings I, Jagle H, Jacobson SG, Apfelstedt-Sylla E, Zrenner E, Sharpe LT, and Wissinger B**. Total colourblindness is caused by mutations in the gene encoding the alpha-subunit of the cone photoreceptor cGMP-gated cation channel. *Nat Genet* 19: 257-259, 1998.

89. **Kohl S, Varsanyi B, Antunes GA, Baumann B, Hoyng CB, Jagle H, Rosenberg T, Kellner U, Lorenz B, Salati R, Jurklies B, Farkas A, Andreasson S, Weleber RG, Jacobson SG, Rudolph G, Castellan C, Dollfus H, Legius E, Anastasi M, Bitoun P, Lev D, Sieving PA, Munier FL, Zrenner E, Sharpe LT, Cremers FP, and Wissinger B**. CNGB3 mutations account for 50% of all cases with autosomal recessive achromatopsia. *Eur J Hum Genet* 13: 302-308, 2005.

90. **Korenbrot JI, and Rebrik TI**. Tuning outer segment Ca2+ homeostasis to phototransduction in rods and cones. *Adv Exp Med Biol* 514: 179-203., 2002.

91. **Korschen HG, Illing M, Selfert R, Sesti F, Williams A, Gotzes S, Colville C, Muller F, Dose A, Godde M, Molday L, Kaupp UB, and Molday RS**. A 240 kDa protein represents the complete β subunit of the cyclic nucleotide-gated channel from rod photoreceptor. *Neuron* 15: 627-636, 1995.

92. **Krishnamoorthy RR, Crawford MJ, Chaturvedi MM, Jain SK, Aggarwal BB, Al-Ubaidi MR, and Agarwal N**. Photo-oxidative stress down-modulates the activity of nuclear factor-kappaB via involvement of caspase-1, leading to apoptosis of photoreceptor cells. *J Biol Chem* 274: 3734-3743, 1999.

93. **Krizaj D, and Copenhagen DR**. Calcium regulation in photoreceptors. *Front Biosci* 7: d2023-2044, 2002.

94. **Kunchithapautham K, and Rohrer B**. Apoptosis and Autophagy in Photoreceptors Exposed to Oxidative Stress. *Autophagy* 3: 2007.

95. **Kunchithapautham K, and Rohrer B**. Autophagy is one of the multiple mechanisms active in photoreceptor degeneration. *Autophagy* 3: 65-66, 2007.

96. **Kurada P, Tonini TD, Serikaku MA, Piccini JP, and O'Tousa JE**. Rhodopsin maturation antagonized by dominant rhodopsin mutants. *Vis Neurosci* 15: 693-700, 1998.

97. **Larsson HP, Baker OS, Dhillon DS, and Isacoff EY**. Transmembrane movement of the shaker K+ channel S4. *Neuron* 16: 387-397, 1996.

98. **Leconte L, and Barnstable CJ**. Impairment of rod cGMP-gated channel alpha-subunit expression leads to photoreceptor and bipolar cell degeneration. *Invest Ophthalmol Vis Sci* 41: 917-926, 2000.

99. **Levine B, and Klionsky DJ**. Development by self-digestion: molecular mechanisms and biological functions of autophagy. *Dev Cell* 6: 463-477, 2004.

100. **Liman ER, and Buck LB**. A second subunit of the olfactory cyclic nucleotide-gated channel confers high sensitivity to cAMP. *Neuron* 13: 611-621, 1994.

101. **Lin JH, Li H, Yasumura D, Cohen HR, Zhang C, Panning B, Shokat KM, Lavail MM, and Walter P**. IRE1 signaling affects cell fate during the unfolded protein response. *Science* 318: 944-949, 2007.

102. **Lisman J, and Fain G**. Support for the equivalent light hypothesis for RP. *Nat Med* 1: 1254-1255, 1995.

103. **Liu C, and Varnum MD**. Functional consequences of progressive cone dystrophy-associated mutations in the human cone photoreceptor cyclic nucleotide-gated channel CNGA3 subunit. *Am J Physiol Cell Physiol* 289: C187-198, 2005.

104. **Liu DT, Tibbs GR, and Siegelbaum SA**. Subunit stoichiometry of cyclic nucleotide-gated channels and effects on Subunit Order on Channel Function. *Neuron* 16: 983-990, 1996.

105. **Lockshin RA, and Zakeri Z**. Apoptosis, autophagy, and more. *Int J Biochem Cell Biol* 36: 2405-2419, 2004.

106. **Lohr HR KK, Sharma AK, Rohrer B.** Multiple, parallel cellular suicide mechanisms participate in photoreceptor cell death. *Exp Eye Res* 83: 380-389, 2006.

107. **Mallouk N, Ildefonse M, Pages F, Ragno M, and Bennett N**. Basis for intracellular retention of a human mutant of the retinal rod channel alpha subunit. *J Membr Biol* 185: 129-136, 2002.

108. **Mattson MP**. Neuronal life-and-death signaling, apoptosis, and neurodegenerative disorders. *Antioxid Redox Signal* 8: 1997-2006, 2006.

109. **Matulef K, and Zagotta WN**. Cyclic nucleotide-gated ion channels. *Annu Rev Cell Dev Biol* 19: 23-44., 2003.

110. **McLatchie LM, and Matthews HR**. Voltage-dependent block by L-cis-diltiazem of the cyclic GMP-activated conductance of salamander rods. *Proc R Soc Lond B Biol Sci* 247: 113-119, 1992.

111. **McLaughlin ME, Ehrhart TL, Berson EL, and Dryja TP**. Mutation spectrum of the gene encoding the beta subunit of rod phosphodiesterase among patients with autosomal recessive retinitis pigmentosa. *Proc Natl Acad Sci U S A* 92: 3249-3253, 1995.

112. **McLaughlin ME, Sandberg MA, Berson EL, and Dryja TP**. Recessive mutations in the gene encoding the beta-subunit of rod phosphodiesterase in patients with retinitis pigmentosa. *Nat Genet* 4: 130-134, 1993.

113. **Michaelides M, Aligianis IA, Ainsworth JR, Good P, Mollon JD, Maher ER, Moore AT, and Hunt DM**. Progressive cone dystrophy associated with mutation in CNGB3. *Invest Ophthalmol Vis Sci* 45: 1975-1982, 2004.

114. **Michaelides M, Hunt DM, and Moore AT**. The cone dysfunction syndromes. *Br J Ophthalmol* 88: 291-297, 2004.

115. **Michalakis S, Geiger H, Haverkamp S, Hofmann F, Gerstner A, and Biel M**. Impaired opsin targeting and cone photoreceptor migration in the retina of mice lacking the cyclic nucleotide-gated channel CNGA3. *Invest Ophthalmol Vis Sci* 46: 1516-1524,

2005.

116. **Miller TJ, Schneider RJ, Miller JA, Martin BP, Al-Ubaidi MR, Agarwal N, Dethloff LA, and Philbert MA**. Photoreceptor cell apoptosis induced by the 2-nitroimidazole radiosensitizer, CI-1010, is mediated by p53-linked activation of caspase-3. *Neurotoxicology* 27: 44-59, 2006.

117. **Min KC, Zvyaga TA, Cypess AM, and Sakmar TP**. Characterization of mutant rhodopsins responsible for autosomal dominant retinitis pigmentosa. Mutations on the cytoplasmic surface affect transducin activation. *J Biol Chem* 268: 9400-9404, 1993.

118. **Muraki-Oda S, Toyoda F, Okada A, Tanabe S, Yamade S, Ueyama H, Matsuura H, and Ohji M**. Functional analysis of rod monochromacy-associated missense mutations in the CNGA3 subunit of the cone photoreceptor cGMP-gated channel. *Biochem Biophys Res Commun* 362: 88-93, 2007.

119. **Nicotera P, and Orrenius S**. The role of calcium in apoptosis. *Cell Calcium* 23: 173-180, 1998.

120. **Nishiguchi KM, Sandberg MA, Gorji N, Berson EL, and Dryja TP**. Cone cGMP-gated channel mutations and clinical findings in patients with achromatopsia, macular degeneration, and other hereditary cone diseases. *Hum Mutat* 25: 248-258, 2005.

121. **Okada A, Ueyama H, Toyoda F, Oda S, Ding WG, Tanabe S, Yamade S, Matsuura H, Ohkubo I, and Kani K**. Functional role of hCNGB3 in regulation of human cone CNG channel: effect of rod monochromacy-associated mutations in hCNGB3 on channel function. *Invest Ophthalmol Vis Sci* 45: 2324-2332, 2004.

122. **Olshevskaya EV, Ennilov AN, and Dizhoor AM**. Factors that affect regulation of cGMP synthesis in vertebrate photoreceptors and their genetic link to human retinal degeneration. *Mol Cell Biochem* 230: 139-147, 2002.

123. **Pacione LR, Szego MJ, Ikeda S, Nishina PM, and McInnes RR**. Progress toward understanding the genetic and biochemical mechanisms of inherited photoreceptor degenerations. *Annu Rev Neurosci* 26: 657-700, 2003.

124. **Palczewski K, Sokal I, and Baehr W**. Guanylate cyclase-activating proteins: structure, function, and diversity. *Biochem Biophys Res Commun* 322: 1123-1130, 2004.

125. **Papermaster DS, and Windle J**. Death at an early age. Apoptosis in inherited retinal degenerations. *Invest Ophthalmol Vis Sci* 36: 977-983, 1995.

126. **Paquet-Durand F, Azadi S, Hauck SM, Ueffing M, van Veen T, and Ekstrom P**.

Calpain is activated in degenerating photoreceptors in the rd1 mouse. *J Neurochem* 96: 802-814, 2006.

127. **Patel KA BK, Fandino RA, Ngatchou AN, Woch G, Carey J, Tanaka JC.** Transmembrane S1 mutations in CNGA3 from achromatopsia 2 patients cause loss of function and impaired cellular trafficking of the cone CNG channel. *Invest Ophthalmol Vis Sci* 46: 2282-2290, 2005.

128. **Pawlyk BS, Li T, Scimeca MS, Sandberg MA, and Berson EL**. Absence of photoreceptor rescue with D-cis-diltiazem in the rd mouse. *Invest Ophthalmol Vis Sci* 43: 1912-1915, 2002.

129. **Payne AM, Downes SM, Bessant DA, Taylor R, Holder GE, Warren MJ, Bird AC, and Bhattacharya SS**. A mutation in guanylate cyclase activator 1A (GUCA1A) in an autosomal dominant cone dystrophy pedigree mapping to a new locus on chromosome 6p21.1. *Hum Mol Genet* 7: 273-277, 1998.

130. **Pearce-Kelling SE, Aleman TS, Nickle A, Laties AM, Aguirre GD, Jacobson SG, and Acland GM**. Calcium channel blocker D-cis-diltiazem does not slow retinal degeneration in the PDE6B mutant rcd1 canine model of retinitis pigmentosa. *Mol Vis* 7: 42-47, 2001.

131. **Peng C, Rich ED, Thor CA, and Varnum MD**. Functionally important calmodulin binding sites in both N- and C-terminal regions of the cone photoreceptor cyclic nucleotide-gated channel CNGB3 subunit. *J Biol Chem* 278: 24617-24623, 2003.

132. **Peng C, Rich ED, and Varnum MD**. Achromatopsia-associated mutation in the human cone photoreceptor cyclic nucleotide-gated channel CNGB3 subunit alters the ligand sensitivity and pore properties of heteromeric channels. *J Biol Chem* 278: 34533-34540, 2003.

133. **Peng C, Rich ED, and Varnum MD**. Functional heterogeneity of cone cyclic nucleotide-gated channel mutations associated with complete achromatopsia. *Biophysical Journal* 80: 633a, 2001.

134. **Peng C, Rich ED, and Varnum MD**. Subunit configuration of heteromeric cone cyclic nucleotide-gated channels. *Neuron* 42: 401-410, 2004.

135. **Perrault I, Rozet JM, Calvas P, Gerber S, Camuzat A, Dollfus H, Chatelin S, Souied E, Ghazi I, Leowski C, Bonnemaison M, Le Paslier D, Frezal J, Dufier JL, Pittler S, Munnich A, and Kaplan J**. Retinal-specific guanylate cyclase gene mutations in Leber's

congenital amaurosis. *Nat Genet* 14: 461-464, 1996.

136. **Pierce EA**. Pathways to photoreceptor cell death in inherited retinal degenerations. *Bioessays* 23: 605-618, 2001.

137. **Pifferi S, Boccaccio A, and Menini A**. Cyclic nucleotide-gated ion channels in sensory transduction. *FEBS Lett* 580: 2853-2859, 2006.

138. **Pittler SJ, and Baehr W**. The molecular genetics of retinal photoreceptor proteins involved in cGMP metabolism. *Prog Clin Biol Res* 362: 33-66, 1991.

139. **Polster BM, Basanez G, Etxebarria A, Hardwick JM, and Nicholls DG**. Calpain I induces cleavage and release of apoptosis-inducing factor from isolated mitochondria. *J Biol Chem* 280: 6447-6454, 2005.

140. **Pugh ENJ, and Lamb TD**. Amplification and kinetics of the activation steps in phototransduction. *Biochim Biophys Acta* 1141: 111-149, 1993.

141. **Pugh ENJ, and Lamb TD**. Cyclic GMP and calcium: the internal messengers of excitation and adaptation in vertebrate photoreceptors. *Vision Res* 30: 1923-1948, 1990.

142. **Quandt FN, Nicol GD, and Schnetkamp PP**. Voltage-dependent gating and block of the cyclic-GMP-dependent current in bovine rod outer segments. *Neuroscience* 42: 629-638, 1991.

143. **Rattner A, Sun H, and Nathans J**. Molecular genetics of human retinal disease. *Annu Rev Genet* 33: 89-131, 1999.

144. **Rispoli G, and Menini A**. The blocking effect of l-cis-diltiazem on the light-sensitive current of isolated rods of the tiger salamander. *Eur Biophys J* 16: 65-71, 1988.

145. **Rohrer B, Pinto FR, Hulse KE, Lohr HR, Zhang L, and Almeida JS**. Multidestructive pathways triggered in photoreceptor cell death of the rd mouse as determined through gene expression profiling. *J Biol Chem* 279: 41903-41910, 2004.

146. **Rojas CV, Maria LS, Santos JL, Cortes F, and Alliende MA**. A frameshift insertion in the cone cyclic nucleotide gated cation channel causes complete achromatopsia in a consanguineous family from a rural isolate. *Eur J Hum Genet* 10: 638-642, 2002.

147. **Roque RS, Rosales AA, Jingjing L, Agarwal N, and Al-Ubaidi MR**. Retina-derived microglial cells induce photoreceptor cell death in vitro. *Brain Res* 836: 110-119, 1999.

148. **Rosenbaum DM, Rosenbaum PS, Gupta A, Michaelson MD, Hall DH, and Kessler JA**. Retinal ischemia leads to apoptosis which is ameliorated by aurintricarboxylic acid. *Vision Res* 37: 3445-3451, 1997.

149. **Rosenbaum PS, Gupta H, Savitz SI, and Rosenbaum DM**. Apoptosis in the retina. *Clin Neurosci* 4: 224-232, 1997.

150. **Ryoo HD, and Steller H**. Unfolded protein response in Drosophila: why another model can make it fly. *Cell Cycle* 6: 830-835, 2007.

151. **Sampath AP, Matthews HR, Cornwall MC, Bandarchi J, and Fain GL**. Light-dependent changes in outer segment free-Ca2+ concentration in salamander cone photoreceptors. *J Gen Physiol* 113: 267-277, 1999.

152. **Sanvicens N, Gomez-Vicente V, Masip I, Messeguer A, and Cotter TG**. Oxidative stress-induced apoptosis in retinal photoreceptor cells is mediated by calpains and caspases and blocked by the oxygen radical scavenger CR-6. *J Biol Chem* 279: 39268-39278, 2004.

153. **Sautter A, Zong X, Hofmann F, and Biel M**. An isoform of the rod photoreceptor cyclic nucleotide-gated channel beta subunit expressed in olfactory neurons. *Proc Natl Acad Sci U S A* 95: 4696-4701, 1998.

154. **Schmucker C, Seeliger M, Humphries P, Biel M, and Schaeffel F**. Grating acuity at different luminances in wild-type mice and in mice lacking rod or cone function. *Invest Ophthalmol Vis Sci* 46: 398-407, 2005.

155. **Schnetkamp PP**. Cation selectivity of and cation binding to the cGMP-dependent channel in bovine rod outer segment membranes. *J Gen Physiol* 96: 517-534, 1990.

156. **Semple-Rowland SL, Gorczyca WA, Buczylko J, Helekar BS, Ruiz CC, Subbaraya I, Palczewski K, and Baehr W**. Expression of GCAP1 and GCAP2 in the retinal degeneration (rd) mutant chicken retina. *FEBS Lett* 385: 47-52, 1996.

157. **Sharma AK, and Rohrer B**. Calcium-induced calpain mediates apoptosis via caspase-3 in a mouse photoreceptor cell line. *J Biol Chem* 279: 35564-35572, 2004.

158. **Sharma AK, and Rohrer B**. Sustained elevation of intracellular cGMP causes oxidative stress triggering calpain-mediated apoptosis in photoreceptor degeneration. *Curr Eye Res* 32: 259-269, 2007.

159. **Sharma RK**. Evolution of the membrane guanylate cyclase transduction system. *Mol Cell Biochem* 230: 3-30, 2002.

160. **Sharpe LT, Nordby, K.** Total colour blindness: an introduction. *Night vision: basic, clinical and applied aspects (Hess RF, Sharpe LT, Nordby K, eds), Cambridge, UK: Cambridge UP* 1990.

161. **Sharpe LT, Stockman, A., Jägle, H., Nathans, J. In:** . Opsin genes, cone photopigments, color vision and colorblindness. . *Color vision: from genes to perception (Gegenfurtner K, Sharpe LT, eds), Cambridge, UK: Cambridge UP* 3-52, 1999.

162. **Shimazawa M, Inokuchi Y, Ito Y, Murata H, Aihara M, Miura M, Araie M, and Hara H**. Involvement of ER stress in retinal cell death. *Mol Vis* 13: 578-587, 2007.

163. **Sidjanin DJ, Lowe JK, McElwee JL, Milne BS, Phippen TM, Sargan DR, Aguirre GD, Acland GM, and Ostrander EA**. Canine CNGB3 mutations establish cone degeneration as orthologous to the human achromatopsia locus ACHM3. *Hum Mol Genet* 11: 1823-1833, 2002.

164. **Simunovic MP, and Moore AT**. The cone dystrophies. *Eye* 12: 553-565., 1998.

165. **Sloan LL, and Feiock K**. Selective impairment of cone function. Perimetric techniques for its detection. *Mod Probl Ophthalmol* 11: 50-62, 1972.

166. **Sokal I, Li N, Surgucheva I, Warren MJ, Payne AM, Bhattacharya SS, Baehr W, and Palczewski K**. GCAP1 (Y99C) mutant is constitutively active in autosomal dominant cone dystrophy. *Mol Cell* 2: 129-133, 1998.

167. **Soo FS, Detwiler PB, and Rieke F**. Light adaptation in salamander L-cone photoreceptors. *J Neurosci* 28: 1331-1342, 2008.

168. **Stearns G, Evangelista M, Fadool JM, and Brockerhoff SE**. A mutation in the cone-specific pde6 gene causes rapid cone photoreceptor degeneration in zebrafish. *J Neurosci* 27: 13866-13874, 2007.

169. **Stern JH, Kaupp UB, and MacLeish PR**. Control of the light-regulated current in rod photoreceptors by cyclic GMP, calcium, and l-cis-diltiazem. *Proc Natl Acad Sci U S A* 83: 1163-1167, 1986.

170. **Sundin OH, Yang JM, Li Y, Zhu D, Hurd JN, Mitchell TN, Silva ED, and Maumenee IH**. Genetic basis of total colourblindness among the Pingelapese islanders.

Nat Genet 25: 289-293, 2000.

171. **Sung CH, Davenport CM, and Nathans J**. Rhodopsin mutations responsible for autosomal dominant retinitis pigmentosa. Clustering of functional classes along the polypeptide chain. *J Biol Chem* 268: 26645-26649, 1993.

172. **Sung CH, Makino C, Baylor D, and Nathans J**. A rhodopsin gene mutation responsible for autosomal dominant retinitis pigmentosa results in a protein that is defective in localization to the photoreceptor outer segment. *J Neurosci* 14: 5818-5833, 1994.

173. **Swaroop A, Branham KE, Chen W, and Abecasis G**. Genetic susceptibility to age-related macular degeneration: a paradigm for dissecting complex disease traits. *Hum Mol Genet* 16 Spec No. 2: R174-182, 2007.

174. **Tan E, Ding XQ, Saadi A, Agarwal N, Naash MI, and Al-Ubaidi MR**. Expression of cone-photoreceptor-specific antigens in a cell line derived from retinal tumors in transgenic mice. *Invest Ophthalmol Vis Sci* 45: 764-768, 2004.

175. **Thirkill CE, Roth AM, and Keltner JL**. Cancer-associated retinopathy. *Arch Ophthalmol* 105: 372-375, 1987.

176. **Trankner D, Jagle H, Kohl S, Apfelstedt-Sylla E, Sharpe LT, Kaupp UB, Zrenner E, Seifert R, and Wissinger B**. Molecular basis of an inherited form of incomplete achromatopsia. *J Neurosci* 24: 138-147, 2004.

177. **Trudeau MC, and Zagotta WN**. An intersubunit interaction regulates trafficking of rod cyclic nucleotide-gated channels and is disrupted in an inherited form of blindness. *Neuron* 34: 197-207, 2002.

178. **Tso MO, Zhang C, Abler AS, Chang CJ, Wong F, Chang GQ, and Lam TT**. Apoptosis leads to photoreceptor degeneration in inherited retinal dystrophy of RCS rats. *Invest Ophthalmol Vis Sci* 35: 2693-2699, 1994.

179. **Tuohy G, Millington-Ward S, Kenna PF, Humphries P, and Farrar GJ**. Sensitivity of photoreceptor-derived cell line (661W) to baculoviral p35, Z-VAD.FMK, and Fas-associated death domain. *Invest Ophthalmol Vis Sci* 43: 3583-3589, 2002.

180. **Ulshafer RJ, Fliesler SJ, and Hollyfield JG**. Differential sensitivity of protein synthesis in human retina to a phosphodiesterase inhibitor and cyclic nucleotides. *Curr Eye Res* 3: 383-392, 1984.

181. **Vallazza-Deschamps G, Cia D, Gong J, Jellali A, Duboc A, Forster V, Sahel JA,**

Tessier LH, and Picaud S. Excessive activation of cyclic nucleotide-gated channels contributes to neuronal degeneration of photoreceptors. *Eur J Neurosci* 22: 1013-1022, 2005.

182. **Varnum MD, Black KD, and Zagotta WN**. Molecular mechanism for ligand discrimination of cyclic nucleotide-gated channels. *Neuron* 15: 619-625, 1995.

183. **Varnum MD, and Zagotta WN**. Subunit interactions in the activation of cyclic nucleotide-gated channels. *Biophysical Journal* 70: 2667-2679, 1996.

184. **Varsanyi B, Wissinger B, Kohl S, Koeppen K, and Farkas A**. Clinical and genetic features of Hungarian achromatopsia patients. *Mol Vis* 11: 996-1001, 2005.

185. **Wang T, Xu H, Oberwinkler J, Gu Y, Hardie RC, and Montell C**. Light activation, adaptation, and cell survival functions of the Na+/Ca2+ exchanger CalX. *Neuron* 45: 367-378, 2005.

186. **Weitz D, Ficek N, Kremmer E, Bauer PJ, and Kaupp UB**. Subunit Stoichiometry of the CNG Channel of Rod Photoreceptors. *Neuron* 36: 881-889, 2002.

187. **Wissinger B, Gamer D, Jagle H, Giorda R, Marx T, Mayer S, Tippmann S, Broghammer M, Jurklies B, Rosenberg T, Jacobson SG, Sener EC, Tatlipinar S, Hoyng CB, Castellan C, Bitoun P, Andreasson S, Rudolph G, Kellner U, Lorenz B, Wolff G, Verellen-Dumoulin C, Schwartz M, Cremers FP, Apfelstedt-Sylla E, Zrenner E, Salati R, Sharpe LT, and Kohl S**. CNGA3 mutations in hereditary cone photoreceptor disorders. *Am J Hum Genet* 69: 722-737, 2001.

188. **Wissinger B, Jagle H, Kohl S, Broghammer M, Baumann B, Hanna DB, Hedels C, Apfelstedt-Sylla E, Randazzo G, Jacobson SG, Zrenner E, and Sharpe LT**. Human rod monochromacy: linkage analysis and mapping of a cone photoreceptor expressed candidate gene on chromosome 2q11. *Genomics* 51: 325-331, 1998.

189. **Wiszniewski W, Lewis RA, and Lupski JR**. Achromatopsia: the CNGB3 p.T383fsX mutation results from a founder effect and is responsible for the visual phenotype in the original report of uniparental disomy 14. *Hum Genet* 121: 433-439, 2007.

190. **Yamamoto S, Sippel KC, Berson EL, and Dryja TP**. Defects in the rhodopsin kinase gene in the Oguchi form of stationary night blindness [see comments]. *Nat Genet* 15: 175-178, 1997.

191. **Yamashima T**. Ca2+-dependent proteases in ischemic neuronal death: a conserved

'calpain-cathepsin cascade' from nematodes to primates. *Cell Calcium* 36: 285-293, 2004.

192. **Yang LP, Wu LM, Guo XJ, Li Y, and Tso MO**. Endoplasmic reticulum stress is activated in light-induced retinal degeneration. *J Neurosci Res* 2007.

193. **Yang LP, Wu LM, Guo XJ, and Tso MO**. Activation of endoplasmic reticulum stress in degenerating photoreceptors of the rd1 mouse. *Invest Ophthalmol Vis Sci* 48: 5191-5198, 2007.

194. **Yau KW, and Baylor DA**. Cyclic GMP-activated conductance of retinal photoreceptor cells. *Annu Rev Neurosci* 12: 289-327, 1989.

195. **Yoon J, Ben-Ami HC, Hong YS, Park S, Strong LL, Bowman J, Geng C, Baek K, Minke B, and Pak WL**. Novel mechanism of massive photoreceptor degeneration caused by mutations in the trp gene of Drosophila. *J Neurosci* 20: 649-659, 2000.

196. **Yoshizawa K, Kiuchi K, Nambu H, Yang J, Senzaki H, Kiyozuka Y, Shikata N, and Tsubura A**. Caspase-3 inhibitor transiently delays inherited retinal degeneration in C3H mice carrying the rd gene. *Graefes Arch Clin Exp Ophthalmol* 240: 214-219, 2002.

197. **Yu TY, Acosta ML, Ready S, Cheong YL, and Kalloniatis M**. Light exposure causes functional changes in the retina: increased photoreceptor cation channel permeability, photoreceptor apoptosis, and altered retinal metabolic function. *J Neurochem* 103: 714-724, 2007.

198. **Zagotta WN, and Siegelbaum SA**. Structure and Function of Cyclic Nucleotide-Gated Channels. *Annu Rev Neurosci* 19: 235-263, 1996.

199. **Zhang K, and Kaufman RJ**. Protein folding in the endoplasmic reticulum and the unfolded protein response. *Handb Exp Pharmacol* 69-91, 2006.

200. **Zhang K, and Kaufman RJ**. The unfolded protein response: a stress signaling pathway critical for health and disease. *Neurology* 66: S102-109, 2006.

201. **Zheng J, Trudeau MC, and Zagotta WN**. Rod Cyclic Nucleotide-Gated Channels Have a Stoichiometry of Three CNGA1 Subunits and One CNGB1 Subunit. *Neuron* 36: 891-896, 2002.

202. **Zheng J, and Zagotta WN**. Stoichiometry and assembly of olfactory cyclic nucleotide-gated channels. *Neuron* 42: 411-421., 2004.

203. **Zhong H, Molday LL, Molday RS, and Yau KW**. The heteromeric cyclic nucleotide-gated channel adopts a 3A:1B stoichiometry. *Nature* 420: 193-198, 2002.